1508

Institut de Géologie
Université de Neuchâtel

Climatic and environmental changes in the Tethys region during the Late Paleocene Thermal Maximum.

Changements climatiques et environnementaux dans la région tethysienne durant le maximum thermique de la fin du Paléocène.

Thèse

Présentée à la Faculté des Sciences de l'Université de Neuchâtel pour l'obtention du grade de docteur ès Sciences

Par

Marie-Pierre Bolle

Janvier 2000

IMPRIMATUR POUR LA THÈSE

Climatic and Environmental Changes in the Tethys Region during the Late Paleocene Thermal Maximum

de Mme Marie-Pierre Bolle

UNIVERSITÉ DE NEUCHÂTEL

FACULTÉ DES SCIENCES

La Faculté des sciences de l'Université de Neuchâtel sur le rapport des membres du jury,

Mmes K. von Salis (ETH Zürich), G. Keller (Princeton USA), MM. J. Remane (directeur de thèse), T. Adatte, K. Föllmi et S. Burns (Uni. Berne)

autorise l'impression de la présente thèse.

Neuchâtel, le 13 janvier 2000

Le doyen:

J.-P. Derendinger

RESUME

Le Paléocène terminal (~55 ma) est caractérisé par des changements environnementaux globaux qui incluent un réchauffement de 6-8°C des eaux océaniques profondes et de surface sous les hautes latitudes (cet épisode est nommé LPTM) et la présence de faunes et flores tempérées à sub-tropicales dans les régions subpolaires des deux hémisphères. Ce réchauffement coincide également avec une excursion négative du $\delta^{13}C$ et une extinction massive (35-50%) des foraminifères benthiques profonds.

A la fin du Paléocène, la Téthys, bassin restreint entouré de vastes mers épicontinentales et soumis à une activité tectonique intense constitue une région clé dans la recherche des mécanismes responsables des changements climatiques et environnementaux globaux qui ont eu lieu durant cette période.

Cette thèse, basée sur une étude pluridisciplinaire, sédimentologique, micropaléontologique, minéralogique et géochimique, a pour but une meilleure compréhension des phénomènes se produisant dans le bassin téthysien à la fin du Paléocène. Malgré la présence d'un hiatus ou de niveaux condensés à la base de l'intervalle LPTM (limite de la subzone P5a/P5b), la plupart des profils sédimentaires étudiés présentent des changements identiques à ceux observés mondialement durant le LPTM. Dans nos profils, cet évènement critique se traduit par une excursion négative du $\delta^{13}C$ observée en roche totale, sur les foraminifères benthiques et planctoniques ainsi que sur les biomarqueurs marins et terrestres. Dans la plupart des profils, le pic négatif du carbon coincide avec une chute drastique de la production carbonatée, une augmentation du détritisme (quartz, feldspath potassique, plagioclase et phyllosilicates), un réchauffement des eaux déduit de la présence d'une excursion négative du $\delta^{18}O$, de l'apparition soudaine d'*Acarinina sibaiyaensis* et/ou *Acarinina africana* ainsi que d'un renouvellement majeur des nanofossiles calcaires. De plus, dans la partie marginale nord-est de la Téthys (Kazakhstan et Ouzbekistan), ces changements coincident avec l'accumulation d'un sédiment riche en matière organique.

Durant le Paléocène inférieur, la Téthys était influencée par un climat chaud et humide avec de fortes précipitations comme l'indique l'abondance de kaolinite observé dans les sédiments marins de cette période. Ce climat uniforme se diversifie durant le Paléocène supérieur, Tandis que les bassins côtiers et les environnements péri-marins de la marge sud et sud-est de la Téthys (sud de la Tunisie et Israel) sont progressivement affectés par des conditions climatiques chaudes et arides (présence de sépiolite et palygorskite), un climat saisonnier avec une alternance de saisons humides et sèches domine la marge sud-ouest et nord-est de la Téthys. Durant le LPTM, un épisode de forte humidité et chaleur affecte la plus grande partie de la Téthys.

Ce fascicule correspond à une forme réduite d'une partie de la thèse.

Le texte intégral de cette thèse a été déposé à la bibliothèque principale de l'Université de Neuchâtel ainsi qu'à la bibliothèque de l'Institut de Géologie de l'Université de Neuchâtel.

Liste des publications majeures

Bolle, M.P., Adatte, T., Keller, G., von Salis, K. and Hunziker, J. (1998). Biostratigraphy, Mineralogy and Geochemistry of the Trabakua Pass and Ermua Sections in Spain: Paleocene-Eocene Transition. *Eclogae geol. Helv.*, 91, 1-25.

Pardo, A., **Bolle, M.P.** and Keller, G. (1999). El eventico bio-climatico del transito P-E en el paratethys boreal: Datos de $\delta^{13}C$, $\delta^{18}O$ y foraminiferos planctonicos. *Rev. Esp. Micropaleontol.,* 31, 91-96.

Bolle, M.P., Adatte, T., Keller, G., von Salis, K. and Burns, S (1999). The Paleocene-Eocene transition in the southern Tethys (Tunisia): Climatic and environmental fluctuations. *Bull. Soc. geol. France* , 170, 661-680.

Bolle, M.P., Pardo, A., Tantawi, A.A., Adatte, T., Hinrichs, K.U., von Salis, K. and Burns, S.(2000). Climatic evolution on the southern and northern margins of the Tethys from the Paleocene to the early Eocene. *GFF,* 122, 31-32.

Bolle, M.P., Tantawi, A.A., Pardo, A., Adatte, T., Burns, S. and Kassab. A. (2000). Climatic and environmental changes documented in the upper Paleocene to lower Eocene Egypt. *Eclogae geol. Helv.,* 93, 33-51.

Bolle, M. P., Pardo, A., Adatte, von Salis, K. and Burns, S. (2000). Climatic evolution on the southern margin of the Tethys (Negev, Israel) from the Paleocene to the early Eocene: Focus on the Late Paleocene thermal Maximum. *J. Geol. Soc. London,* 157, 929-941.

Sous presse

Bolle, M. P., Pardo, A., Hinrichs, K.-U., Adatte, T., von Salis, K., Burns, S., Keller, G. and Muzylev, N. The Paleocene-Eocene transition in the marginal northern Tethys (Kazakhstan and Uzbekistan).*Geologische Rundschau.*

Bolle, M.P. and Adatte, T. Paleocene-Early Eocene climatic evolution in the Tethyan realm: Clay minerals evidence. *Clay minerals.*

0012-9402/98/010001-25 $1.50 + 0.20/0
Birkhäuser Verlag, Basel, 1998

Eclogae geol. Helv. 91 (1998) 1–25

Biostratigraphy, mineralogy and geochemistry of the Trabakua Pass and Ermua sections in Spain: Paleocene-Eocene transition

MARIE-PIERRE BOLLE[1], THIERRY ADATTE[1], GERTA KELLER[2], KATHARINA VON SALIS[3] & JOHANNES HUNZIKER[4]

Key words: Paleocene-Eocene transition, Basque Basin, potential stratotype, planktic foraminifera, calcareous nannofossils, stable isotopes, clay-minerals, geochemistry

ABSTRACT

Isotopic, geochemical and bulk mineralogical analyses in the Trabakua and Ermua sections, Basque Basin, reveal major changes across the Paleocene-Eocene transition. Expanded sedimentary records exhibit a gradual decrease of 1.0 ‰ in $\delta^{13}C$ values in the lower part of Zone P5 followed by a more rapid 3 ‰ negative excursion. The 3 ‰ $\delta^{13}C$ excursion is associated with an abrupt decrease in carbonate sedimentation, increased detrital flux and decreased grain size which suggest changes in marine/atmospheric currents and/or size and structure of the ocean carbon reservoir. The clays recognized at Trabakua record a deep burial diagenesis as indicated by two generations of chlorite, the presence of mixed-layers chlorite-smectite and illite-smectite, the absence of smectite and the near absence of kaolinite. The very low $\delta^{18}O$ values (< -3.5‰) throughout the Trabakua and Ermua sections reflect diagenetic alteration rather than paleotemperatures. Because of deep burial diagenesis and very poorly preserved microfossils, the Trabakua Pass and Ermua sections are not optimal potential stratotypes for the Paleocene-Eocene boundary.

RESUME

Différentes analyses, faunistiques, minéralogiques, isotopiques et géochimiques, effectuées sur des sédiments provenant des profils de Trabakua et Ermua localisés dans le pays basque espagnol montrent des changements majeurs à la transition Paléocène-Eocène. Cette dernière est marquée lithologiquement par un intervalle argileux d'une épaisseur de 3 mètres. La transition Paléocène-Eocène est caractérisée par une diminution graduelle de 1‰ du $\delta^{13}C$ dans la partie inférieure de la Zone P5, suivie par une excursion négative abrupte de 3 ‰ du $\delta^{13}C$. Cette excursion négative est associée à une importante diminution de la sédimentation carbonatée, une augmentation des apports détritiques ainsi qu'à une réduction de la taille des particules. Ces changements suggèrent une diminution de la productivité biologique primaire ainsi que des variations dans la source des sédiments et/ou des courants océaniques/atmosphériques. Deux générations de chlorite, la présence d'interstratifiés illite-smectite et chlorite-smectite, ainsi que l'absence de smectite et kaolinite indiquent que les sédiments de Trabakua ont subi une diagenèse importante. En raison de la mauvaise préservation des microfossiles et de la diagenèse qui affecte les sédiments, le choix combiné des profils de Trabakua et Ermua comme stratotype de la limite Paléocène – Eocène ne serait pas optimal.

Introduction

The Paleocene-Eocene transition is characterized by a 6-8° warming in the deep ocean and high latitude surface ocean as indicated by foraminiferal $\delta^{18}O$ analyses and by a major change in the carbon budget as indicated by a negative excursion of 2.5–3‰ in carbonate $\delta^{13}C$ values (Kennett & Stott 1991; Koch et al. 1992; Pak & Miller 1992; Stott 1992; Lu & Keller 1993; Bralower et al. 1995; Canudo et al. 1995; Lu et al. 1996; Thomas & Shackleton 1996; Stott et al. in press). Clay mineral associations suggest a time of exceptionally high precipitation on Antarctica (Robert & Kennett 1994), but an arid climate in the Tethys region (Adatte et al. 1995). Coincident with the negative $\delta^{13}C$ excursion, carbonate sedimentation decreased drastically in all major basins as well as on continental margins (O 'Connell 1990; Canudo et al. 1995; Thomas & Shackleton 1996), indicating significant changes in ocean chemistry which might have affected atmospheric CO_2 concentrations. The reorganization of ecosystems associated with the P-E global change is marked by a mass extinction in benthic foraminifera known as the benthic extinction event (BEE) (Miller et al. 1987; Thomas 1990; Katz & Miller 1991; Pak & Miller 1992; Speijer 1994a, 1994b; Canudo et al. 1995; Thomas & Shackleton 1996), and the radiation and proliferation of

[1] Institut de Géologie, 11 Emile-Argand, Université de Neuchâtel, CH–2007 Neuchâtel. marie-pierre.bolle@geol.unine.ch
[2] Dpt of Geosciences, Princeton University, Princeton, USA–NJ 08544
[3] Geologisches Institut, ETH-Zentrum, CH–8092 Zürich
[4] Institut de Minéralogie et Pétrographie, BFSH2, Université de Lausanne, CH–1015 Lausanne

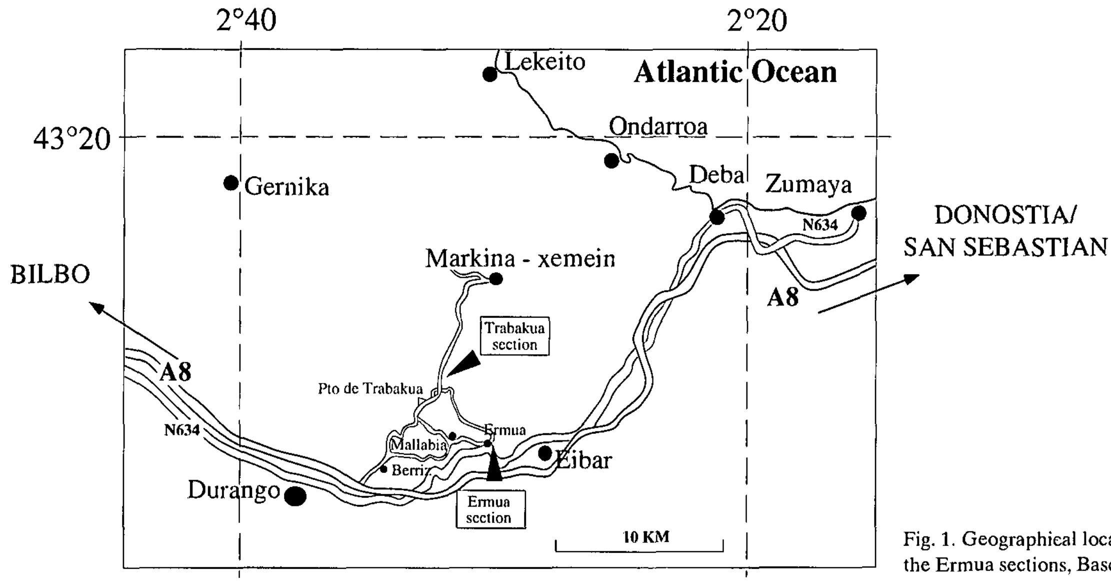

Fig. 1. Geographical location of the Trabakua Pass and the Ermua sections, Basque Basin, North of Spain.

thermophilic species in marine plankton and terrestrial vertebrates and plants (Gingerich 1980, 1986; Wing et al. 1991; Axelrod 1992; Wing & Greenwood 1993; Lu & Keller 1993, 1995a, 1995b).

The Tethys is generally considered as a crucial region for investigating the potential cause(s) and mechanism(s) of the global P-E change (Kennett & Stott 1990, 1991; Lu et al. 1996). During the P-E transition, the Tethys was a semi-restricted basin surrounded by vast shallow epicontinental seas and undergoing intense tectonic activity (Oberhänsli & Hsü 1986; Klootwijk et al. 1992; Oberhänsli 1992; Selverstone & Gutzler 1993). These unique geographic and tectonic features suggest that the Tethys region was most likely a major source and/or sink of organic carbon (Raymo & Ruddiman 1992; Selverstone & Gutzler 1993) and potentially a major source of warm saline deep water (Kennett & Stott 1990, 1991), two conditions that are probably the primary driving forces for the P-E global climatic and environmental changes (Lu et al. 1996).

The Trabakua Pass section has been proposed by Coccioni et al. (1994) and Orue-Etxebarria et al. (1996) as potential stratotype section for the Paleocene/Eocene boundary. According to these authors, this section fullfils most of the requirements for a stratotype section as suggested by the International Commission on Stratigraphy (Remane et al. 1997): a) easy access, b) hemipelagic sedimentation, c) continuous, if somewhat condensed, sedimentation across the boundary, d) absence of synsedimentary and tectonic disturbances, e) absence of diagenetic alteration or redeposition, f) abundance and diversity of well preserved fossils, and g) good magnetostratigraphic and isotopic records. Moreover, this section can be correlated with the Ermua section, located about 10 km to the south of the study area which shows resedimented deposits from a coeval carbonate platform. The proposed boundary section offers therefore the possibility to intercalibrate the biostratigraphic scales of the most important deep and shallow marine fossil groups across the Paleocene/Eocene boundary (Orue-Etxebarria et al. 1996).

To evaluate the Trabakua Pass section as potential P-E boundary stratotype, we conducted a detailed investigation of mineralogical, geochemical, isotopic and faunal changes across the P-E transition of the Trabakua Pass and Ermua sections. The main objectives of this study are: 1) to test the choice of the Trabakua Pass section as potential stratotype with the aid of mineralogical, chemical and isotopic data. 2) To confirm the correlation, based on biostratigraphic data between the two sections. And 3) to correlate this section with others located in the Tethyan realm (Alamedilla, Caravaca).

Location and paleogeographical setting

The Trabakua Pass and Ermua sections are located in the northwestern part of the Pyrenees (Basque Region) of northern Spain and can be reached by the road from Bilbo to Durango (Fig. 1). The Ermua section is located near the village of Ermua and the Trabakua Pass section is 1 km north of the Trabakua Pass.

During the late Cretaceous to early Eocene, the Basque Basin in which the Trabakua and Ermua sections are located, was an interplate trough of intermediate water depth (Plaziat 1981; Pujalte et al. 1992, 1993, 1994). This basin was elongated in a E-W direction, opening westward into the Bay of Biscay, and surrounded by shallow shelf areas to the south, east and north. Within this basin, the Ermua section was located at the base of the slope, whereas the Trabakua Pass section was deposited in a more basinward location.

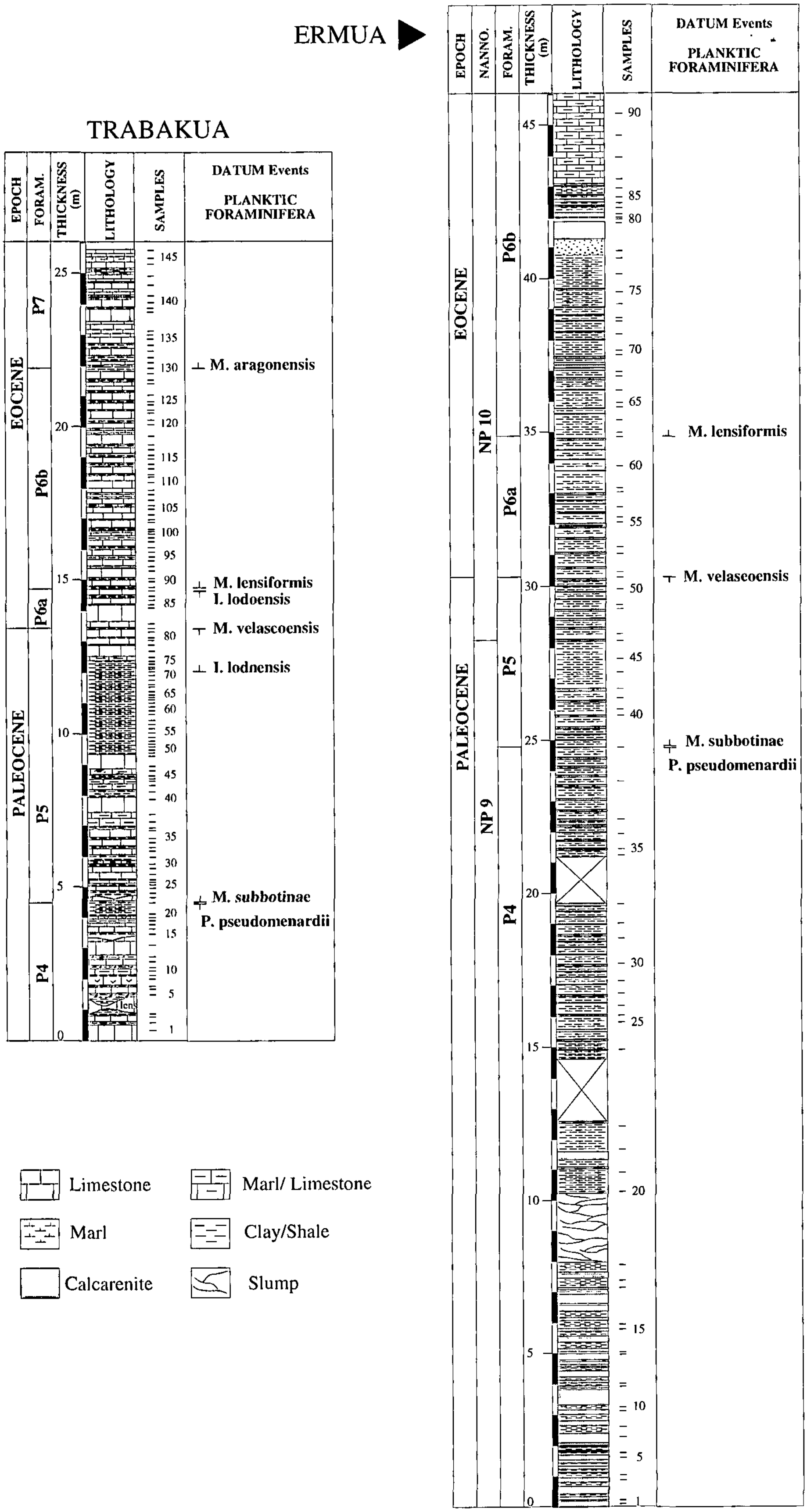

Fig. 2. Lithological description of the Trabakua Pass and the Ermua sections. Planktic foraminifera and calcareous nannoplankton zonation used in this study.

Lithology and sampling

The Trabakua section is about 26 m thick and spans the Paleocene-Eocene (P-E) transition (Fig.2). The lower part of the section (0 to 9.3 m) consists of alternating hemipelagic marls and limestones. The middle part (9.3 to 12.3 m) is composed of green laminated clays alternating with reddish clays and the upper part of the section (12.3 to 25.7 m) consists of alternating hemipelagic limestones and marl layers. This interval consists of more massive limestone and marl layers than the lower part of the section. We sampled the section at 10 to 20 cm intervals, except in the green/reddish clay layers where samples were collected at 5 to 10 cm intervals. A total of 146 samples were analyzed for this study.

The Ermua section is about 45 m thick and also spans the P-E transition (Fig. 2). This succession is mainly built up of turbidites grading upward from coarse grained sandy calcarenites into hemipelagic marls. The calcarenites are rich in quartz and other reworked detrital material. Limestones and marl layers are more massive in the uppermost three meters of the section. Samples in the marly layers were collected at 10 to 90 cm intervals. A total of 90 samples were analyzed for this study.

Methods

Foraminifera:

Sediments were soaked in water and washed through a 63 μm sieve. An ultrasonic bath was used to further clean the recovered foraminiferal tests. Washed residues were dried in an oven. Foraminifera were picked from the residues (>106 μm) for identification and biostratigraphic determinations.

Calcareous nannofossils:

Simple smearslides were prepared and studied with the light microscope at a magnification of 1000 x.

Mineralogical analyses:

X-Ray Diffraction (XRD) analyses of whole rock and clay mineral studies were conducted at the Geological Institute of the University of Neuchâtel, Switzerland, using a SCINTAG XRD 2000 Diffractometer. Whole rock samples were prepared following the method of Kübler (1987). For each rock sample, approximately 20 g were ground to obtain small rock chips (1 to 5 mm). Of these, 5 g were dried at a temperature of 60 °C and then ground again to a homogenous powder with particle size < 40 μm. 800 mg of this powder was compressed (20 bars) in a powder holder and analyzed by XRD. Whole rock composition was determined using external standards based on the methods described by Ferrero (1965, 1966), Klug & Alexander (1974), Kübler (1983), and Moore & Reynolds (1989).

Clay mineral analyses were based on the methods of Kübler (1987). Ground chips were mixed with de-ionized water (pH 7–8) and agitated. The carbonate fraction was removed with 10% HCl (1.25 N) at room temperature for 20 minutes or more until all the carbonate was dissolved. Ultrasonic disaggregation was performed for 3 minutes. The insoluble residue was washed and centrifuged (5–6 times) until a neutral suspension was obtained (pH 7–8). Separation of different grain size fractions (< 2 μm and 2–16 μm) was obtained by the timed settling method based on Stokes law. The selected fraction was then pipetted onto a glass plate and air-dried at room temperature. XRD analyses of oriented clay samples were made after air-drying in ethylen-glycol solvated conditions for the fraction < 2 μm. The intensities of selected XRD peaks characterizing each clay mineral (e.g., chlorite, mica, kaolinite, chlorite-smectite and illite-smectite mixed-layers) were measured for semi-quantitative estimates of the proportion of clay minerals present in the size-fractions < 2 μm and 2–16 μm. Clay minerals are therefore given in relative percent abundance without correction factors.

Stable isotopes:

Oxygen and carbon isotope analyses were conducted on bulk rock samples at the stable isotope laboratory at the University of Lausanne, Switzerland. Carbonate samples were prepared following the conventional procedure of McCrea (1950). CO_2 released from a 2 hour reaction between powdered bulk samples and 100% phosphoric acid at 50 °C was analyzed. The $\delta^{13}C$ and the $\delta^{18}O$ composition of the released CO_2 gas was measured on a Finnigan MAT 251 spectrometer. The results are reported in the usual per mil δ -notation relative to the PDB (Pee Dee Belemnite) international isotopic standard. In the isotope laboratory at the University of Lausanne, calibration to PDB is performed by Carrara marble versus NSB19 standard. Replicate analysis of selected samples showed a reproducibility of 0.05 per mil for $\delta^{13}C$ and better than 0.1 per mil for $\delta^{18}O$. (Bartolini et al. 1996)

Organic matter:

Organic carbon was analyzed using a CHN Carlo-Erba Elemental Analyzer NA 1108. This instrument analyzes total carbon, hydrogen and nitrogen in solid samples by flash combustion at 1020 °C. The sample was placed in a tin container and introduced into a combustion column reactor by means of an auto-sampler (Verardo et al. 1990). The combustion product, a mixture of CO_2, NO and H_2O, is transported through the combustion reactor by a mobile phase of helium into a second column. Due to their different velocities, N is first detected, followed by C and H. Total carbon was first measured on bulk samples (0.01–0.02 g). Total organic carbon (TOC) was determined after dissolving carbonate with hydrochloric acid (HCl 10%). TOC values were determined by comparing the values obtained from the analysis of the sample with the analysis of a suitable standard (Cyclohexanone–2,4 dinitrophenyl Hydrazone ($C_{12}H_{14}N_4O_4$)) and the use of a known reference k-factor (Erba, C., instruction manual 1990). Analytical precision is ± 0.003% of the measured value.

Granulometry:

Measurements have been carried out using a Galai CIS I laser system. This system is based on a rotating He-Ne laser, where the time it takes to pass over a particle is related to the particle diameter. The standard measuring range extends from 0.5 µm to 150 µm in steps of 0.5 µm (Jantschik et al. 1992).

Atomic absorption:

The presence of the elements Ca, Sr, Fe, Mn, Mg and K was determined with a Perkin-Elmer 5100 PC Atomic Absorption Spectrophotometer in the Laboratory of petrology and mineralogy at the Institute of Geology, University of Neuchâtel, Switzerland.

Results

Biostratigraphy

Foraminifera

Planktic and benthic foraminifera in both the Trabakua and Ermua sections are very poorly preserved, recrystallized and/or phosphatized though common at Trabakua, but rare at Ermua in most samples. In general, up to a dozen species can be identified per sample. This is generally enough to obtain biostratigraphic control, though placement of zonal boundaries may be tentative because of the rarity and poor preservation of index species.

Nevertheless, biostratigraphic determinations of this study are in relatively good agreement with earlier studies by Coccioni et al. (1994) and Orue-Etxebarria et al. (1996). The planktic foraminiferal zonation used in this study is the revised zonation of Berggren et al. (1995). For the Paleocene-Eocene interval, this zonal scheme differs from earlier zonations, where the original Zone P5 had been eliminated or effectively included in Zone P6a. Now, Zone P5 is used in a larger sense, including P5 and P6a of earlier publications. Thus this zonal name change will cause great confusion when sections are correlated with earlier published P-E studies where the benthic extinction event and carbon-13 shift is known to occur in Subzone P6a, which is now labelled Zone P5.

Zone P4: This zone is defined by the total range of *Planorotalites pseudomenardii.* At the Trabakua and Ermua sections this taxon disappears at 4.5 m and 25 m from the base respectively (Fig. 2). In both sections the faunal assemblages in this interval are dominated by subbotinids (e.g. *Subbotina triloculinoides, S.hornibrooki, S.velascoensis*) and conicate acarinids (e.g. *Acarinina subsphaerica, A.mckannai, A.nitida). Igorina pusilla, Planorotalites pseudoimitata, P. pseudomenardii* and *P. ehrenbergi* are generally present.

Morozovellids are extremely rare (single occurrence of *M. occlusa* and very rare *M. acuta*). In contrast, tropical assemblages of Zone P4 are dominated by discoidal morozovellids, including *M. occlusa* and *M. velascoensis* (Lu & Keller 1995a). The near absence of these tropical taxa in the Pyreneean sections indicates a relatively cool water environment as also suggested by the abundance of subbotinids.

Chiloguembelinids (e.g. *C. crinita, C. wilcoxensis* and *C. subcylindrica*) are present in the Ermua section in the uppermost part of Zone P4 (21.4 m) and continuing upwards into Zone P5 (29.5 m). The presence of these low oxygen tolerant taxa, as well as the generally dwarfed size of acarinids and subbotinids, particularly in the lower part of this interval, and the presence of low oxygen tolerant benthic foraminifera (bolivinids and buliminids), suggest that low oxygen conditions prevailed at this time. No chiloguembelinids were observed in the Trabakua section in Zone P4, however, many samples were barren due to dissolution in the upper part of Zone P4. The basal part of the Ermua section investigated contains only rare subbotinids and small acarinids. No *P. pseudomenardii* were found, though Orue-Etxebarria et al. (1996) noted the presence of this index species in this interval. We therefore tentatively identify the basal part as Zone P4.

Zone P5: This zone marks the biostratigraphic interval between the last occurrence of *Planorotalites pseudomenardii* and the last occurrence of *Morozovella velascoensis.* Note that this zonal re-definition by Berggren et al. (1995) includes the formerly known Zone P5 which marked the interval between the last occurrence of *P. pseudomenardii* and the first occurrence of *M. subbotinae* (Berggren & Miller 1988), and the formerly known Zone P6a, which marked the interval between the first occurrence of *M. subbotinae* and the last occurrence of *M. velascoensis.* The benthic extinction event, rapid faunal turnover and increased diversity in planktic foraminifera, and the carbon-13 isotopic excursion occur in the upper part of this interval worldwide within a carbonate-poor clay layer (e.g. Canudo et al. 1995; Lu et al. 1995; Lu & Keller 1995a, 1995b; Schmitz et al. 1995; Ortiz 1996; Thomas & Shackleton 1996).

At Trabakua and Ermua, the base of Zone P5 is at 4.5 m and 25 m respectively, marked by the last appearance of *P. pseudomenardii* and the first appearance of *M. subbotinae* within the same sample (Fig. 2). The top of this zone can only be tentatively identified in these sections because many samples have only rare foraminifera due to dissolution. This is particularly the case in the clay layer at Trabakua (9.3 to 12.3 m), and intermittently in the Ermua section. At Trabakua, the last *Morozovella velascoensis* was observed at 13.5 m which is about 1m above the top of the clay layer. At DSDP Site 577, Lu & Keller (1995a) noted that the short ranging species *Igorina lodoensis* marks the interval equivalent to Subzone P6a. *Igorina lodoensis* first appears at Trabakua near the top of the clay layer (12 m). This suggests that the Zone P5/P6a boundary may be lower. At Ermua, *M. velascoensis* disappears at 30.3 m; *Igorina lodoensis* was not observed. Zone P5 assemblages at Trabakua and Ermua are dominated by acarininids (*A. mckannai, A. nitida, A. densa, A. pseudotopilensis*) and few morozovellids *(M. aequa, M. occlusa).*

Zone P6a: This zone is defined by the stratigraphic interval from the last *M. velascoensis* to the first appearance of *M. formosa* and/or *M. lensiformis. Morozovella lensiformis* is constantly present in the Trabakua and Ermua sections and we base the top of P6a at the first appearance of this taxon. At Trabakua, *M. lensiformis* appears at 14.5 m and only one meter above the last *M. velascoensis* (Fig. 2). This suggests either diachronous species occurrences, or a very condensed interval above the clay layer. There is no evidence for the latter in these limestone/marl layers, though a short hiatus could be present. At Ermua the first *M. lensiformis* was observed at 35 m and hence indicates that Zone P6a spans 5 m (Fig. 2). In both sections, Zone P6a is marked by higher planktic foraminiferal diversity than either above or below. This was also observed at other sections in Spain and elsewhere (Canudo et al. 1995; Lu & Keller 1995a, 1995b; Lu et al. 1996). The assemblages in this interval contain more morozovellids *(M. aequa, M. quetra, M. subbotinae, M. marginodentata).* In addition, rounded acarininids dominate *(A. pseudotopilensis, A. soldadoensis, A. praepentacamerata)* and replace the earlier conicate acarininid assemblage *(A. nitida, A. subsphaerica, A. mckannai)* as also observed in sections elsewhere (see Lu & Keller 1995a, 1995b). This major faunal turnover between P5 and P6a correlates with the maximum warming following the benthic extinction event and carbon-13 shift in other Tethyan (e.g. Caravaca, Zumaya, Allamedilla) in Spain (Canudo et al. 1995) and Negev sections (Lu et al. 1996).

Zone P6b: This zone spans the interval from the first appearance of *M. lensiformis* to the first appearance of *M. aragonensis.* At Trabakua, *M. aragonensis* appears at 22 m and the zone spans 7.5 m (14.5–22 m) (Fig. 2). At Ermua, *M. aragonensis* was not encountered in the examined interval; Zone P6b thus spans from 35 m to the top of the section (Fig. 2). The faunal assemblages in this interval are diverse. Rounded acarininids still dominate, though angulate morphotypes appear *(A. nicoli, A. densa),* and morozovellids are more common.

Zone P7: The base of Zone P7 is defined by the first appearance of *M. aragonensis.* This zone was only sampled at Trabakua where *M. aragonensis* was observed at 22 m; thus the upper most 4 m of the section belong to Zone P7. The assemblage is dominated by large rounded and angulate acarininids (e.g. *A. densa, A. triplex, A. primitiva, A. appressocamerata, A. soldadoensis, A. pseudotopilensis*) and morozovellids *(M. aragonensis, M. lensiformis).*

Calcareous nannofossils

Only the calcareous nannofossils of the Ermua section were studied in detail. While some samples were barren of any calcareous nannofossils, they are very rare to common in others. The preservation is usually poor, sometimes poor to moderate.

Zones NP9 and NP10: *Discoaster multiradiatus* is present from the lowermost studied sample on upwards thus indicating the presence of NP9, the *Discoaster multiradiatus* Zone of Martini (1971) in the lower part of the section (Tab. 1). A subdivision of NP9 has been suggested by various authors based on the first occurrence (FO) of *Campylosphaera dela* or the FO of *Rhomboaster sp.* This subdivision can only be applied in assemblages with a better preservation than the one observed in the present material.

The base of NP10, the *Rhomboaster bramlettei* Zone of Martini (1971), is defined by the FO of the namegiving species. In recent papers there has been an as of yet unresolved controversy about the correct determination and generic assignment – *Rhomboaster* or *Tribrachiatus* – of this species.

Representatives of *Rhomboaster/Tribrachiatus* were only found over a short part of the section (Tab. 1) and include *Rhomboaster* sp., *R. cuspis, R. bramlettei* and *R. spineus. Fasciculithus sidereus,* a species which has its last occurrence (LO) in the basal part of NP10 according to Bybell & Self-Trail (1995), was found by these authors and also at Ermua to overlap with *Rhomboaster bramlettei* and *R. spineus.* Bybell & Self-Trail (1995) have lumped together *R. cuspis* and other species of *Rhomboaster* into an enlarged *R. bramlettei,* thus lowering the base of NP10 below the level where authors separating *R. cuspis* and *R. bramlettei* would place it. *R. cuspis* usually appears before *R. bramlettei.* Wei & Zhong (1996) included some forms previously assigned to *R. bramlettei, R. calcitrapa, R. spineus* and *R. bitrifida* into the stratigraphically oldest species of the genus, *R. cuspis.* They assigned the remaining bramlettei to Tribrachiatus. Angori & Monechi (1996) included *R. cuspis, R. calcitrapa* and *R. bitrifida* in *R. bramlettei,* while retaining *R. spineus.* They then went on to register *R. bramlettei* with "short arms" (oldest), "long arms" and "var. T" (youngest), the latter appearing still before *R. contortus.* In conclusion, the lower boundary of NP10 is presently applied differently by different authors according to their concept of the defining species *R. bramlettei.*

Orue-Etxebarria et al. (1996) did not report *F. sidereus* from the Ermua section, but found other fasciculiths to overlap with *R. spineus* and *R. bramlettei* (their *Tribrachiatus nunnii*). The NP9/NP10 boundary is in this study placed at the first occurrence of *R. bramlettei,* following the original definition of the zonal boundary.

Aubry (1996) has subdivided NP10 based on the evolution of *Rhomboaster/Tribrachiatus.* This seems to be not applicable in the present section due to the scarcity or absence of *Rhomboaster* and *Tribrachiatus* respectively in the upper part of the section. Also the subdivision based on the FO of *Discoaster diastypus* could not be applied, since this species was not found in the scarce and poorly preserved assemblages available from that part of the section. It was, however, found by Orue-Etxe-

Samples	ER6	ER12	ER14	ER18	ER19	ER20	ER22	ER23	ER25	30,34,38	ER46	ER48	ER54	ER64	ER65	ER67	ER73	ER76	ER77	ER80	ER83	ER84	ER85	ER86	ER87	ER88	ER89
Abundance	F			Fc	Fc	Fr	R	C		*		X	X	C	R	F	F	F	*		F	R	R	X	X	X	X
Preservation	P			Pm	P	P	vP	Pm		*		vP	vP	Pm	Pm	Mp	P	Mp	*		Pm	P	P	P	vP	P	P
Biantolithus sparsus																				R							
Braarudosphaera bigelowii								X															R				
Campylosphaera (eo)dela																					R						
Chiasmolithus cf. C. bidens				X																							
Chiasmolithus cf. C. gigas									X																		
Coccolithus crassus				X				X	X					X								X					
Coccolithus eopelagicus					R				X						X											X	X
Coccolithus pelagicus	F		F	R	F	R	R	X	X		X	X	X	R	R	F	X	F			F	R	R		X	X	X
Cruciplacolithus primus								?													R						
Cruciplacolithus sp. 10µ																					R						
Cyclagelosphaera margerelii	?		?	?				?																?			
Chiasmolithus sp.			R																								
Discoaster delicatus (4-8µ)				X										X		X	X										
Discoaster falcatus				?										X													
Discoaster lenticularis																					R				?		
Discoaster megastypus								?																			
Discoaster mohleri														X			?	?		R	R						
Discoaster multiradiatus	?		?	R	R	X	X	X	X				?	R	R	X	X	X		R	R		R			X	
Ellipsolithus? sp. "bisectus"				X				X									X					X					
Ellipsolithus sp.						X												X									
Ericsonia sp. (round)															X		X										
Fasciculithus clinatus																				R							
Fasciculithus involutus				X				X						X				X									
Fasciculiths cf. F. involutus	R																										
Fasciculithus lillianae	R			?												X											
Fasciculithus sidereus														X													
Fasciculithus tonii/rich.?			R					X																			
Fasciculithus tympaniformis	R				R	X	X	X	X																		
Fasciculithus sp.			R		R	X	X	X	X					R			X			R		X					
Fasciculithus/Sphenoliths? sp.								X						X													
Heliolithus?. sp.								X																			
Micrantolithus sp.																						X					
Neochiastozygus cearae																?		?			R						
Neochiastus concinnus								X																			
Neochiastozygus distentus			R	X										X							R				?		
Neochiastozygus c.f N. perfectus									X						X						R						
Placozygus sigmoides														X	X												
Pontosphaera rimosa																					R						
Prinsius bisulcus					R			R													R						
Prinsius tenuiculus	R																										
Prinsius sp. round 5µ					R																						
Rhomboaster/Bianthollthus? sp.											X																
Rhomboaster bramlettei														X		X	?	X									
Rhomboaster cuspis													X	F	X	X		X									
Rhomboaster spineus														X		X											
Rhomboaster sp.																				R							
Scapholithus rhombicus			R																								
Semihololithus biskayae	F	F	F		Fc	X	X	F													R	X	R				
Semihololithus cf. S. kerabyi			R	X	R			R													R						
Sphenolithus anarrhopus																				R							
Sphenolithus sp.	R			R	R	R	X	X	X					R		X	X	R		Rf	R	R	R		X	X	
Sullivania californica																	X										
Sullivania consuetus														X	X		X	X									
Sullivania "maxi" >15µ			R					X																			
Thoracosphaera sp.								X							X					R							
Toweius eminens				X				X	X									X		R							
Toweius magnicrassus									X																		
Toweius sp.	R	X	F					R							X		X				R	X	R		X	X	
Zygodiscus bramlettei																							R				
Zygrhablithus bijugatus						R			X												R	X					
Cretaceous (reworked): Arkhangelskiella cymbiformis																	X										
Cretaceous (reworked): Cribrosphaera ehrenbergii												X															
Cretaceous (reworked): Eiffellithus turriseiffelii									X																		
Cretaceous (reworked): Micula decussata								X	X		X	X		X						R							
Cretaceous (reworked): Prediscosphaera cretaceae														X													
Cretaceous (reworked): Watznaueria barnesae									X			X					X										
NP, Martini, 1971	**9**										**10**																

* = barren
X = present
R = rare
F = few
C = common
vP = very poor
P = poor
M = moderate

Tab. 1. Ermua section: Relative abundance, degree of preservation of calcareous nannofossils.

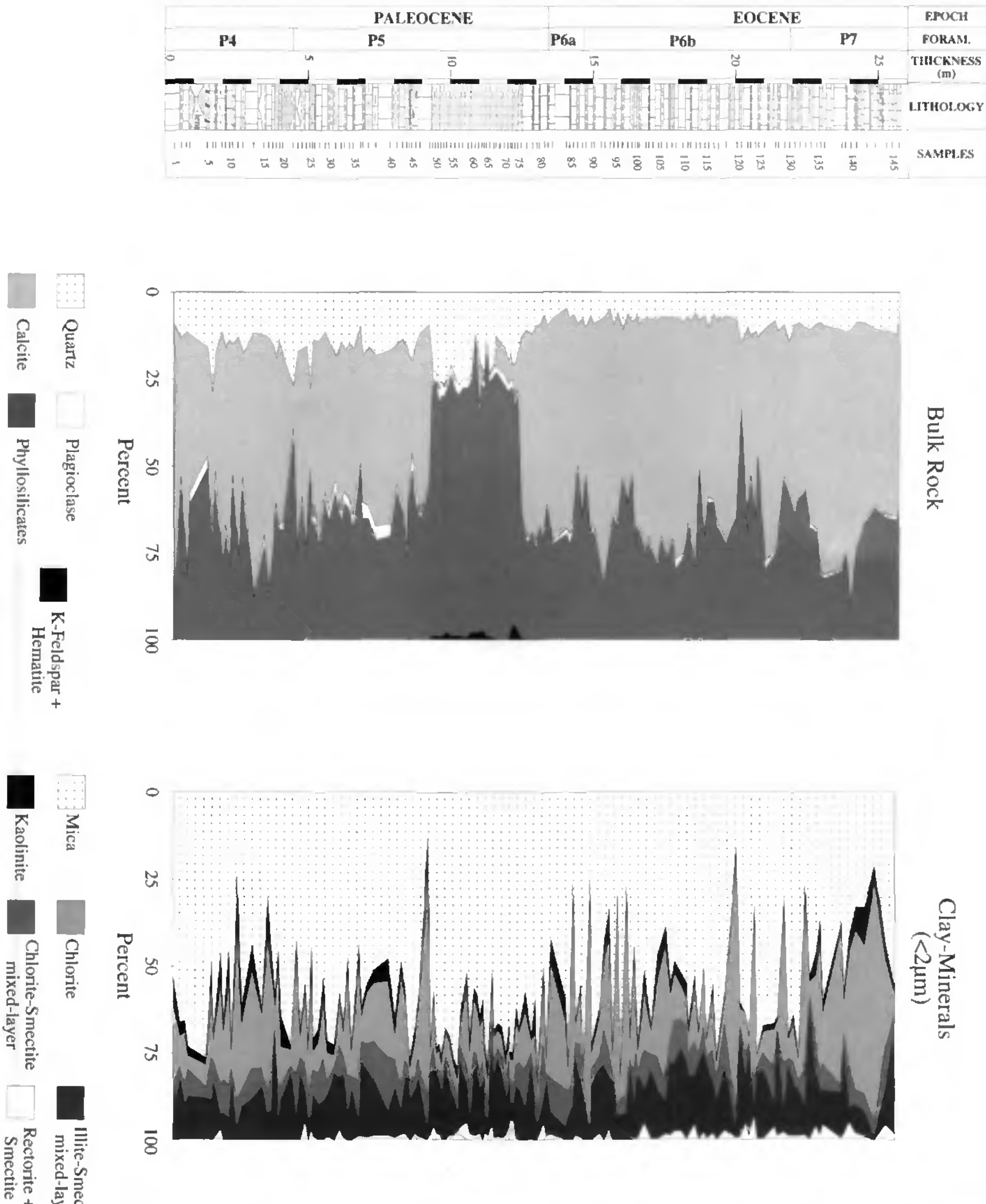

Fig. 3. Mineralogical Composition (Bulk Rock and Clay-Minerals, fraction <2µm) across the Paleocene-Eocene (P/E) transition, Trabakua, Spain.

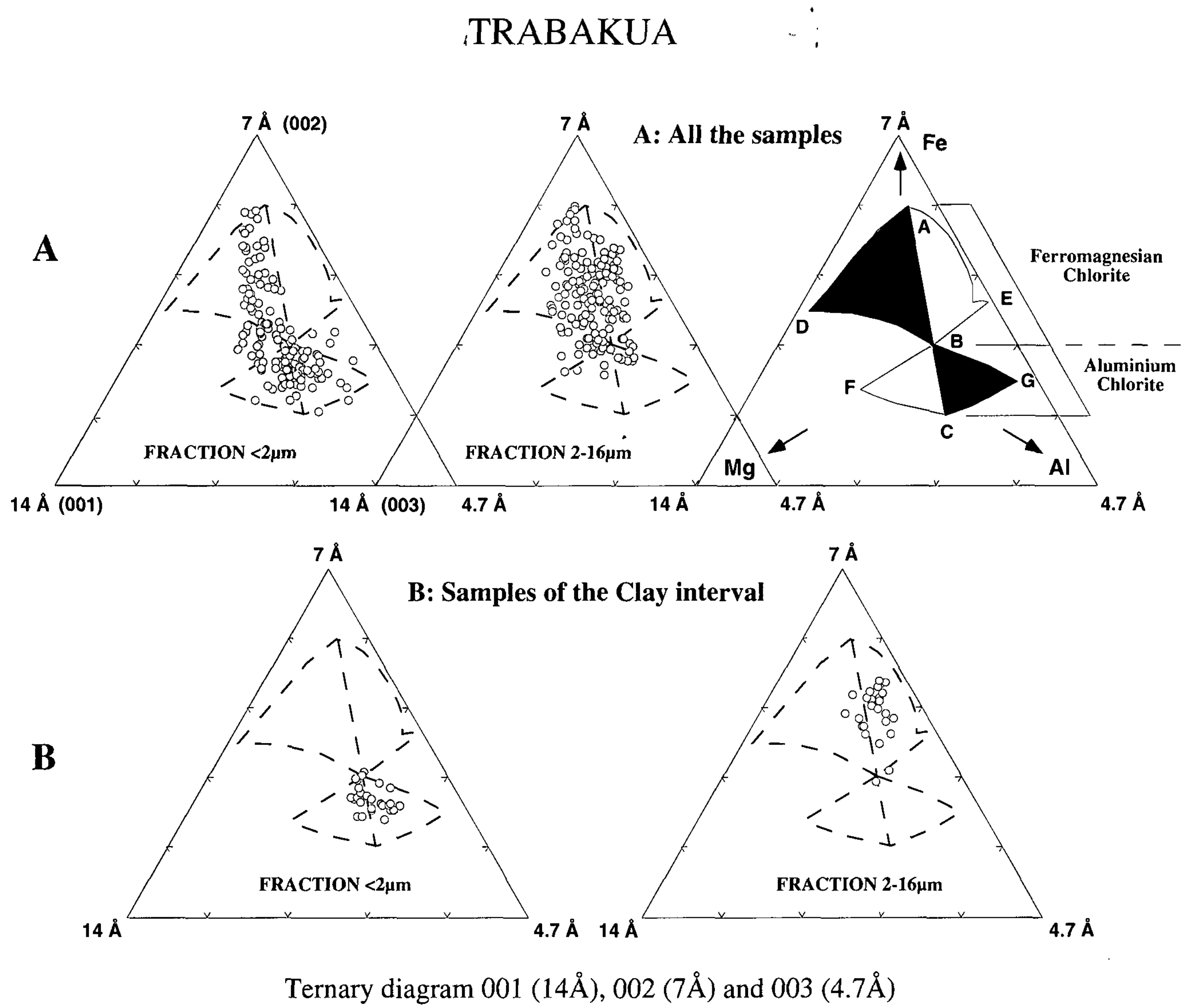

Fig. 4. Chemical nature of chlorite, Trabakua, Spain.
Ternary diagramm after Oinuma, Shimoda & Sudo, 1972.
Field ABDE indicates ferromagnesian chlorites. Field ABD = Iron excess in silicate layers. Field ABE = Iron excess in hydroxyl layers. Field BFCG indicates aluminium chlorites. Field BCG = Aluminium excess in silicate layers. Field BCF = aluminium excess in hydroxyl layers.

barria et al. (1996) who had samples also from higher up in the section.

Reworked Cretaceous coccoliths are very rare and include only relatively solution resistant forms (Tab. 1).

Mineralogy

Trabakua Pass section

Bulk rock analyses of the Trabakua Pass section indicate that calcite is the dominant component in the limestone-marl sequence between 0 to 9.3 m, with a mean value of 48% (Fig. 3). In the upper more massive limestone-marl sequence, between 12.3 and 25.75 m, calcite averages 58%. The 3 m thick interval of green/reddish clay (9.3 to 12.3 m) is marked by an abrupt decrease in calcite to 2%. The dramatic decrease in calcite coincides with a corresponding increase in phyllosilicates, from an average of 32–34% above and below the clay layer to an average of 75% and a maximum of 83%.

Detrital minerals are a minor component of the sediments and include primarily quartz, some plagioclase and K-feldspar. Quartz averages 17% below the clay layer and 11% above it. Within the clay layer, quartz content increases to 25% in the lower half and decreases to an average of 17% in the upper half of the clay interval. Plagioclase and K-feldspar reach 3% and 1% respectively in this interval. Hematite, a strong coloring agent, has been observed in the reddish layers of the clay interval and may be responsible for the color. Under oxidizing conditions, this mineral forms at neutral to high pH (Velde 1995).

These mineralogical changes across the clay layer probably indicate a decrease in the primary productivity of carbonates and variations in sediment sources and/or oceanic currents.

The composition of the clay mineral association (< 2 µm fraction) varies strongly throughout the section with mica as the dominant mineral, averaging 55% to 57%. In the clay layer, mica increases to 67% (Fig. 3). Chlorite is present throughout the section with an average of 19%, but decreases in the clay interval to 9%. Kaolinite averages 3.5% (0 to 11%) and is a minor component. Mixed-layer illite-smectite (IS) and chlorite-smectite (CS) contents have mean values of 14% and 7% respectively. Smectite and rectorite contents are very low (< 1%). The clay mineral distributions of the clay interval are thus not significantly distinct from those in the rest of the section. Only a slight increase in mica and decrease in chlorite can be observed.

The chemical composition of chlorite is shown in ternary diagrams (Fig. 4 after Oinuma et al. 1972) where the poles 14Å, 7Å and 4.7Å indicate magnesian, iron and aluminium respectively. The chemical nature of chlorite within the clay interval depends on the grain size. Chlorite is aluminous in the fraction < 2 µm and ferromagnesian in the fraction 2–16 µm. The ferromagnesian chlorite in the fraction < 2 µm is restricted to the field ABD which shows an iron excess in the chlorite's silicate layers. Two generations of chlorite can be observed, a ferromagnesian and an aluminous generation which have two origins, the first more important one detrital and the second one diagenetic. Magnesium and iron released during the transformation of smectite to illite could favor the formation of diagenetic chlorite (Hower et al. 1976). Kaolinite is also a potential source of Al and Si for aluminous chlorite formation during burial diagenesis (e.g. Muffler & White 1969; Perry & Hower 1970; Boles & Francks 1979).

Clay minerals generally reflect climatic conditions. For example, high abundance of kaolinite indicates warm, or humid climates, well-drained continental areas with high precipitation and accelerated leaching of parent rocks (Millot 1970; Chamley 1989; Weaver 1989). Increased chlorite and mica contents indicate cold or arid (desert) conditions with active mechanical erosion (Millot 1970). However, post-depositional diagenetic alteration may obliterate or obscure the climate signal.

For example in the Trabakua section, the near absence of smectite and the low kaolinite content (< 4%) are not linked to climatic conditions, nor to a particular depositional environment, but to a diagenetic overprint. This is suggested by the presence of diagenetic chlorite, mixed-layers chlorite/smectite and illite-smectite, the near absence of smectite, rectorite and kaolinite. The clay mineral contents of the Trabakua Pass sediments thus indicate deep burial diagenesis that corresponds approximately to the end of zone 3 of Kübler et al. (1979). In contrast, the Zumaya section, located in the Basque basin about 30 kilometers to the north-east, in a similar sedimentary environment, has retained the climatic signals. In this section, during the Paleocene-Eocene transition, the clay mineral composition consists of mica, mixed-layers illite-smectite, chlorite and large amounts of smectite and kaolinite (Adatte et al. 1995). The presence of smectite and the increase in chlorite and mica during the P-E transition suggest arid conditions in the adjacent continental areas where kaolinite is absent. Kaolinite would probably have been transported from lower latitude by oceanic currents.

Ermua section

Bulk rock composition of the Ermua section shows high variability (Fig. 5). In the lower part of the section (0 to 16 m) calcite is the dominant component in the hemipelagic marls and the carbonate turbidites with a mean value of 42% and 31% respectively. In the upper more massive carbonate turbidite sequence between 41 to 46 m, calcite averages 49%. Between these lithologies (16 to 41 m), calcite content decreases drastically with a mean value of 4% in hemipelagic marls and 21% in calcarenites. This decrease coincides with an increase in phyllosilicates in the hemipelagic marls, from an average of 36% below the middle part of the section (16 to 41 m) to an average of 67%. In the calcarenites, the phyllosilicates increase also from a mean value of 21% to 57%. In the upper massive limestone, the phyllosilicate content reaches an average of 35%. Detrital minerals are a minor component of the sediments and include primarily quartz, some plagioclase and K-feldspar. Below 16 m, quartz averages in the hemipelagic marls and in the calcarenites 17% and 36% respectively. Above 41 m quartz reaches a mean value of 11%. Between 16 m and 41 m, the proportion of quartz in the calcarenites decreases to a mean value of 17% and increases in the hemipelagic marls to an average of 25%. Plagioclase and K-feldspar are minor throughout the section with a mean value < 6% and < 1% respectively. Pyrite, goethite and apatite (phosphate) have been observed in the sandstones between 25 m and 39 m indicating a low oxygen environmental deposit.

Clay mineral contents also are variable throughout the section. In the lower part of the section (between 0 and 16 m) (Fig. 5) mica is the dominant mineral averaging 63 and 57% in hemipelagic marls and in calcarenites respectively. In the middle part (16–41 m) mica decreases with a mean value of 27% in calcarenites and 51% in marls. In the upper more massive limestones (41 to 46 m) mica increases to an average of 43%. The decrease in mica coincides with an increase in chlorite

Fig. 5. Mineralogical composition (Bulk Rock and Clay Minerals, fraction < 2 µm), Ermua, Spain.

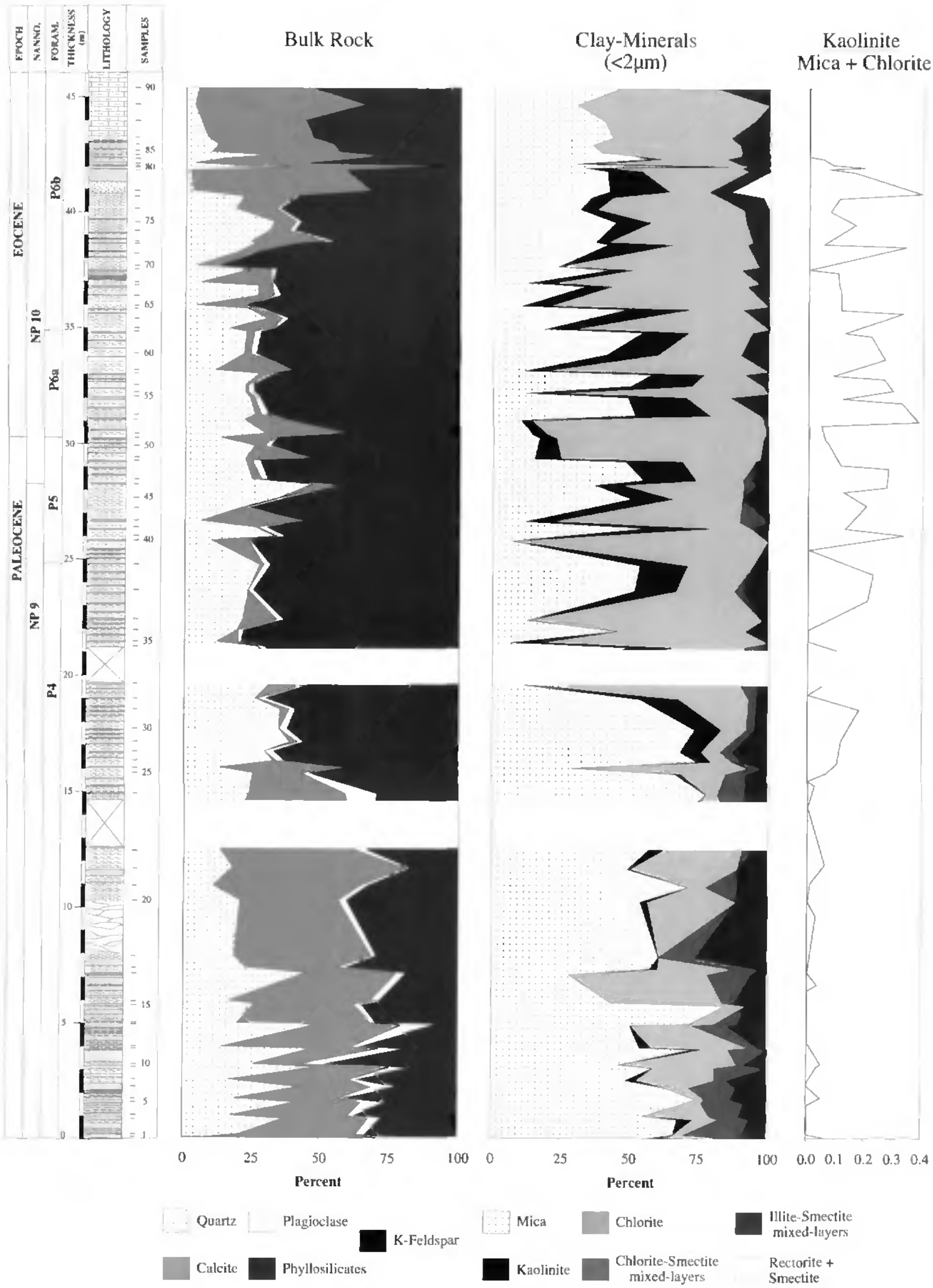

EPOCH
NANNO.
FORAM.
THICKNESS (m)
LITHOLOGY
SAMPLES
EOCENE
PALEOCENE
NP 10
NP 9
P6b
P6a
P5
P4
Bulk Rock
Clay-Minerals (<2μm)
Kaolinite
Mica + Chlorite
Percent
Percent
Quartz
Plagioclase
K-Feldspar
Calcite
Phyllosilicates
Mica
Chlorite
Illite-Smectite mixed-layers
Kaolinite
Chlorite-Smectite mixed-layers
Rectorite + Smectite

from an average of 17% to 74% in the calcarenites. In the hemipelagic marls, chlorite increases only from 22 to 26%. In the upper limestones (41 to 46 m), chlorite reaches a mean value of 40%. Kaolinite is a minor component in the sediments with a mean value < 2% between 0 and 16 m, an average of 14% and 6% in hemipelagic marls and calcarenites respectively between 16 m and 41 m, and a mean value of 3% in the last 5 meters. Mixed-layer illite-smectite (IS) contents have a mean value of 10% in the hemipelagic marls throughout the section. In the calcarenites (0 to 16 m), the IS content attains an average of 6% and decreases to 2% between 16 m and 41 m. Mixed-layer chlorite-smectite (CS) shows a mean value of 17% in the calcarenites and 7% in the hemipelagic marls between 0 and 16 m. In the middle part the CS content decreases to an average of 1% in the two lithologies. The upper, more calcareous sediments are marked by the absence of CS and by an IS content with a mean value of 9%.

Major changes were observed in the interval between 16 m and 41 m which is marked in the hemipelagic marls by an increase in kaolinite and chlorite and an important decrease in mica. In the calcarenites of this interval, mica and IS decrease whereas chlorite and kaolinite increase. The relatively high amount of kaolinite in the interval between 16 and 43 m suggests that the sediments are less affected by burial diagenesis and/or tectonic activity than in the Trabakua Pass section. In the Ermua section clay minerals retain therefore climatic signals. Chlorite and mica indicate cold or arid (desert) conditions with active mechanical erosion. In contrast kaolinite typically develops in tropical soils on poorly drained surfaces with high precipitation. The joint increase of chlorite and kaolinite between 16 m and 41 m and the higher content of kaolinite in hemipelagic marls compared to calcarenites imply different sources characterized by opposite climatic conditions and different ways of transport. Therefore, these mixed associations suggest that arid conditions prevailed in the adjacent coastal area whereas kaolinite was brought from lower latitudes by oceanic currents.

Stable isotopes

Trabakua Pass section

Bulk rock carbonate was analyzed for $\delta\,^{13}C$ and $\delta\,^{18}O$ isotopes in the interval between 3 m and 20 m at the Trabakua Pass section (Fig. 6 and Tab. 2).

In sediments of the Trabakua section, carbonates are affected by recrystallization/diagenesis which obscure, alter or obliterate the $\delta\,^{18}O$ signals, but not the $\delta\,^{13}C$ signals. Early diagenetic alteration of carbonate $\delta\,^{18}O$ and $\delta\,^{13}C$ of the K/T and early Paleocene sediments in the Negev of Israel has been studied by Magaritz et al. (1992). By comparing the isotopic values from whole-rock and two fine fractions, these authors concluded that $\delta\,^{13}C$ signals were not significantly altered, whereas $\delta\,^{18}O$ signals were strongly affected by meteoric water during early diagenesis. Dissolution and recrystallization often

Tab. 2. Trabakua section: Analyses of stable isotopes ($\delta\,^{13}C$ and $\delta\,^{18}O$), total carbon and calcite.

Samples	δ 13 C	δ 18 O	Total Carbon	Calcite
	(‰)		(%)	
TB14	2,54	-4,45		75,98
TB19	2,52	-4,62	7,50	53,90
TB28	2,00	-4,63	7,12	56,49
TB34	1,68	-4,67	6,39	45,36
TB38	1,88	-4,73	6,10	45,95
TB40	1,69	-4,72	6,28	49,99
TB41	1,46	-4,99	4,99	40,08
TB42	1,87	-3,92	6,63	48,12
TB43	1,42	-4,80	5,87	57,61
TB44	1,06	-4,84	4,32	39,03
TB45	0,71	-4,66	2,77	26,32
TB46	0,92	-4,58	5,06	41,28
TB62	-0,59	-4,57	0,70	12,99
TB72	-1,14	-4,20	1,05	8,04
TB74	-1,42	-4,56	1,04	10,17
TB75	-1,00	-4,62	1,36	10,89
TB76	0,32	-4,75	6,01	47,87
TB77	0,85	-4,67	8,13	60,09
TB78	0,67	-4,45	6,74	56,99
TB79	1,03	-4,66	8,66	63,08
TB80	0,69	-4,40	7,17	57,76
TB81	1,04	-4,63	9,45	63,50
TB85	0,97	-4,48	7,72	62,00
TB90	1,27	-4,65		62,37
TB95	0,84	-4,47	6,07	57,37

do not significantly influence the magnitude of the $\delta\,^{13}C$ shift in deep sea sequences whereas the primary oxygen isotope is overprinted by diagenesis (Veizer 1983). $\delta\,^{18}O$ values are very negative (–3.8 to –4.9 ‰) and constant throughout the Trabakua section, thus indicating secondary recrystallization or alteration by meteoric water.

Below the clay layer, between 3 m to 9.3 m, $\delta\,^{13}C$ values gradually decrease from 2.5 to 0.95 ‰. A similar decrease preceding the clay layer was also observed at Alamedilla, Spain (Lu et al. 1996, Fig. 12). Within the clay layer $\delta\,^{13}C$ values decrease by 1.4‰ and reach minimum values (– 1.4‰) between 12.15 and 12.45 m. The absence of $\delta\,^{13}C$ data in the lower part of the clay layer is due to the very low carbonate content (<2%). Between 12.45 m and 12.5 m, $\delta\,^{13}C$ values rapidly increase by 1.3‰. Above this interval (12.65 m), bulk $\delta\,^{13}C$ values gradually increase (0.8 to 1.2‰).

Bulk $\delta\,^{13}C$ values correlate well with the carbonate curve (Fig. 6). In both datasets, there is a gradual decrease below the clay layer, an abrupt decrease within, and a gradual increase above it.

Fig. 6. Stable isotopic changes ($\delta\,^{13}C$ and $\delta\,^{18}O$) across the Paleocene-Eocene transition, correlated with Organic Matter, Total Carbon and Calcite variations, Trabakua, Spain.

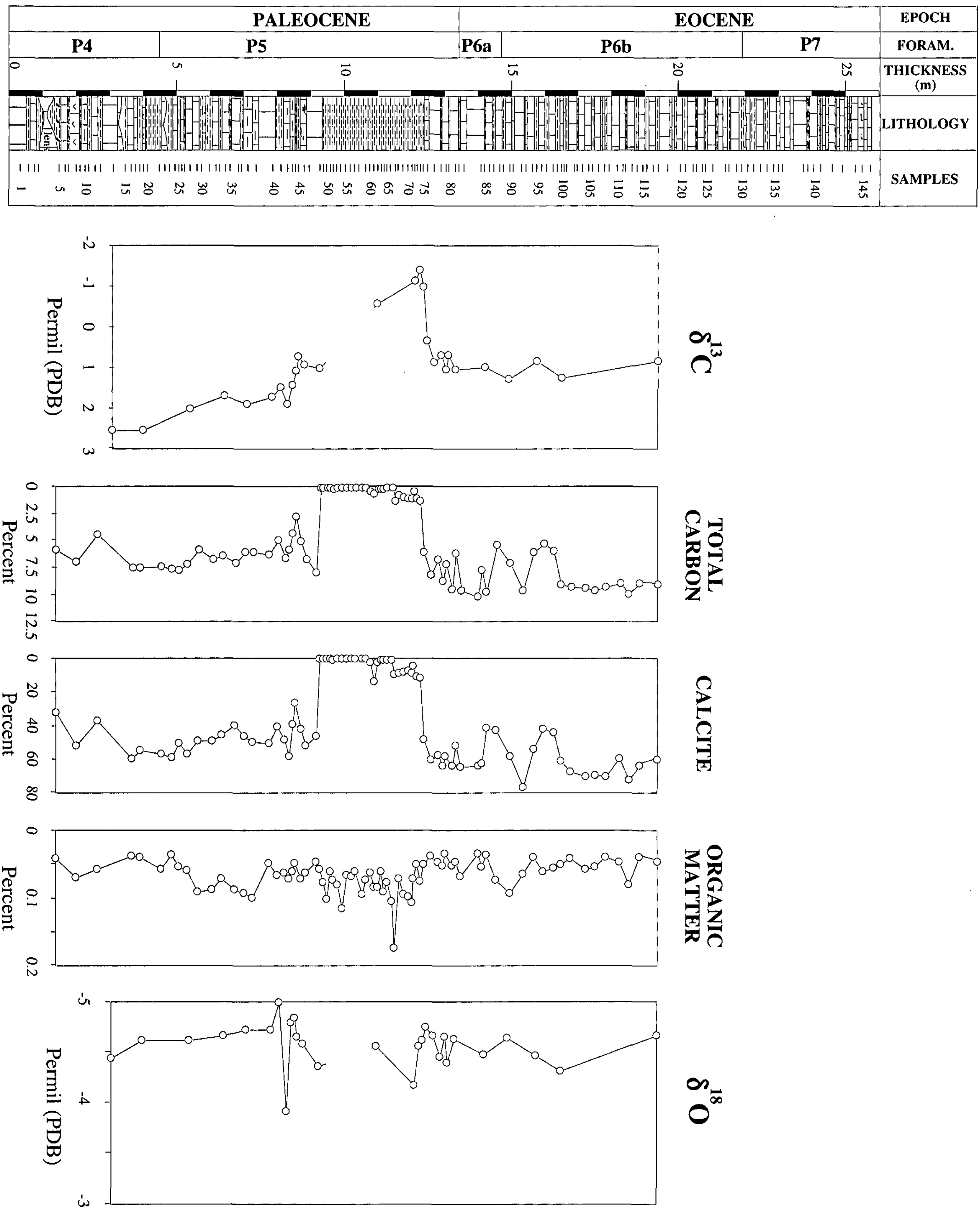
PALEOCENE
EOCENE
EPOCH
P4
P5
P6a
P6b
P7
FORAM.
THICKNESS (m)
LITHOLOGY
SAMPLES
Permil (PDB)
$\delta^{13}C$
Percent
TOTAL CARBON
Percent
CALCITE
Percent
ORGANIC MATTER
Permil (PDB)
$\delta^{18}O$

Ermua section

Bulk rock carbonate was analyzed for $\delta\,^{13}C$ and $\delta\,^{18}O$ isotopes in hemipelagic marls between 0.2 m and 44 m in the Ermua section (Fig. 7 and Tab. 3) in order to determine the presence of a $\delta\,^{13}C$ shift correlative with the clay layer at Trabakua. Unfortunately, relatively few samples are rich in calcite and hence isotopic data are of low sample resolution and low reliability in some samples. However, the following trends can be tentatively determined. Between 0 and 15 m where calcite averages 40% $\delta\,^{13}C$ values gradually decrease from 1.4 to 0.6‰. Between 16 and 41 m, where calcite is nearly zero (< 2%) $\delta\,^{13}C$ values are very low with an average of – 2.6‰. These very low values of $\delta\,^{13}C$ may be explained by the presence of lithologies very poor in carbonates but enriched in organic matter. In the limestone interval at the top of the section $\delta\,^{13}C$ values increase from – 0.6 to 0.9‰.

At Ermua, the negative $\delta\,^{13}C$ excursion occurs in the middle part of the Zone P4 contrary to the carbon–13 isotopic excursion in the upper part of P5 in the Trabakua section within a carbonate-poor clay layer. The two negative $\delta\,^{13}C$ excursion are thus not correlatable and cannot be used as chronostratigraphic markers.

As in the Trabakua section, oxygen isotope values (–4.6 to –5.7‰) reflect diagenetic alteration rather than original paleotemperatures.

Tab. 3. Ermua section: Analyses of stable isotopes ($\delta^{13}C$ and $\delta^{18}O$), total carbon, organic matter and calcite.

Samples	δ 13 C (‰)	δ 18 O (‰)	Total Carbon (%)	Organic Matter (%)	Calcite (%)
ER2	1,45	-4,36	5,06	0,20	43,09
ER6	1,09	-4,30	4,43	0,22	38,07
ER14	1,18	-4,57	5,80	0,12	49,16
ER19	0,89	-4,54			50,24
ER20	0,78	-4,68	4,01	0,14	36,23
ER22	0,70	-4,50	7,19	0,11	62,88
ER23	0,60	-4,73			49,53
ER25	-2,82	-5,39	2,46	0,11	17,91
ER40	-2,58	-5,01	6,79	0,19	13,52
ER49	-2,67	-5,11	6,14	0,11	24,49
ER65	-2,06	-5,09	9,81	0,14	18,23
ER76	-2,43	-5,13			14,54
ER77	-2,94	-5,66	2,36	0,20	18,39
ER79	0,81	-4,75	11,65	0,06	57,08
ER84	-0,64	-5,59			40,77
ER85	0,16	-4,57	8,10	0,08	47,16
ER86	0,51	-4,60			40,90
ER87	0,63	-4,87	10,44	0,10	38,21
ER88	0,86	-4,32			37,45

Organic matter

Trabakua sediments are extremely poor in organic matter (< 0.10%): below 0.1% values are considered background noise (Fig. 6). Only one sample within the clay layer reaches 0.197%. Ermua sediments have a relatively higher organic content (Fig. 8), varying between 0.1 to 0.5%. In the hemipelagic marls between 20 m and 40 m organic matter increases from an average of 0.15% to 0.25% whereas in the calcarenites it attains a mean value of 0.1%.

Oxygenation at the sea floor is controlled by the input of organic matter (e.g. Calvert 1987), oxygen content of bottom water, and circulation intensity. The oxygen depletion results from oxidation of organic matter which sinks through the water column, or is transported laterally (Wetzel 1991). An oxygen-depleted environment favours the formation of reduced minerals like pyrite. The absence of organic matter at Trabakua prevents the development of reducing conditions and favours the formation of iron oxides like hematite, a mineral observed in the clay layer. In the Ermua section the presence of organic matter and of pyrite seem to indicate a more reducing environment than at Trabakua.

Grain size

Grain size analyses in the Trabakua Pass section indicate that an average of 44% of the grains are in the < 4 µm size fraction which includes < 1 µm, 1–2 µm and 2–4 µm size fractions (Fig. 8). However, in the clay interval an average of 52% is contained in the < 4 µm fraction. The larger fraction 4–8 µm averages 38% throughout the section. The coarser grain fractions (between 8 and 32 µm) average 16% between 0 and 9.25 m and 18% in the interval between 12.45 m and 25.7 m. The coarse fraction decreases to an average of 10% in the clay interval. The decrease in the grain size in the clay interval suggests changes in ocean currents and/or reduction in the intensity of atmospheric circulation.

Geochemistry

Trabakua Pass

Significant changes occur in the clay layer of the Trabakua Pass section in all major components (Fig. 9). For example, calcium averages a mean value of 23% and 27% below and above the clay interval respectively, but decreases to 3% within the clay layer (9.3 to 12.3 m). Strontium averages 0.05% except in the clay layer where values decrease to 0.002%. Manganese averages 0.09% above and below the clay layer, but

Fig. 7. Stable isotopic changes ($\delta\,^{13}C$ and $\delta\,^{18}O$) across the Paleocene-Eocene transition, correlated with Organic Matter, Total Carbon variations, Ermua, Spain.

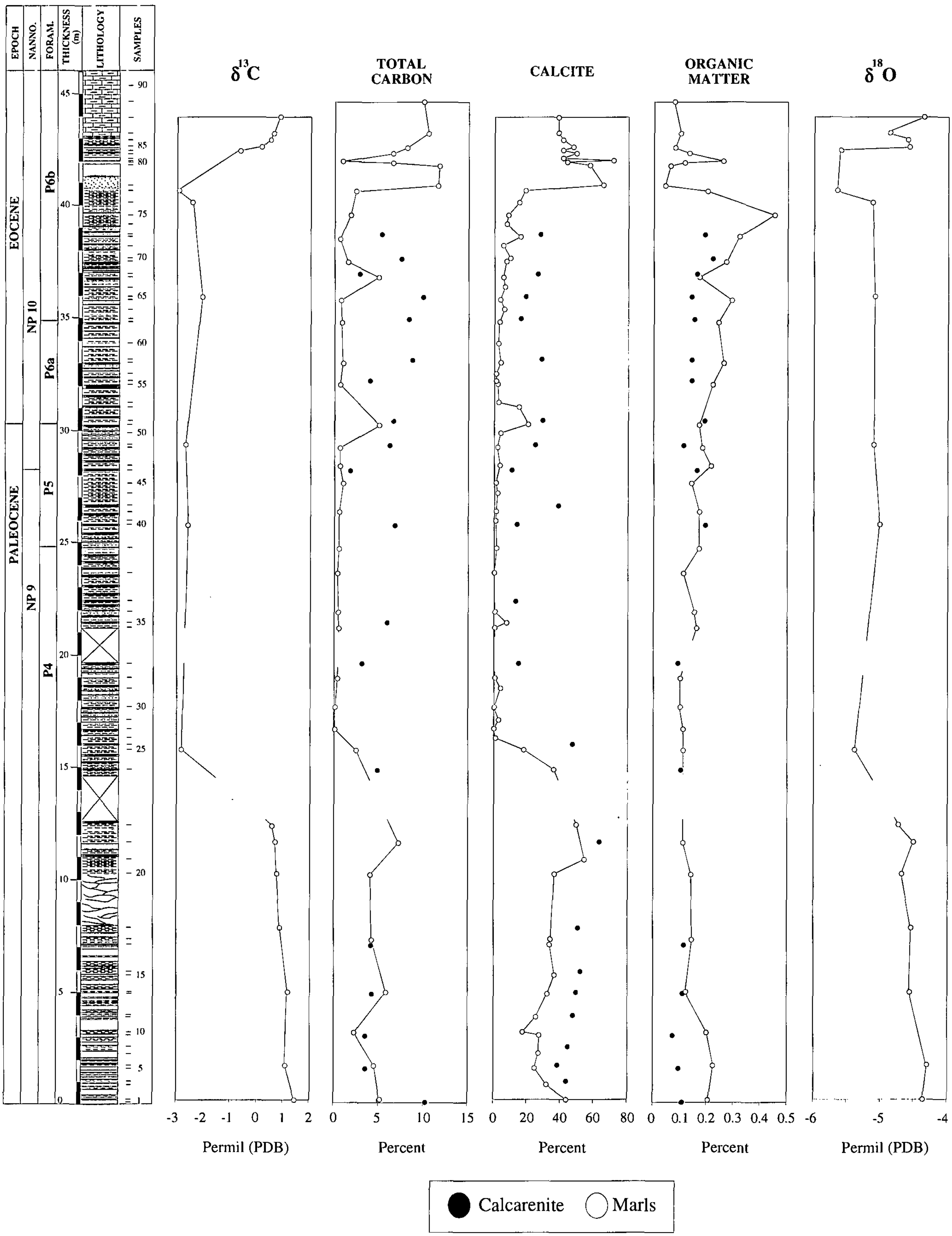

EPOCH
NANNO.
FORAM.
THICKNESS (m)
LITHOLOGY
SAMPLES
EOCENE
PALEOCENE
NP 10
NP 9
P6b
P6a
P5
P4
$\delta^{13}C$
TOTAL CARBON
CALCITE
ORGANIC MATTER
$\delta^{18}O$
Permil (PDB)
Percent
Percent
Percent
Permil (PDB)
Calcarenite
Marls

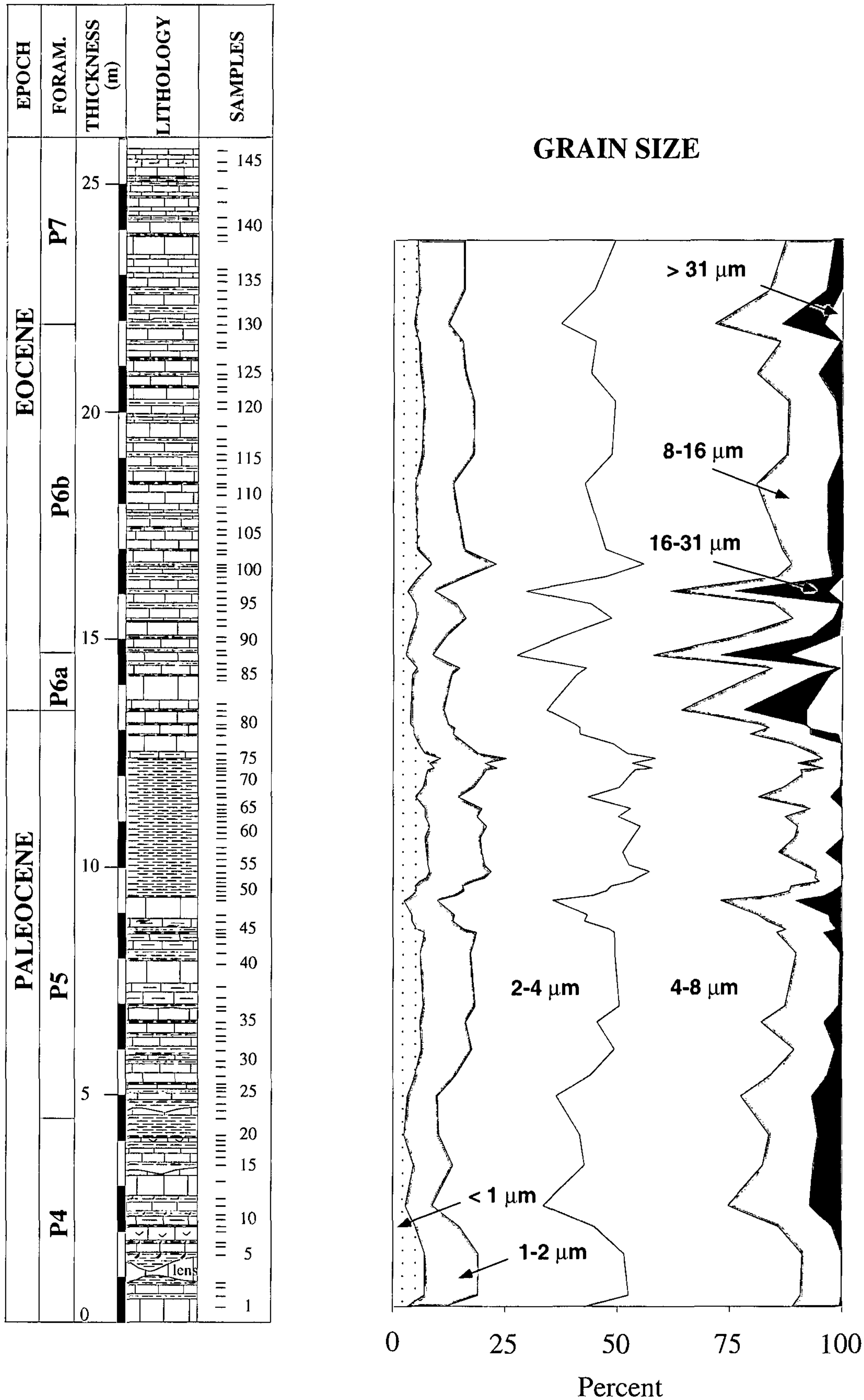
EPOCH
FORAM.
THICKNESS (m)
LITHOLOGY
SAMPLES
EOCENE
PALEOCENE
P7
P6b
P6a
P5
P4
0
5
10
15
20
25
1
5
10
15
20
25
30
35
40
45
50
55
60
65
70
75
80
85
90
95
100
105
110
115
120
125
130
135
140
145
lens
GRAIN SIZE
> 31 µm
8-16 µm
16-31 µm
2-4 µm
4-8 µm
< 1 µm
1-2 µm
0
25
50
75
100
Percent

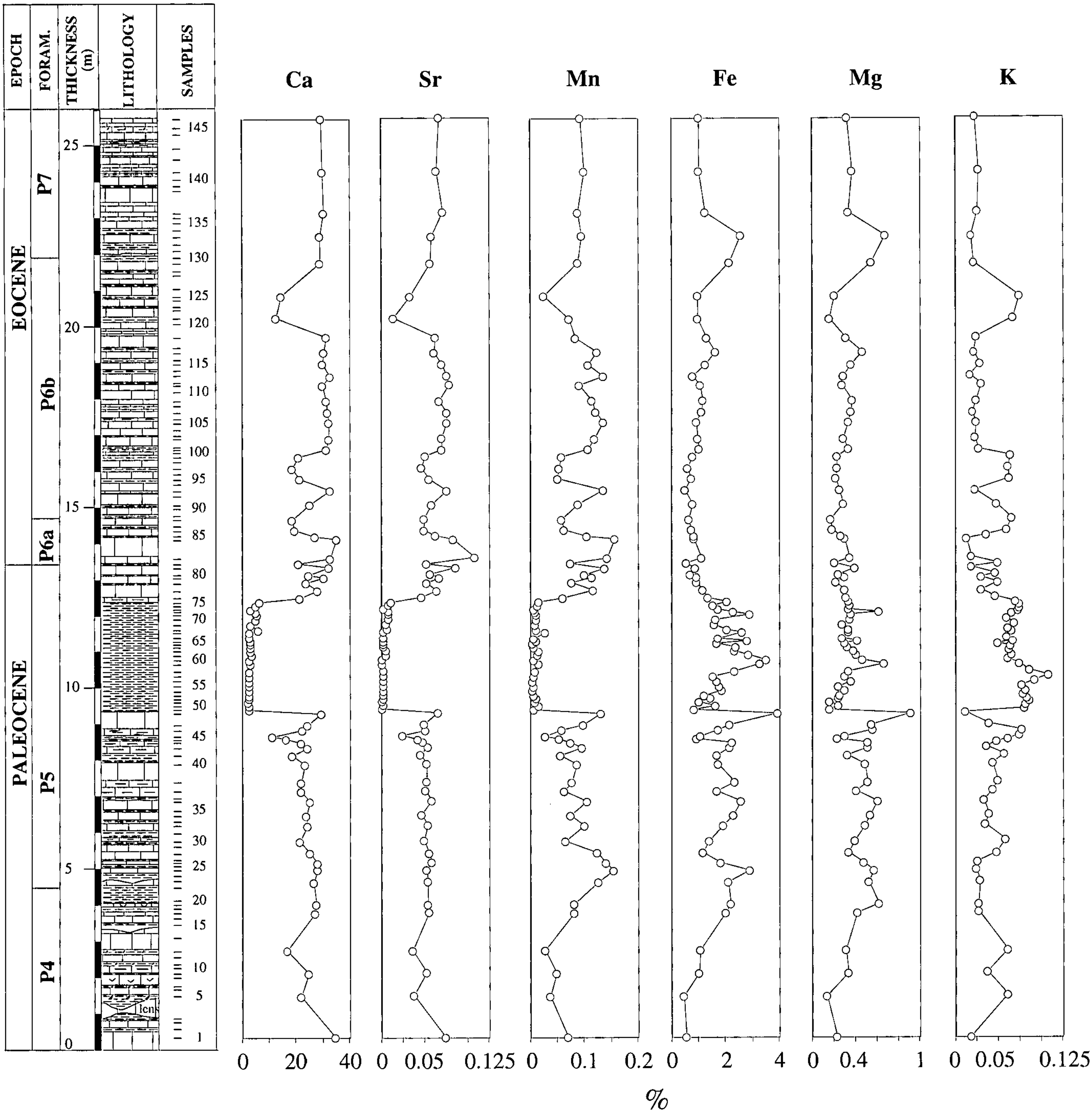

Fig. 9. Chemical elements: variations of Ca, Sr, Mn, Fe, Mg and K across the P/E transition, Trabakua, Spain.

Fig. 8. Grain size changes across the P/E transition, Trabakua, Spain.

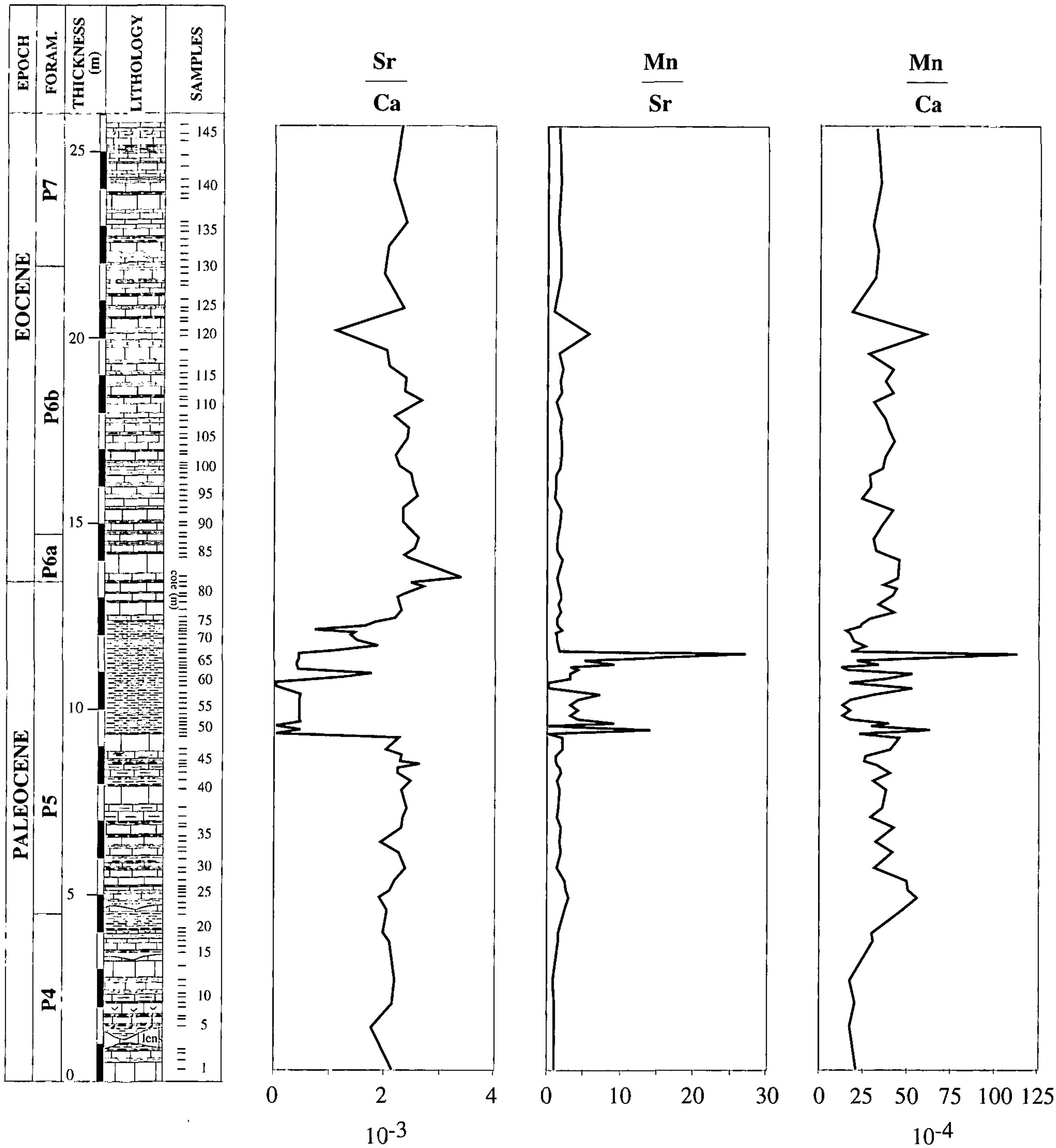

Fig. 10. Sr/Ca, Mn/Sr and Mn/Ca ratios across the P/E transition, Trabakua, Spain.

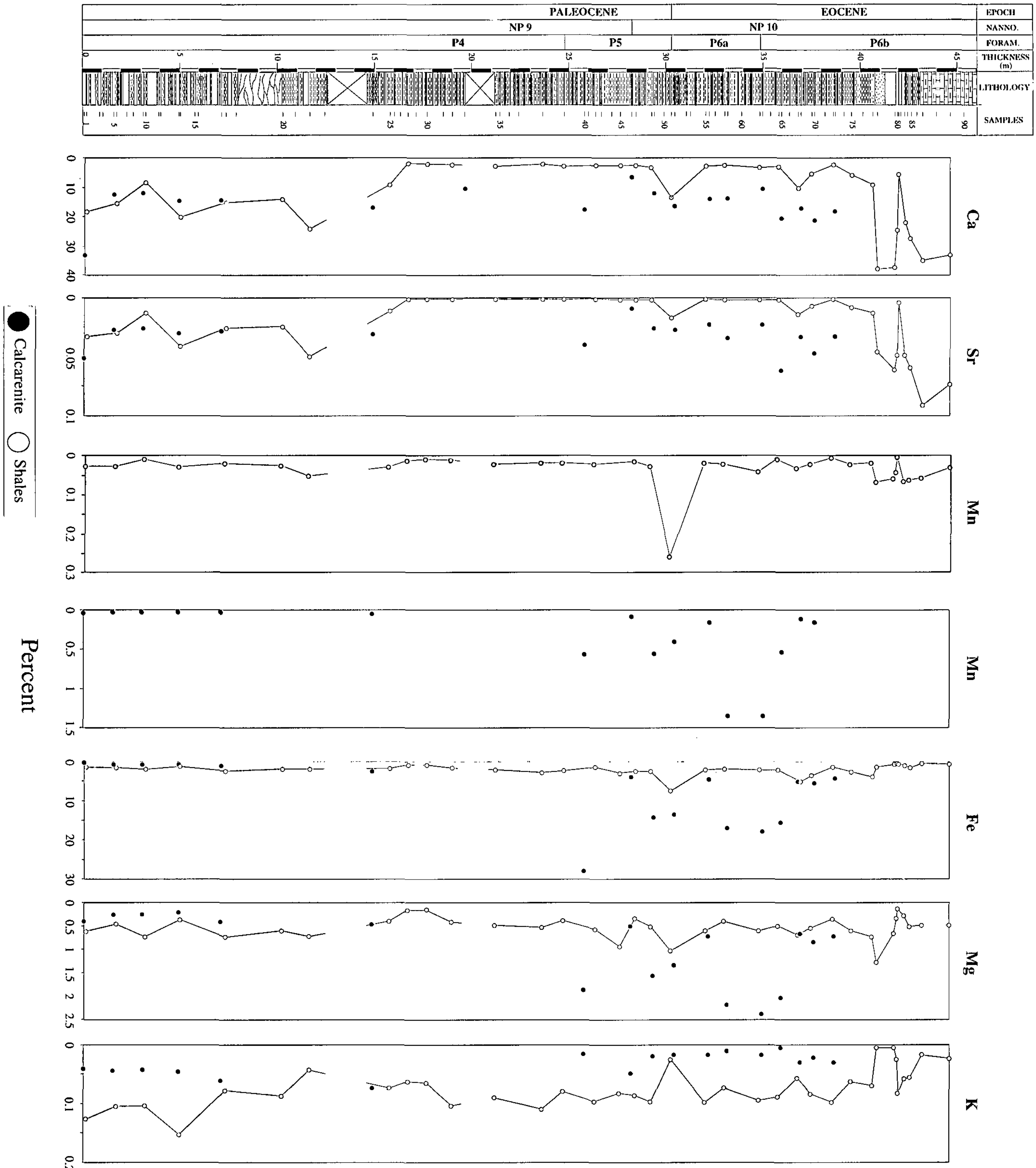

Fig. 11. Chemical elements: variations of Ca, Sr, Mn, Fe, Mg and K across the P/E transition, Ermua, Spain.

decreases to an average of 0.008% within it. Iron increases only slightly (1.8% to 2%) in the clay layer, and decreases to about 1% in the upper marl/limestone interval. Mg averages between 0 and 9.3 m 0.45% and decreases to 0.3% between 9.3 and 26 m. Potassium averages 0.04% except in the clay interval where it reaches 0.07%.

Thus, calcium, strontium and manganese have parallel trends with very low values (near zero) in the clay layer and higher though variable values above and below. Calcium is mainly present in limestone and a decrease to near zero in the clay layer coincides with the decrease in carbonates in this interval (9.3 to 12.3 m). Strontium co-precipitates frequently with aragonite and calcite (Handbook of Geochemistry 1978) and the parallel trend indicates that Sr is associated with calcium in the carbonate fraction. The higher Mn abundance in carbonate rocks is probably derived from diagenetic mobilization of Mn under reducing conditions. The decrease of Mn associated with the decrease of Ca and Sr in the clay interval may indicate significant changes in the reducing conditions during sediment deposition. The ratios of Mn/Sr and Mn/Ca which are very high in the clay interval (Fig. 10) indicate probably an increase of Mn during the Paleocene-Eocene transition. The origin of this manganese could be linked to the increase of the volcanic activity in the North Atlantic during this period (Ritchie & Hitchen 1996).

Magnesium is present in the sediments mainly in phyllosilicates, such as chlorite. The decrease in Mg in the clay layer corresponds to a decrease in chlorite as described in the discussion of the clay minerals (Fig. 3). Potassium in carbonate sediments is almost exclusively contained in the non-carbonate fraction. In the Trabakua Pass section, the K fraction is contained within the siliceous detritus that is present in marls and limestones above and below the clay layer. Within the clay layer, the K fraction is primarily a function of the clay mineral content and secondarily the amount of K-feldspar.

Detrital influx plays an important role in the supply of K, Mg and Fe to the ocean sediments. The increase of these elements across the Paleocene-Eocene transition is due to the increased detrital accumulation in this interval. Major changes in these minerals associated with clay deposition suggest changes in sediments source and/or oceanic circulation.

Ermua

Significant changes occur throughout the Ermua section in all major components (Fig. 11). In the calcarenites calcium and strontium values are very constant with respectively an average of 15% and 0.03% throughout the section. In the hemipelagic marls, calcium and strontium average between 0 m and 16 m respectively 16% and 0.03% and decrease drastically in the middle part (16 m to 41 m) with a mean value of 3% and 0.004% respectively. In the upper more massive limestone (41 to 46 m), calcium averages 25% whereas strontium reaches a mean value of 0.06%. Between 0 and 16 m, manganese averages 0.03% in the two lithologies but increases with a mean value of 0.49% only in the calcarenites between 16 m and 41 m. In the upper calcareous sequence, Mn has a mean value of 0.06%. Potassium decreases from an average of 0.05% below the middle part to an average of 0.02% in it in the calcarenites and from a mean value of 0.1% to 0.08% in the hemipelagic marls. Iron and magnesium average 0.54% and 2.4% respectively in the marls throughout the section. In the calcarenites Mg and Fe increase strongly between 25 m and 39 m from a mean value of 0.33% and 1% to 1.3% and 11% respectively. In the upper massive limestone, K, Mg and Fe reach an average of 0.03%, 0.57% and 0.94% respectively.

Thus, calcium, strontium and manganese have parallel trends in the hemipelagic marls with very low values between 16 m and 41 m and higher though variable values above and below. Calcium decreases to 2% in the middle part coinciding with the decrease in carbonates in this interval (16 m to 41 m). Strontium is associated with calcium in the carbonate fraction and manganese is one of the few minor elements which is more abundant in carbonates than in the detrital fraction.

The calcarenites seem not affected by the decrease of the carbonate sedimentation observed in the marls. Between 25 m and 39 m Fe and Mg increase strongly in the sandstones. The presence of pyrite and goethite described in the bulk rock analyses and the presence of low oxygen tolerant benthic foraminifera indicate low-oxygen environment and explain the very high content of iron. High magnesium content is linked to the increase of chlorite described in clay minerals (Fig. 4) during this interval and its origin is detrital.

Discussion

The P/E transition is globally characterized by a mass extinction in benthic foraminifera, diversification in planktic foraminifera, an abrupt negative $\delta^{13}C$ excursion, a decrease in calcite, an increase in detrital minerals and negative anomalies in Sr and Mn, all of which are present also in the Trabakua section. Moreover, the Trabakua clay layer is more expanded than in deep-sea sections where this interval is concentrated in a few to a few tens of centimeters, However, this interval seems still to be condensed at Trabakua as suggested by the presence of glauconite. Isotopic, geochemical and mineralogical bulk rock analyses of the P-E transition at Trabakua give similar results as those obtained at Caravaca and Alamedilla, located in the Tethyan Realm (Fig. 12). At the coeval Ermua section, these characteristic trends can not be identified (Fig. 12). The turbiditic sedimentation with its low content of carbo-

Fig. 12. Biostratigraphic correlation between Trabakua and Ermua, Atlantic realm and Alamedilla and Caravaca, Tethyan realm. Correlations are based on planktic foraminiferal datum events. The shaded interval corresponds to the carbon-13 isotopic excursion. The Alamedilla data are from Lu et al. (1996). The Caravaca data are from Ortiz (1996).

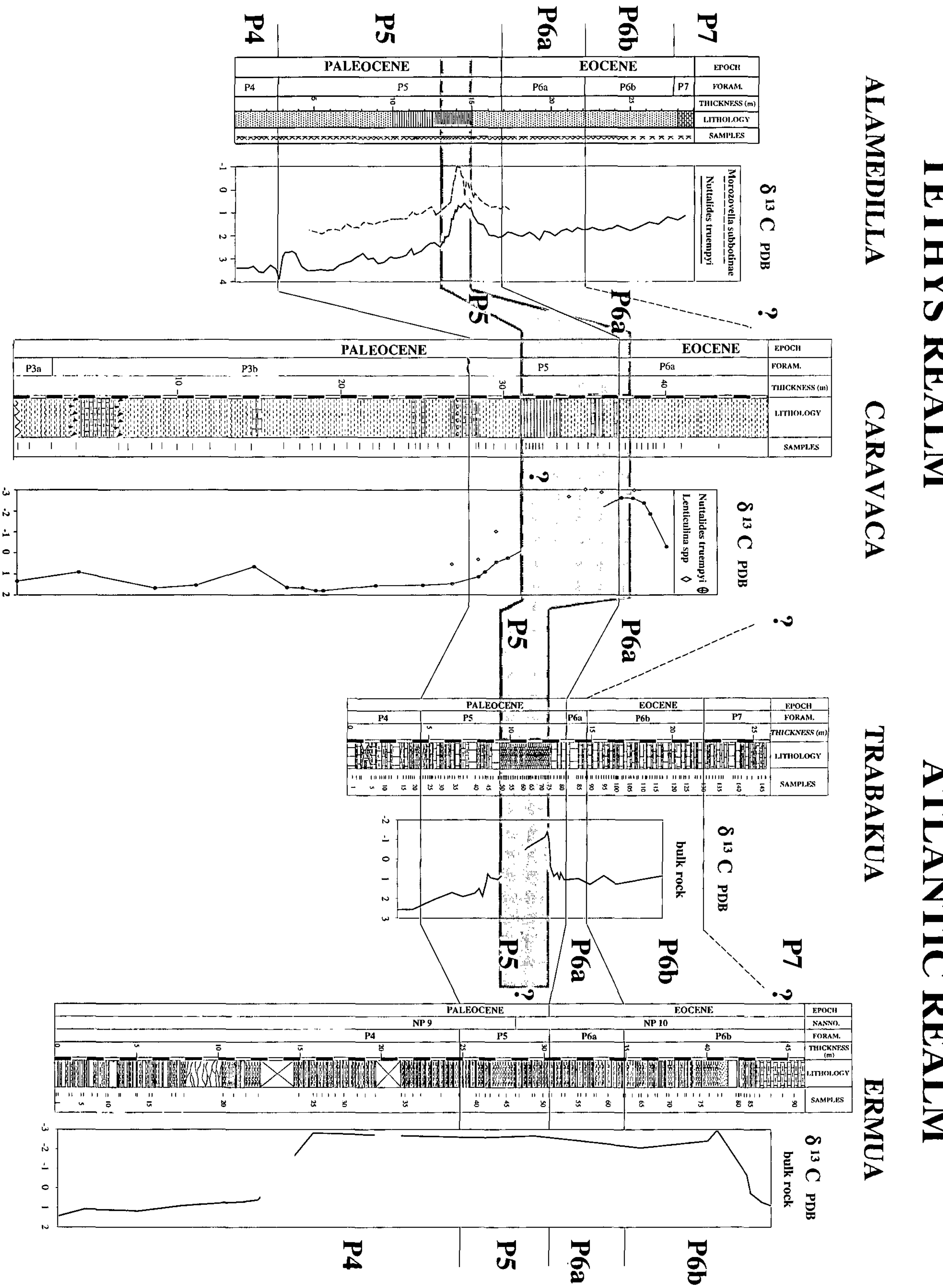
TETHYS REALM
ALAMEDILLA
CARAVACA
ATLANTIC REALM
TRABAKUA
ERMUA
P4
P5
P6a
P6b
P7
PALEOCENE
EOCENE
EPOCH
FORAM.
NANNO.
NP 9
NP 10
THICKNESS (m)
LITHOLOGY
SAMPLES
P3a
P3b
δ 13 C PDB
Morozovella subbotinae
Nuttalides truempyi
Lenticulina spp
bulk rock

nates and high content of clays in the hemipelagic marls associated with organic matter seems to obscure or obliterate the isotopic and geochemical signals.

Stable isotope and biostratigraphic data show that the Trabakua section is relatively complete (see also Orue-Etxebarria et al. 1996). During the latest Paleocene (Zone P5), the oceanic carbon reservoir changed dramatically, beginning with a gradual decrease by 1.0‰ of $\delta\,^{13}C$ values in the lower part of Zone P5, followed by a 3‰ decrease in the clay layer in the upper Zone P5 interval. In the limestone overlying the clay layer, $\delta\,^{13}C$ values rapidly increase by 2.5‰ and remain steady upsection. The decrease in $\delta\,^{13}C$ values in the clay layer coincides with a reduction in carbonate to near zero. A similar isotopic profile has been observed in the Alamedilla section of southern Spain (Fig. 12) where Lu et al. (1996), first noted that the rapid excursion in the clay is preceded by a gradual prelude decrease and followed by a gradual recovery. The gradual prelude decrease, rapid excursion and gradual recovery are accompanied by similar trends in calcite concentrations in sediments (Fig. 6). The concomitant decrease in $\delta\,^{13}C$ and calcite values can be explained by a decrease in primary productivity. Detrital influx, particulary quartz, plagioclase, K-feldspar, phyllosilicates, increased in the clay interval whereas grain size decreased. These changes in detrital influx suggest variations in source rocks and in the intensity of weathering and erosion. This oceanographic event is observed globally and is accompanied by a major mass extinction in benthic foraminifera (~ 50% species extinct) and a major faunal turnover in planktic foraminifera (e.g. Thomas 1990; Lu & Keller 1995a, 1995b; Lu et al. 1996; Ortiz 1996; Thomas & Shackleton 1996).

Clues to environmental conditions in the Pyreneean basin during the P-E transition can be gleaned from clay minerals. Clay mineral assemblages, if not altered by deep burial, reflect continental morphology and tectonic activity linked to the structural evolution of the margins, as well as climatic evolution and associated variations of atmospheric and/or marine circulation (Robert & Chamley 1987). Moreover, detrital clay mineral compositions in marine sediments record qualitative signals of regional climatic changes (Millot 1970; Chamley 1989). For instance, kaolinite forms abundantly in soils of intertropical land masses characterized by warm, humid climates. Kaolinite abundance increases toward the Equator in all oceanic basins (Chamley 1989). In contrast, detrital chlorite increases toward cold latitudinal zones parallel to the decrease of continental hydrolysis. Chlorite forms also in cold and dry or frozen regions. Mica tends to increase toward high latitudes, similar to chlorite, which reflects decreased chemical weathering and increased mechanical erosion under cold climatic conditions (Chamley 1989).

Although clays in the Trabakua and Ermua sections have undergone significant burial diagenesis, mica and chlorite are partly detrital, indicating that the adjacent areas were characterized by a dry climate. Sediments at Ermua contain higher kaolinite percentages in marls (15–23%) than at Trabakua where kaolinite does not exceed 8%. At Ermua, in calcarenites which contain reworked shallow-water carbonate platform sediments, kaolinite reaches a maximum of 10% and averages 7%. These data suggest that the kaolinite is transported by oceanic currents and does not come from adjacent land areas. In the Zumaya section, kaolinite first appears 6 m below the Paleocene/Eocene transition and rapidly disappears upward. The presence of kaolinite close to coastal areas and the extinction of benthic foraminifera are likely to be the result of a global turnover in oceanic circulation (Adatte et al. 1995).

Trabakua Pass section: a potential Paleocene/Eocene GSSP?

The Paleocene/Eocene boundary is usually placed at the P5/P6 (Berggren et al. 1995) zonal boundary by planktic foraminiferal specialists. Calcareous nannoplankton specialists generally use the NP9/NP10 zonal boundary. Designation of suitable markers for this boundary and the problems associated with chosing an oceanographic event as marker, are currently investigated and examined by workers of the IGCP Project 308 (Paleocene/Eocene Boundary Events in Time and Space) (see Berggren & Aubry 1995; Aubry et al. 1995; Berggren et al. 1995).

A potential GSSP candidate section for the P/E boundary has to fulfil certain conditions suggested by the International Commission on Stratigraphy. These conditions include: a) easy access, b) open marine sedimentation, c) continuous sedimentation across the boundary, d) absence of synsedimentary and tectonic disturbances, e) absence of redeposition or diagenetic alteration, f) abundance and diversity of well preserved fossils, and g) good magnetostratigraphic and isotopic records (Remane et al. 1997).

Previous reports on the Trabakua section concluded that most of these conditions were satisfied and that Trabakua could be considered as suitable global stratotype section and point (Coccioni et al. 1994; Orue-Etxebarria et al. 1996). Our study partly concurs with this assessment insofar as the global biostratigraphic, geochemical and isotopic markers are present. However, the section is not ideal for several reasons. 1) Microfossils are very poorly preserved, phosphatized, recrystallized or completely replaced by diagenetic calcite. The poor preservation and often sporadic occurrence makes it difficult to positively identify species. This is a serious problem which we observed in trying to reproduce the biostratigraphies of Coccioni et al. (1994) and Orue-Etxebarria et al. (1996) in the same section. As stratotype, Trabakua would necessarily cause problems when correlating this section with well-preserved faunas and floras of other sections. Moreover, no paleotemperature signals can be obtained from the recrystallized calcite of the Trabakua section. 2) Sedimentation across the clay layer may be discontinuous, as suggested by the presence of glauconite. 3) The clays are affected by deep burial diagenesis corresponding approximately to the upper part of Zone 3 (> 100 °C) of Kübler et al. (1979). We conclude therefore that the Trabakua Pass section is not an optimal stratotype for the Paleocene-Eocene transition.

Conclusions

Expanded sedimentary records from Trabakua, Spain, reveal unique faunal, isotopic, geochemical, mineralogical and sedimentary compositional changes across the Paleocene-Eocene (P-E) transition. Unlike in the open oceans, the Trabakua section exhibits a gradual decrease of 1.3‰ in $\delta^{13}C$ values prior to the rapid $\delta^{13}C$ excursion. Associated with the $\delta^{13}C$ excursion is a decrease in calcite preservation, increase in detrital content and reduction in the grain size.

These major changes across the P/E transition are explained by a reduced intensity of sea-surface circulation with a concomitant decrease in the primary biological productivity. The decline in carbonate productivity is partially reflected in the negative shift of $\delta^{13}C$ values which occurred exactly at the same time.

The increase in detrital minerals together with a decrease of grain sizes across the P/E transition indicate changes of global oceanic currents and/or reduction of the intensity of atmospheric circulation probably associated with changes in sediments sources.

Acknowledgements

We thank X. Arostegui, X. Orue-Etxebarria and V. Pujalte from the University of Bilbao, Spain, for guiding us in the field. Thanks to C. Beck for conducting geochemical analyses and J. Richard for conducting X-ray preparations at the laboratory of mineralogy and petrology, University of Neuchâtel, Switzerland. We thank also J. Remane, Institute of Geology, Neuchâtel, A–C. Bartolini from the stable isotope laboratory at the University of Lausanne, Switzerland for providing important comments and suggestions on an early draft. We sincerely thank H.P Luterbacher (Tübingen) and X. Orue-Etxebarria (Bilbao) for a stimulating review of the manuscript.

This study was supported by Swiss National Foundation, N° 2100–043450.95/1

REFERENCES

ADATTE, T., LU, G. & KELLER, G. 1995: Clay mineral correlation across the Paleocene-Eocene boundary: evidence for global paleo-oceanographic turnover. GSA 1995, annual meeting, New Orleans, USA, abstract p. 405.

ANGORI, E. & MONECHI, S. 1996: High resolution calcareous nannofossil biostratigraphy across the Paleocene/Eocene boundary at Caravaca (southern Spain). Israel. J. of Earth Sc. 44, 197–206.

AUBRY, M.P., BERGGREN, W.A., STOTT, L.D. & SINHA, A. 1995: The upper Paleocene-lower Eocene stratigraphic record and the Paleocene-Eocene boundary isotope excursion: implications for geochronology. In Correlation of the Early Paleogene in Northwestern Europe. (Ed. by KNOX, R.O.B., CORFIELD, R.M. & DUNNAY, R.E.) London: Special Publication of the Geological Society, 1996, 353–380.

AUBRY, M.P. 1996: Towards an Upper Paleocene-Lower Eocene High Resolution Stratigraphy Based on Calcareous Nannofossil Stratigraphy. Israel. J. of Earth Sc. 44, 239–253.

AXELROD, D.I. 1992: What is an equable climate? Palaeogeogr., Palaeoclimatol., Palaeoecol. 91, 1–12.

BARTOLINI, A.C, BAUMGARTNER, P.O. & HUNZIKER, J. 1996: Middle and Late Jurassic carbon stable-isotope stratigraphy and radiolarite sedimentation of the Umbria-March Basin (Central Italy). Eclogae geol. Helv. 89/2, 811–844.

BERGGREN, W.A. & AUBRY, M.P. 1995: A Late Paleocene-early Eocene NW European and North Sea magnetobiochronology correlation network: A sequence stratigraphic network. In Correlation of the Early Paleogene in Northwestern Europe. (Ed by KNOX, R.O.B., CORFIELD, R.M. & DUNNAY, R.E.) London: Special Publication of the Geological Society, 1996, 309–352.

BERGGREN, W.A, KENT, D.V., SWISHER, C.C. & AUBRY, M.P. 1995: A revised Cenozoic geochronology and chronostratigraphy. In Geochronology, time scale and global stratigraphy correlation. (Ed. by BERGGREN, W.A., KENT, D.V., AUBRY, M.P. & J. HARDENBOL) Tulsa, Oklahoma, USA: SEPM Special Publication N°54, 129–212.

BERGGREN, W.A & MILLER, K.G. 1988: Paleogene planktonic foraminiferal biostratigraphy and magnetobiostratigraphy. Micropaleontology 34, 362–380.

BOLES, J.R. & FRANCKS, S.G. 1979: Clay diagenesis in Wilcox sandstones of Southwest Texas: implications of smectite diagenesis on sandstone cementation. J. Sed. Petr. 49, 55–70.

BRALOWER, T.J., ZACHOS, J.C., THOMAS, E., PARROW, M., PAUL, C.K., KELLY, D.C., PREMOLI SILVA, I., SLITER, W.V. & LOHMANN, K.C. 1995: Late Paleocene to Eocene paleoceanography of the equatorial Pacific Ocean: Stable isotopes recorded at Ocean Drilling Program Site 865, Allison Guyot. Paleoc. 10, 841–865.

BYBELL, L.M. & SELF-TRAIL, J.M. 1995: Evolutionary, Biostratigraphic, and Taxonomic Study of Calcareous Nannofossils from a Continous Paleocene-Eocene Boundary Section in New-Jersey. U.S. Geol. Survey Prof. Paper. 1554, 1–36.

CALVERT, S.E. 1987. Oceanographic controls on the accumulation of organic matter in marine sediments. In Marine petroleum source rocks. (Ed. by BROOKS, J. & FLEETS, A.J.). Geol. Soc. London Spec. Publ.

CANUDO, J.I., KELLER, G., MOLINA, E. & ORTIZ, N. 1995: Planktic foraminiferal turnover and $\delta^{13}C$ isotopes across the Paleocene-Eocene transition at Caravaca and Zumaya, Spain. Palaeogeogr., Palaeoclimatol., Palaeoecol. 114, 75–100.

CHAMLEY, H. 1989: Clay Sedimentology. Springer-Verlag. Berlin–Heidelberg, 623.

COCCIONI, R., DI LEO, R., GALEOTTI, S. & MONECHI, S. 1994: Integrated biostratigraphy and benthic foraminiferal faunal turnover across the Paleocene-Eocene boundary at Trabakua Pass section, Northern Spain. Palaeopelagos 4, 87–100.

ERBA, INSTRUMENTS CARLO. 1990: Instruction manual, eager 2000. (Ed. by FISONS).

FERRERO, J. 1965: Dosage des principaux minéraux des roches par diffraction de Rayon X. Rapport C.F.P (Bordeaux), inédit.

– 1966: Nouvelle méthode empirique pour le dosage des minéraux par diffraction R.X. Rapport C.F.P (Bordeaux), inédit, 26.

GINGERICH, P.D. 1980: Evolutionary patterns in early Cenozoic mammals. Ann. Rev. Earth Planet. Sci. 8, 407–424.

– 1986: Evolution and fossil record: patterns, rates and processes. Canadian Journal of Zoology 65, 1053–1060.

HANDBOOK OF GEOCHEMISTRY 1978: Springer-Verlag. Berlin–Heidelberg–New York, 1200.

HOWER, J., ESLINGER, E.V., HOWER, M.E. & PERRY, E.A. 1976: Mechanisms of burial metamorphism of argillaceous sediment: 1. Mineralogical and chemical evidence. Geol. Soc. Amer., Bull. 87, 725–737.

JANTSCHIK, R., NYFFELER, F. & DONARD, O.F.X. 1992: Marine particle size measurement with a stream-scanning laser system. Marine Geology 106, 239–250.

KATZ, M.E. & MILLER, K.G. 1991: Early Paleogene benthic foraminiferal assemblages and stable isotopes in the Southern Ocean. Proc. ODP, Sci. Res. 114, 481–512.

KENNETT, J.P. & STOTT, L.D. 1990: Proteus and Proto-Oceanus: Paleogene oceans as revealed from Antarctica stable isotopic results. In Proc. ODP, Sci. Res. 113, 865–879.

– 1991: Abrupt deep-sea warming, palaeoceanographic changes and benthic extinctions at the end of the Paleocene. Nature 353, 225–229.

KLOOTWIJK, C.T., GEE, J.S., PEIRCE, J.W., SMITH, G.M. & MCFADDEN, P.L. 1992: An early India-Asia contact: Paleomagnetic constraints from Ninetyeast Ridge, ODP Leg 121. Geology 20, 395–398.

KLUG, H.P. & ALEXANDER, L. 1974: X-ray Diffraction Procedures for Polycrystalline and Amorphous Materials. (Ed. by JOHN WILEY and SONS, INC.). New York.

KOCH, P.L., ZACHOS, J.C. & GINGERICH, P.D. 1992: Correlation between isotope records in marine and continental carbon reservoir near the Paleocene/Eocene boundary. Nature 358, 319–322.

KÜBLER, B. 1983: Dosage quantitatif des minéraux majeurs des roches sédimentaires par diffraction X. Cahier de l'institut de Géologie de Neuchâtel Série AX N°1.1 & 1.2.

– 1987: Cristallinité de l'illite, méthodes normalisées de préparations, méthodes normalisées de mesures. Cahiers de l'Institut de Géologie de Neuchâtel Série ADX, 1–8.

KÜBLER, B., PITTION, J.C., HERIOUX, Y., CHAROLLAIS, J. & WEIDMANN, M. 1979: Sur le pouvoir réflecteur de la vitrinite dans quelques roches du Jura, de la Molasse et des Nappes préalpines, helvétiques et penniques (Suisse occidentale et Haute-Savoie). Eclogae geol. Helv. 72, 347–373.

LU, G. & KELLER, G. 1993: The Paleocene-Eocene transition in the Antarctic Indian Ocean: inference from planktic foraminifera. Mar. Micropaleontol. 21, 101–142.

– 1995a: Planktic foraminiferal faunal turnovers in the subtropical Pacific during the late Paleocene to early Eocene. J. Foram. Res. 26, 97–116.

– 1995b: Ecological stasis and saltation: species richness change in planktic foraminifera during the late Paleocene to early Eocene, DSDP Site 577. Palaeogeogr., Palaeoclimatol., Palaeoecol. 117, 211–227.

LU, G., KELLER, G., ADATTE, T. & BENJAMINI, C. 1995: Abrupt change in the upwelling system along the southern margin of the Tethys during the Paleocene-Eocene transition event, Israel. J. Earth Sci. 44, 185–195.

LU, G., KELLER, G., ADATTE, T., ORTIZ, N. & MOLINA, E. 1996: Long-term (10^5) or short-term (10^3) $\delta\ ^{13}C$ excursion near the Palaeocene-Eocene transition: evidence from the Tethys. Terra Nova 8, 347–355.

MAGARITZ, M., BENJAMINI, C., KELLER, G. & MOSHKOVITZ, S. 1992: Early diagenetic isotopic signal at the Cretaceous/Tertiary boundary, Israel. Palaeogeogr., Palaeoclimato., Palaeoecol. 91, 291–304.

MARTINI, E. 1971: Standard Tertiary and Quaternary calcareous nannoplankton zonation. In Proc. 2nd Planktonic Conference. (Ed by FARINACCI, A.). Roma: Tecnoscienza, 739–785.

MCCREA, J.M. 1950: On the Isotopic Chemistry of the Carbonates and a Paleotemperatures Scale. Jour. Chem. Phys. 18, 849–857.

MILLER, K.G., JANECEK, T.R., KATZ, M.E. & KEIL, D.J. 1987: Abyssal circulation and benthic foraminiferal changes near the Paleocen-Eocene boundary. Paleoceanography. 2, 741–761.

MILLOT, G. 1970: Geology of Clays. Springer Verlag. Berlin, Heidelberg, New York, 499.

MOORE, D. & REYNOLDS, R. 1989: X-Ray-diffraction and the identification and analysis of clay-minerals. Oxford University Press, 332.

MUFFLER, L.P.J. & WHITE, D.E. 1969: Active metamorphism of Upper Cenozoic sediments in the Salton Sea geothermal fild and the Salton Trough, southeastern California. Geol. Soc. Amer., Bull. 80, 157–182.

O'CONNELL, S.B.O. 1990: Variations in upper Cretaceous and Cenozoic calcium carbonate percentages, Maud Rise Weddell Sea. In: Proc. ODP, Sci. Res. 113, 971–984.

OBERHÄNSLI, H. 1992: The Influence of the Tethys on the bottom waters of the early Tertiary ocean. In The Antarctic Paleoenvironment: A Perspective on Global Change. (Ed. by KENNETT, J.P.), 167–184.

OBERHÄNSLI, H. & HSÜ, K.J. 1986: Paleocene-Eocene paleoceanography. In Mesozoic and Cenozoic Oceans. Geodynamic Series. 15, 85–100.

OINUMA, K., SHIMODA, S. & SUDO, T. 1972: Triangular diagrams of surveying chemical compositions of chlorites. J. Tokyo Univ. 15, 1–13.

ORTIZ, N. 1996: Differential patterns of benthic foraminiferal extinctions near the Paleocene/Eocene boundary in the North Atlantic and the western Tethys. Mar. Micropaleontol. 26, 341–359.

ORUE-ETXEBARRIA, X., APELLANIZ, E., BACETA, J.I., COCCIONI, R., DI LEO, R., DINARES-TURELL, S., GALEOTTI, S., MONECHI, S., NUNEZ-BETELU, K., PARES, J.M., PAYROS, A., PUJALTE, V., SAMSO, J.M., SERRA-KIEL, J., SCHMITZ, B. & TOSQUELLA, J. 1996: Physical and biostratigraphic analysis of two prospective Paleocene-Eocene Boundary Stratotypes in the intermediate-deep water Basque Basin, western Pyrenees: The Trabakua Pass and Ermua sections. N. Jb. Geol. Paläont., Abh. 200, 1–64.

PAK, D.K. & MILLER, K.G. 1992: Paleocene to Eocene benthic foraminiferal isotopes and assemblages:implications for deepwater circulation. Paleoceanography. 7, 741–761.

PERRY, E. & HOWER, J. 1970: Burial diagenesis in Gulf Coast pelitic sediments. Clays and clay minerals 18, 165–177.

PLAZIAT, J.C. 1981: Late Cretaceous to late Eocene Paleogeographic evolution of southwest Europe. Palaeogeogr., Palaeoclimatol., Palaeoecol. 36, 263–320.

PUJALTE, V., BACETA, J.I., DINARÈS-TURELL, J., ORUE-ETXEBARRIA, X. PARES, J.M. & PAYROS, A. 1995: Biostratigraphic and magnetostratigraphic intercalibration of latest Cretaceous and Paleocene depositional sequences from the deep-water Basque Basin, Western Pyrenees, Spain. Earth and Planetary Sci. Lett. 136, 17–30.

PUJALTE, V., BACETA, J.I., PAYROS, A., ORUE-ETXEBARRIA, X. & SERRA-KIEL, J. 1994: Late Cretaceous-middle Eocene sequence stratigraphy and biostratigraphy of SW and W Pyrenees (Pamplona and Basque Basin, Spain. Guide-book of a field seminar of the Groupe d'étude du Paléocène and IGCP 286, 118.

PUJALTE, V., ROBLES, S., BACETA, J. & ORUE-ETXEBARRIA, X. 1992: Latest Cretaceous-early Eocene sedimentation in the deep-water Basque Basin (northern Spain): Eustatic and Tectonic influences. Field Trip guide book of the International Symposium on "Mesozoic and Cenozoic Sequence Stratigraphy of European Basins". Dijon, France.

PUJALTE, V., ROBLES, S., ROBADOR, A., BACETA, J. & ORUE-ETXEBARRIA, X. 1993: Shelf-to-Basin Paleocene Palaeogeography and depositional sequences, Western Pyrenees, North Spain. In Sequence Stratigraphy and Facies Association. (Ed. by POSAMENTIER, H.W., SUMMERHAYES, C.P., HAQ, B.U. & ALLEN, G.P). Special Publication Int. Assoc. Sedimentologists. 18, 369–395.

RAYMO, M.E., RUDDIMAN, W.F. 1992: Tectonic forcing of Late Cenozoic climate. Nature 359, 117–122.

REA, D.K., ZACHOS, J.C., OWEN, R.M. & GINGERICH, P.D. 1990: Global changes at the Paleocene-Eocene boundary: climate and evolutionary consequences of tectonic events. Palaeogeogr., Palaeoclimatol., Palaeoecol. 79, 117–128.

REMANE, J., BASSETT, M.G., COWIE, J.W., GOHRBANDT, H.K., LANE, H.R., MICHELSEN, O. & WANG, N. 1996: Revised guidelines for the establishment of global chronostratigraphic standards by the international commission on stratigraphy (ICS). Episodes 19/3, 77–81.

RITCHIE, J.D.& HITCHEN, K. 1996: Early Paleogene offshore igneous activity to the northwest of the UK margin and its relationship to the North Atlantic Igneous Province. In Correlation of the Early Paleogene in Northwest Europe. (Ed. by KNOX, R.W., CORFIELD, R.M. & DUNAY, R.E.) London. The Geological Society, 1996, 63–78.

ROBERT, C. & CHAMLEY, H. 1987: Cenozoic evolution of continental humidity and paleoenvironment, deduced from the kaolinite content of oceanic sediments. Paleogeogr., Paleoclimatol., Paleoecol. 60, 171–187.

ROBERT, C. & KENNETT, J.P. 1994: Antarctic subtropical humid episode at the Paleocene-Eocene boundary; Clay-mineral evidence. Geology 22, 211–214.

SCHMITZ, B., SPEIJER, R.P. & AUBRY, M.P. 1995: Latest Paleocene benthic extinction event on the southern Tethyan shelf (Egypt): Foraminiferal stable isotopic $\delta\ ^{13}C$ and $\delta\ ^{18}O$ records. Geology 24, 347–350.

SELVERSTONE, J. & GUTZLER, D.S. 1993: Post-125 Ma carbon storage associated with continent-continent collision. Geology 21, 885–888.

SPEIJER, R.P. 1994a: Extinction and recovery patterns in benthic foraminiferal paleocommunities across the Cretaceous/Paleogene and Paleocene/Eocene boundaries. Geologica Ultraiectina, University of Utrecht.

– 1994b: The late Paleocene benthic foraminiferal extinction as observed in the Middle East. Bull. Soc. belge Géol. 103, 267–280.

STOTT, L.D. 1992: Higher temperatures and lower oceanic pCO2: a climate enigma at the end of the Paleocene Epoch. Paleoceanography. 7, 395–404.

STOTT L.D., SINHA, A. TIRY, M. AUBRY, M.P. & BERGGREN, W.A. in press: The transfer of $\delta\ ^{12}C$ changes from the ocean to the terrestrial biosphere across the Paleocene-Eocene boundary: criteria for terrestrial-marine correlations. Geol. Soc. Spec. Publ.

THOMAS, E. 1990: Late Cretaceous through Neogene deep-sea benthic foraminifers (Maud Rise, Weddell Sea, Antarctica). In: Proc. ODP. Sci. Results 113, 571–594.
THOMAS, E. & SHACKLETON, N.J. 1996: The latest Palaeocene benthic foraminiferal extinction and stable isotope anomalies. J. Geol. Soc. London 101, 421–441.
VEIZER, J. 1983: Trace elements and isotopes in sedimentary carbonates. In Carbonates: mineralogy and chemistry (Ed. by REEDER, R.J). Min. Soc. Am. Rev. Min, 11, 265–299.
VERARDO, D.J., FROELICH, P.N. & MCINTYRE, A. 1990: Determination of organic carbon and nitrogen in marine sediments using the Carlo Erba NA-1500 Analyzer. Deep Sea Research 57, 157–165.
WEAVER, C.E. 1989: Clays, Muds, and Shales. Elsevier Science Publishers B.V. Amsterdam, 819.
WEI, W. & ZHONG, S. 1996: Taxonomy and magnetobiochronology of Tribrachiatus and Rhomboaster, two genera of calcareous nannofossils. J. Paleont. 70, 7–22.
WING, S.L., BOWN, T.M. & OBRADOVICH, J.D. 1991: Early Eocene biotic and climatic change in interior western America. Geology 19, 1189–1192.
WING, S.L. & GREENWOOD, D.L. 1993: Fossils and fossil climate: The case for equable continental interiors in the Eocene. Royal Soc. London Philo. Trans. ser. 341, 243–252.

Manuscript received February 22, 1997
Revision accepted June 8, 1997

Bull. Soc. géol. France, 1999, t. 170, n° 5, pp. 661-680

Séance spécialisée : SGF-APF-CFS
La limite Paléocène-Eocène en Europe
Paris, 19-20 janvier 1998

The Paleocene-Eocene transition in the southern Tethys (Tunisia) : climatic and environmental fluctuations

MARIE P. BOLLE[1], THIERRY ADATTE[1], GERTA KELLER[2], KATHARINA VON SALIS[3] and STEVE BURNS[4]

Key words. – Climate, Environment, Tunisia, Biostratigraphy, Phosphate, Clay-minerals, Stable isotopes.

Abstract. – This study, based on a multidisciplinary approach including micropaleontology, sedimentology, mineralogy and geochemistry, evaluates the Paleocene-Eocene transition in Tunisia. At Foum Selja, sediment deposition occurred in the shallow, restricted Gafsa Basin influenced by the adjacent Saharan Platform. During the early Paleocene this area experienced a warm and humid climate that changed to warm but arid climatic conditions during the Paleocene-Eocene transition. At Elles the sediment deposition in the El Kef Basin occurred in an open marine environment connected to the Tethys. During the late Paleocene, the Tethyan region was submitted to a seasonal warm climate changing to a warm and humid climate across the P/E transition and becoming seasonal/arid in the early Eocene. From Africa to northern Europe, kaolinite, a strong marker of warmth and humidity disappeared diachronously suggesting a latitudinal shift in the source area of this mineral and consequently in the climatic zones, from lower to higher latitudes. The P/E transition observed at Elles corresponds to a 2.7 m thick clay layer and is marked by a drastic decrease in carbonate sedimentation, a negative $\delta^{13}C$ excursion of 1.3‰ and increased detrital input. The presence of a condensed interval, the accumulation of phosphate deposits after the P/E event, which obliterate the original isotopic signal and strong dissolution of the planktic fauna and flora in these phosphatic layers, all are criteria that prevent the Elles section to be a potential GSSP candidate for the P/E boundary.

La transition Paléocène-Éocène dans la partie sud de la Téthys (Tunisie) : fluctuations climatiques et environnementales

Mots clés. – Climat, Environnement, Tunisie, Biostratigraphie, Phosphates, Minéraux argileux, Isotopes stables.

Résumé. – Cette étude, basée sur une approche multidisciplinaire incluant micropaléontologie, sédimentologie, minéralogie et géochimie, a pour objet l'évaluation de la transition Paléocène-Eocène en Tunisie. A Foum Selja, les sédiments, sous influence de la plate-forme saharienne adjacente se sont déposés dans le bassin peu profond de Gafsa. Au Paléocène précoce, cette région est marquée par un climat chaud et humide qui devient aride à la transition Paléocène-Eocène. Au contraire, à Elles, les sédiments se déposent dans le bassin d'El Kef sous influence téthysienne. Au Paléocène tardif, cette région est soumise à un climat saisonnier qui devient chaud et humide au Paléocène-Eocène et franchement aride à l'Eocène. De l'Afrique au nord de l'Europe, la kaolinite, indicatrice d'humidité et de chaleur, disparaît diachroniquement suggérant un déplacement latitudinal de la zone de production de ce minéral et par conséquent des zones climatiques chaudes et humides, des basses vers les hautes latitudes. La transition Paléocène-Eocène observée à Elles se marque lithologiquement par un intervalle argileux d'une épaisseur de 2,7 mètres. Cet intervalle est caractérisé par une importante diminution de la sédimentation carbonatée, une excursion négative de 1,3‰ du $\delta^{13}C$, et par une augmentation des apports détritiques. Toutefois, en raison de la présence d'un intervalle condensé, de l'apparition de dépôts phosphatés surmontant la transition Paléocène-Eocène et d'une forte dissolution affectant la faune et flore planctoniques dans ces niveaux phosphatés, la coupe d'Elles ne peut être considérée comme une candidate potentielle de la limite Paléocène-Eocène.

VERSION FRANÇAISE ABRÉGÉE

La transition Paléocène-Eocène est caractérisée par des changements environnementaux globaux qui incluent un réchauffement de 6°C des eaux océaniques de surface sous les hautes latitudes [Zachos *et al.*, 1994], et la présence de faunes et flores tempérées à sub-tropicales dans les régions subpolaires des deux hémisphères [Estes et Hutchison, 1980; Wolfe, 1980; Axelrod, 1984]. Ce réchauffement coïncide également avec une excursion négative du $\delta^{13}C$ et une extinction massive des foraminifères benthiques [Thomas, 1990; Kennett et Stott, 1991]. La composition des minéraux argileux reflète une période de précipitations exceptionnellement élevées en Antarctique [Robert et Kennett, 1994] mais au contraire un climat aride dans une partie de la région téthysienne [Adatte et Lu, 1995].

La Téthys, bassin restreint entouré de vastes mers épicontinentales et soumis à une activité tectonique intense constitue une région clé dans la recherche des mécanismes responsables des changements climatiques et environnementaux globaux qui ont eu lieu durant la transition Paléocène-Eocène (P/E) [Kennett et Stott, 1990, 1991; Lu *et al.*, 1996].

L'étude de deux profils, Foum Selja et Elles (marge sud de la Téthys), basée sur une approche pluridisciplinaire, sédimentologique, micropaléontologique, géochimique (isotopes stables) et minéralogique fournit ainsi une nouvelle base de données nécessaires à la compréhension des phénomènes se produisant à la transition P/E.

Le profil de Foum Selja est situé dans le bassin peu profond de Gafsa entre l'île de Kasserine au nord et la plate-forme saharienne au sud (fig. 1). L'absence de communications avec la Téthys durant la transition P/E est due à la présence de petites zones surélevées et de golfes qui agissaient comme barrières. La sédimentation dans ce bassin est principalement influencée par la plate-forme saharienne adjacente. La partie étudiée de ce profil comprend les zones de nannofossiles NP(4)-5 à NP10 (fig. 2 et photo 1). Le profil de Foum Selja se divise en trois formations; Thelja (séquence évaporitique), Chouabine (séquence phosphatique) et Kef Eddour (séquence évaporitique) [Regaya *et al.*, 1991]. Le profil d'Elles est situé dans le bassin d'El Kef, au nord de l'île de Kasserine (fig. 1). La sédimentation dans cet

[1] Institut de Géologie, 11 Emile Argand, Université de Neuchâtel, 2007 Neuchâtel, Switzerland.
[2] Dpt of Geosciences, Princeton University, Princeton, NJ 08544, USA.
[3] Geologisches Institut, ETH-Zentrum, 8092 Zürich, Switzerland.
[4] Geologisches Institut, Balzerstrasse, Universität Bern, 3000 Bern, Switzerland.
Manuscrit déposé le 10 juin 1998 ; accepté après révisions le 7 avril 1999.

environnement marin ouvert est principalement influencée par la région téthysienne. La partie étudiée de ce profil comprend les zones de nannofossiles NP7 à NP10 et de foraminifères planctoniques P4a à P6a. Trois bancs sableux riches en glauconie séparent une alternance de marnes, argiles et petits bancs calcaires noduleux (fig. 2 et photo 2).

A Elles, la transition P/E correspond à un intervalle argileux d'une épaisseur de 2,70 mètres. Cet intervalle se marque minéralogiquement par une diminution importante de la sédimentation carbonatée de 30 % à 7 %. Cette chute des carbonates coïncide avec une augmentation des phyllosilicates et l'apparition de feldspath potassique. La présence de ce minéral et le rapport détritique/carbonate maximal (fig. 5) suggèrent une augmentation des apports détritiques durant cette période. Ces changements minéralogiques reflètent probablement une diminution de la productivité biologique primaire et/ou de la dissolution ainsi qu'une augmentation de l'érosion dans la région téthysienne. La transition P/E se marque également par une diminution graduelle du $\delta^{13}C$ de 1,6 ‰ de la zone P4 à la partie inférieure de la zone P5, suivie par une excursion négative de 1,3‰ du $\delta^{13}C$ (fig. 8). La présence d'apatite fluoro-carbonatée (francolite) dans le banc glauconieux qui surmonte l'intervalle argileux P/E (fig. 2 et 5) coïncide avec des valeurs très négatives du $\delta^{13}C$ et du $\delta^{18}O$ (fig. 8 et tab. II). La francolite formée durant la diagenèse primaire se caractérise par des valeurs fortement négatives du $\delta^{13}C$ (– 12‰) et du $\delta^{18}O$ (– 11‰) [Kastner *et al.*, 1984; Mertz, 1984] masquant ou oblitérant ainsi le signal isotopique originel. La présence de cet intervalle glauconieux coïncidant avec l'apparition de dépôts phosphatés, la forte dissolution qui affecte la faune et flore planctoniques rend difficile le choix du profil d'Elles comme candidat potentiel GSSP de la limite Paléocène/Eocène.

A Foum Selja, les valeurs négatives du $\delta^{13}C$ (entre –2 et –12‰) et du $\delta^{18}O$ (entre – 0,7 et – 5,5 ‰) coïncident également avec les plus fortes teneurs en phosphates (fig. 8 et tab. III). Dans ce profil, la diagenèse primaire caractérisée par la présence de francolite masque l'excursion négative du $\delta^{13}C$ observée dans la majeur partie des profils P/E [Thomas, 1990; Kennett et Stott, 1991; Bolle *et al.*, 1998].

A Foum Selja, la distribution des minéraux argileux reflète les variations climatiques sur la plate-forme saharienne. Le rapport kaolinite/smectite très élevé, observé dans les premiers 20 mètres indique un climat chaud et humide sur la plate-forme pendant l'intervalle biozonal NP4-5 (fig. 6). La disparition de kaolinite et l'abondance de smectite associée à la formation d'évaporites suggèrent le développement d'un climat saisonnier, voir aride, devenant très aride sur la plate-forme à la transition P/E comme l'indique l'abondance de palygorskite et de sépiolite (fig. 6).

A Elles, la faible représentation de la kaolinite, mais l'abondance de smectite suggèrent un climat saisonnier dans la région téthysienne de P4a à P4c. Le rapport kaolinite/smectite maximal à la transition P/E implique un climat chaud et humide pour cette période. L'abondance de smectite et la disparition de kaolinite à l'Eocène inférieur indiquent le retour à un climat plus aride dans cette région (fig. 7).

A Elles, mais également dans le sud de l'Espagne, à Caravaca et Alamedilla, le cortège des minéraux argileux indique des conditions climatiques humides et chaudes à la transition Paléocène-Eocène qui coïncident avec l'excursion négative du $\delta^{13}C$. L'abondance de smectite indique une augmentation de l'aridité dans la région téthysienne juste après l'événement P/E. Du sud au nord, la kaolinite disparaît diachroniquement, dans la zone NP5 à Foum Selja, dans la zone NP9 à Elles et Caravaca et seulement dans la zone NP11 à Zumaya (nord de l'Espagne). Cette disparition diachronique de la kaolinite suggère donc un déplacement latitudinal de la zone de production de ce minéral et par conséquent des zones climatiques chaudes et humides, des basses vers les hautes latitudes (fig. 9).

Au Paléocène terminal, la marge sud de la Téthys pourrait avoir été affectée par l'activité intermittente de courant d'upwellings. A Foum Selja, l'accumulation de phosphates est favorisée par des conditions climatiques arides sur la plate-forme saharienne et par un apport détritique réduit dans le bassin de Gafsa (figs. 4 and 6). Le développement d'un climat plus aride dans la région téthysienne et l'apport réduit de détritiques après l'événement P/E (figs. 5 and 7) pourraient être la principale cause de l'accumulation tardive des phosphates dans le bassin d'El Kef (zone NP9) en comparaison du bassin de Gafsa où les dépôts phosphatés apparaissent dans la zone NP4/5 (fig. 4).

INTRODUCTION

The Paleocene-Eocene transition is marked by major global environmental changes, which caused various palaeontological, sedimentological and isotopical variations that include a 6°C warming in high latitude surface waters of the southern oceans [Zachos *et al.*, 1994], and the presence of sub-tropical to temperate faunas and floras in subpolar regions of both hemispheres [Estes and Hutchison, 1980; Wolfe, 1980; Axelrod, 1984]. In addition, the high latitude warming coincides with a major rapid negative $\delta^{13}C$ excursion and the extinction of 35 to 50 % of deep-sea benthic foraminiferal species [Thomas, 1990; Kennett and Stott, 1991; Speijer, 1994].

The rapid negative $\delta^{13}C$ excursion implies a significant addition of ^{12}C into the combined ocean-atmosphere inorganic carbon reservoir which cannot be explained by the two conventional hypotheses of the addition of volcanogenic CO_2 and/or transfer of ^{12}C from the terrestrial biomass because mantle CO_2 is insufficiently enriched in ^{12}C and the biomass is insufficiently large [Dickens *et al.*, 1995; Thomas and Shackleton, 1996]. Dickens *et al.* [1997] suggest that the release of methane hydrates, which are present in pore spaces of deep marine sediments, could be the source for the negative excursion during the thermal maximum.

During the Paleocene-Eocene, the Tethys was a semi-restricted basin surrounded by vast shallow epicontinental seas and was undergoing intense tectonic activity [Oberhänsli and Hsü, 1986; Klootwijk *et al.*, 1992; Oberhänsli, 1992]. The geographic and tectonic features suggest that the Tethys is a key region for the investigation of global climatic and oceanic changes during the Paleocene-Eocene [Kennett and Stott, 1990, 1991; Lu *et al.*, 1996].

This study evaluates the Paleocene-Eocene transition in central and southern Tunisia based on two sections, Foum Selja, and Elles, and is an integrated multidisciplinary approach that includes micropalaeontology, sedimentology, mineralogy and geochemistry (stable isotopes). The palaeogeographic location of these sections provides an important new database that aids our understanding of the climatic and environmental changes across the Paleocene-Eocene transition, in shallow marginal seas of the Tethys as well as their potential influence in contributing to global environmental changes.

LOCATION AND PALAEOGEOGRAPHICAL SETTING

The Elles section is located in the El Kef Basin and can be reached by the road from Siliana to El Kef. The Foum Selja section is located in a gorge about 10 km west of the city of Metlaoui and is reached by following the road from Metlaoui to Tozeur (fig. 1A).

During the Palaeogene, Tunisia was located at the southern margin of the Tethys and was the site of major phosphate deposition. The phosphate deposition occurred mainly in the shallow Gafsa Basin of southern Tunisia during the late Paleocene to early Eocene and to a lesser extent in the El Kef Basin (Tunisian Trough) of west-central Tunisia (fig. 1B) [Berthon, 1928; Visse, 1952, 1973; Burollet, 1956, 1967; Sassi, 1974, 1980; Fournié, 1980; Svoboda, 1983, 1985, 1989; Beji-Sassi, 1985]. In the Foum Selja section in the Gafsa Basin we analyzed a sequence comprising the Thelja, Chouabine and Kef Eddour Formations [Regaya

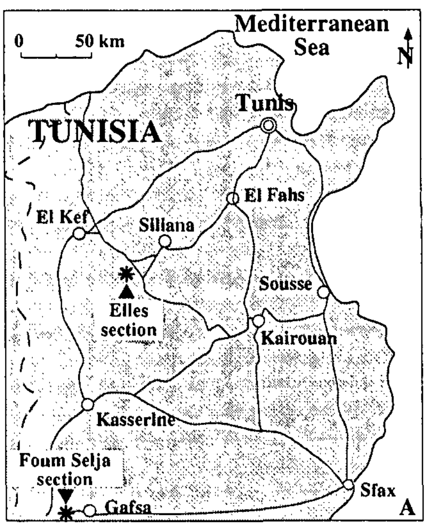

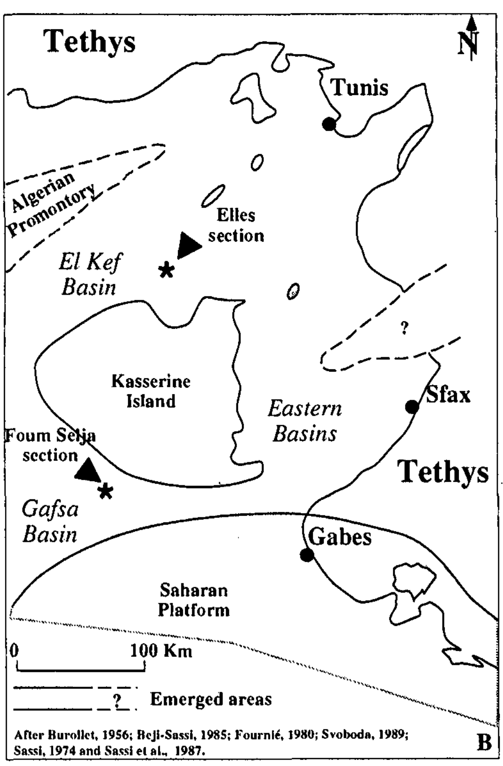

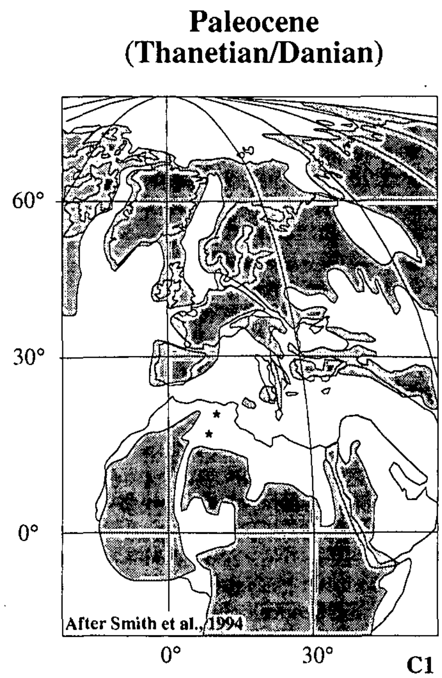

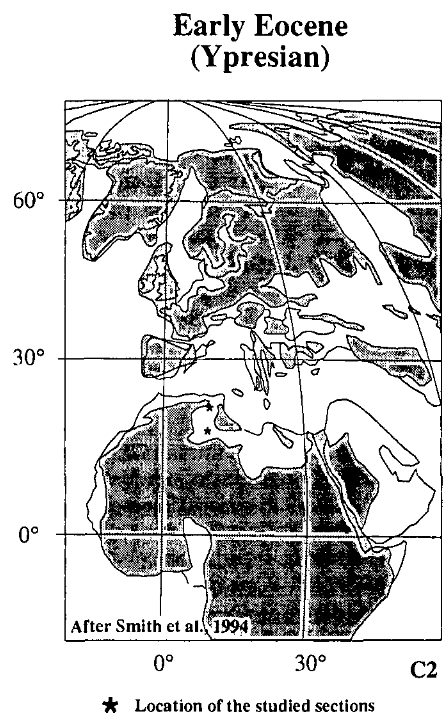

FIG. 1
A – Geographic location of the Elles and Foum Selja sections in Tunisia.
A – *Localisation géographique des profils d'Elles et de Foum Selja, Tunisie.*
B – Palaeogeography during the Paleocene and early Eocene in Tunisia.
B – *Paléogéographie de la Tunisie du Paléocène à l'Eocène inférieur.*
C1 – Palaeocoastline map during the Paleocene at 60 Ma (Thanetian-Danian).
C1 – *Carte des paléocôtes au Paléocène (60 Ma).*
C2 – Palaeocoastline map during the early Eocene at 53 Ma (Ypresian).
C2 – *Carte des paléocôtes à l'Eocène inférieur (53 Ma).*

et al., 1991] in order to observe the global environmental changes across the Paleocene/Eocene transition (fig. 2). These three formations are equivalent to the Lower, Middle and Upper Metlaoui Formations previously defined by Lucas *et al.* [1979]. Another P/E transition, the Elles section in the El Kef Basin was analyzed. The studied sequence comprises one part of the El Haria Formation [Said, 1978].

Palaeogeographic reconstructions for the Paleocene and early Eocene reveal several tectonic events that may have affected climate and ocean circulation (fig. 1B and C). These events include the closing of the north-south seaway between the southern Tethys and the South Atlantic, and the onset of the opening of the North Atlantic, between Greenland and Great Britain (fig. 1, C1 and C2). In Tunisia, the closure of the seaway to the south is accompanied by the re-emergence of Kasserine Island. At the time of the Paleocene-Eocene transition, Tunisia was divided into three emerged areas, the Saharan Platform, Kasserine Island and the Algerian Promontory separated by the Gafsa, the El Kef and the Eastern Basins (fig. 1B).

The palaeogeography of the region significantly influenced the nature of sediment deposition. At Foum Selja, in the Gafsa Basin, sedimentation was primarily influenced by the adjacent land areas, the Saharan Platform and Kasserine Island, whereas at Elles in the El Kef Basin, sedimentation was primarily influenced by Kasserine Island and the Tethys ocean.

LITHOLOGY

Foum Selja

The part of the section studied is about 135 m thick and spans at least nannofossil Zones NP4-5 to NP10 (fig. 2). The Thelja Formation [Lower Metlaoui after Lucas *et al.*, 1979] consists of a 56 m thick, evaporitic sequence that contains three massive evaporite beds, each several metres thick. These evaporite beds are interbedded with grey shales and thin calcareous beds enriched in shells and gastropods. The top of this interval is marked by a phosphatic hard ground (Hg, in fig. 2). The Chouabine Formation [Middle Metlaoui after Lucas *et al.*, 1979] consists of a 44 m thick phosphatic sequence (56 to 100 m, fig. 2). The lower 20 metres consist of grey shales alternating with thin calcareous layers enriched in oysters and gastropods. Upsection, sediments are increasingly more massive and more phosphatic. The Kef Eddour Formation [Upper Metlaoui after Lucas *et al.*, 1979] is 60 m thick with the basal 2 metres composed of discontinuous, lenticular, and highly bioturbated (Thalassinoides) phosphatized limestones [Sassi *et al.*, 1987] (ph. 1). Visse [1952] designated this facies as "conglomerate layer". The top of the studied section consists of two thick shelly limestones separated by alternating phosphates, marls and limestones containing cherts.

Thin sections of the phosphatic sequence in the Chouabine Formation show rounded phosphatic particles, phosphate-coated grains, phosphatized shells of gastropods, oysters, fish and vertebrate debris and a few detrital quartz grains. The phosphatic grains, phosphatized shells and the non-phosphatized micritic matrix indicate the absence of in situ phosphatogenesis and a probable allochthonous reworking. Nevertheless the absence of extraclasts produced by erosion of older sediments in these phosphatic layers could suggest that phosphate formation is nearly contemporaneous with the deposits (Föllmi, oral comm., 1998).

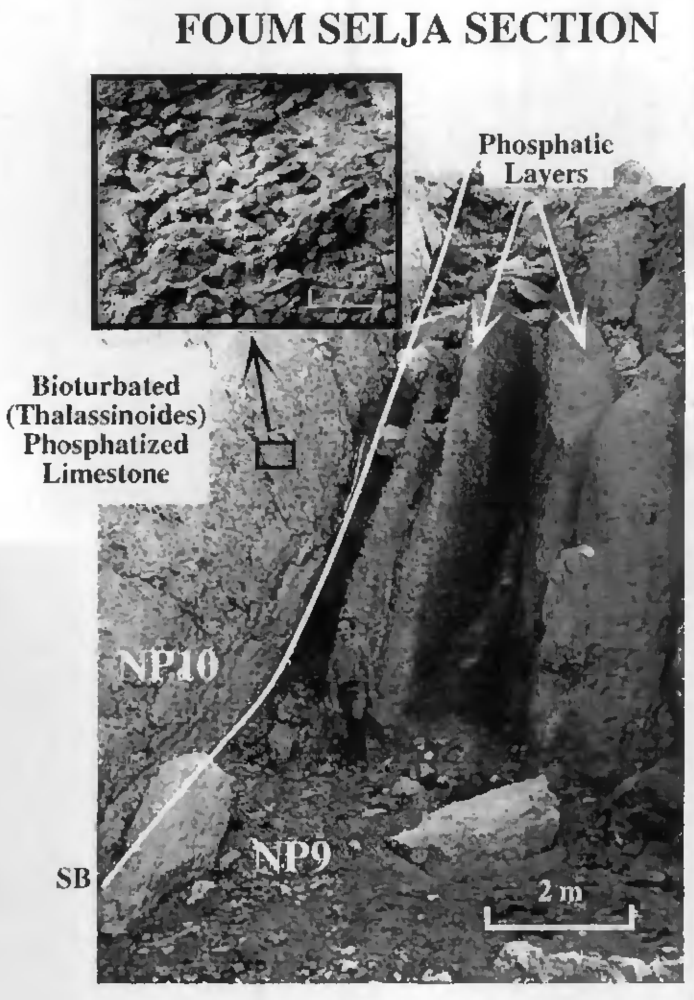

PH. 1. – Upper part of the phosphatic sequence at Foum Selja (SB = sequence boundary).

PH. 1. – *Partie supérieure de la séquence phosphatique à Foum Selja (SB = limite de séquence).*

Elles

This section is about 55 m thick and spans the upper Paleocene to lower Eocene nannofossil Zones NP7 to NP10, and foraminiferal Zones P4a to P6a (fig. 2). Three coarse glauconitic layers are present. The basal glauconitic bed is

FIG. 2. – Lithologic description of the Foum Selja and the Elles sections with sample locations. Planktic foraminiferal and nannofossil biozonations used in this study are from Berggren *et al.* [1995] and Martini [1971]. Sea level fluctuations and sequence boundaries (SB) are estimated by lithologic changes, abrupt change in faunal assemblages, variations in terrigenous and phosphatic influx, and by sedimentological criteria such as reworking, hard grounds and condensed or eroded surfaces.

FIG. 2. – *Description lithologique des profils de Foum Selja et Elles avec la position des échantillons. Les biozonations de foraminifères planctoniques et de nannofossiles utilisées dans cette étude sont celles de Berggren* et al. *[1995] et Martini [1971]. Les changements abrupts dans les assemblages faunistiques, les variations des apports détritiques et phosphatés ainsi que les critères sédimentologiques tels que surfaces érodées, condensées ou remaniement permettent d'évaluer les variations du niveau marin et les limites de séquence.*

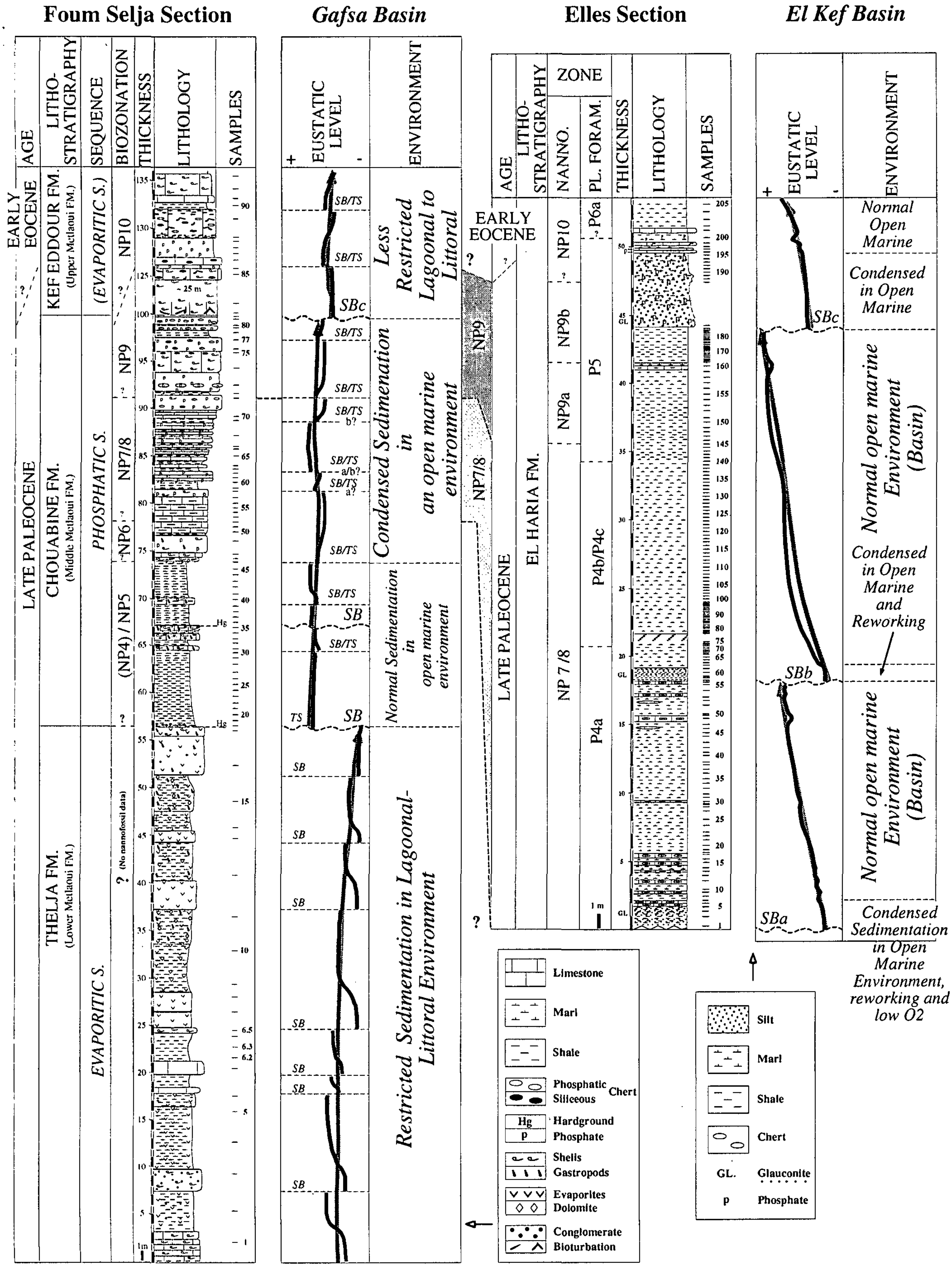
Foum Selja Section
Gafsa Basin
Elles Section
El Kef Basin
AGE
LITHO-STRATIGRAPHY
SEQUENCE
BIOZONATION
THICKNESS
LITHOLOGY
SAMPLES
EARLY EOCENE
LATE PALEOCENE
KEF EDDOUR FM. (Upper Metlaoui FM.)
CHOUABINE FM. (Middle Metlaoui FM.)
THELJA FM. (Lower Metlaoui FM.)
(EVAPORITIC S.)
PHOSPHATIC S.
EVAPORITIC S.
NP10
NP9
NP7/8
NP6
(NP4) / NP5
? (No nannofossil data)
EUSTATIC LEVEL
ENVIRONMENT
SB/TS
SBc
SB
TS
Less Restricted Lagoonal to Littoral
Condensed Sedimentation in an open marine environment
Normal Sedimentation in open marine environment
Restricted Sedimentation in Lagoonal-Littoral Environment
ZONE
NANNO.
PL. FORAM.
EL HARIA FM.
NP9a
NP9b
NP 7/8
P6a
P5
P4b/P4c
P4a
Limestone
Marl
Shale
Phosphatic
Siliceous
Chert
Hardground
Phosphate
Shells
Gastropods
Evaporites
Dolomite
Conglomerate
Bioturbation
Normal Open Marine
Condensed in Open Marine
Normal open marine Environment (Basin)
Condensed in Open Marine and Reworking
SBb
SBa
Condensed Sedimentation in Open Marine Environment, reworking and low O2
Silt
GL.
Glauconite
p

1.8 m thick and is overlain by 17 m of alternating grey marls and thin calcareous beds with chert nodules. The second glauconitic layer is overlain by 15 m of marls followed by 10 m of shales and shaly marls (fig. 2 and ph. 2). The third glauconitic layer is 6 m thick and contains phosphatic grains. This glauconitic layer is overlain by alternating phosphate and marl layers.

Thin sections show that the first two coarse glauconitic beds consist predominantly of glauconitic particles. The presence of this authigenic mineral suggests condensed sedimentation in an open marine environment, reworking and low oxygen conditions. The third glauconite layer contains in addition to phosphatic and glauconitic particles, small benthic and planktic foraminifera and detrital quartz. The phosphatic particles are irregular in size, but generally well-rounded. The co-existence of phosphate which indicates high nutrients and oxic or suboxic conditions and glauconite implies formation of these mineral grains in two different open marine environments and subsequent reworking. Reworking in these sediments is also suggested by the presence of detrital quartz and the absence of a phosphatized matrix (no *in situ* phosphatogenesis, Föllmi, oral comm., 1998).

METHODS

In the field, the sections were measured and samples collected from all lithologic units. More closely spaced samples were collected from marls, shales and clays (Elles) than from the evaporites (Foum Selja). A total of 93 samples were collected from the Foum Selja section and 205 samples from the Elles section. Analyses of planktic foraminifera for identification and biostratigraphic determinations were based on the size fraction greater than 106 µm. For calcareous nannofossil studies, simple smearslides were studied with the light microscope at a magnification of 1000x. Oxygen and carbon stable isotopes analyses were based on powdered samples. Analyses were conducted at the stable isotope laboratory of the University of Berne, Switzerland, using a VG Prism II ratio mass spectrometer equipped with a common acid bath (H_3PO_4). The results were calibrated to the PDB scale with the standard errors of 0.1‰ for $\delta^{18}O$ and 0.05‰ for $\delta^{13}C$. X-Ray Diffraction (XRD) analyses of whole rock and clay mineral studies were conducted at the Geological Institute of the University of Neuchâtel, Switzerland using a SCINTAG XRD 2000 Diffractometer. Whole rock compositions were determined by XRD based on methods described by Ferrero (unpublished) and Kübler [1983]. This method for semi-quantitative analysis of the bulk rock mineralogy used external standards. Clay mineral analyses followed the analytical method of Kübler [1987] described in Adatte *et al.* [1996]. We present here data from the 2µm fraction. Clay minerals are given in relative percent abundance and the clay mineral ratios are calculated from XRD mineral peak data in counts per minute.

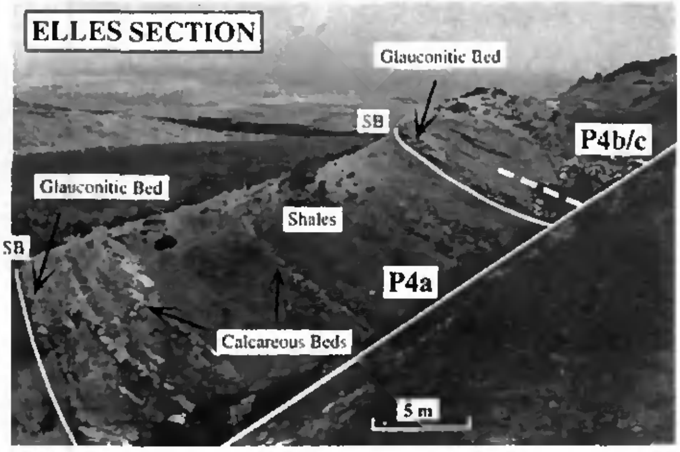

PH. 2. – Alternance of shales, marls and thin calcareous beds in P4a and P4b/c intervals at Elles (SB = sequence boundary).

PH. 2. – *Alternance de shales, marnes et minces bancs calcaires des intervalles P4a et P4b/c à Elles (SB = limite de séquence).*

RESULTS

Biostratigraphy

Foraminifera

Samples from the Foum Selja section lack planktic foraminifera and frequently also benthic foraminifera. At Elles, preservation of planktic foraminifera is variable with a relatively well preserved fauna in carbonate-rich intervals and strong dissolution in phosphate-rich intervals. In addition, there is considerable reworking of Cretaceous and Danian faunas which may reach up to 30 % of the total assemblage in the lower part of the section (Zone P4a), though reworking is relatively minor upsection. The planktic foraminiferal zonation used in this study is that of Berggren *et al.* [1995]. For the Paleocene interval this zonation differs from other zonal schemes in that the original Zone P5 has been eliminated, or effectively included in Zone P6a. Thus, the name "Zone P5" includes the interval formerly encompassed by Zones P5 and P6a. In the new zonation, the ^{13}C shift and benthic extinction event which characterize the P/E boundary interval (and Subzone P6a in previous studies) are now within Zone P5.

Zone P4

The base of the Elles section (up to 20.7 m) contains planktic foraminiferal assemblages characteristic of Subzone P4a, which include the concurrent ranges of the marker species *Globanomalina pseudomenardii* and *Acarinina subsphaerica* (fig. 3). Other characteristic species within this interval include *Acarinina mckannai*, *A. nitida*, *Morozovella velascoensis*, *M. apanthesma*, *Subbotina triangularis* and *S. velascoensis* (fig. 3). Subzones P4b and P4c mark the interval between 20.7 m and 34.3 m and are characterized by the last appearance of *A. subsphaerica* at the base of P4b and the last appearance of *G. pseudomenardii* at the top of P4c. The two subzones could not be differentiated because the marker species for the b/c boundary, *A. soldadoensis*, is already present at the top of Subzone P4a. This suggests a range overlap of *A. subsphaerica* and *A. soldadoensis* and possibly condensation or a hiatus with part of P4b missing. An abrupt change in the faunal assemblage at 20.7 m, maximum reworking between 19-20.7 m, plus a lithological change across this interval all point towards a sea level fall and erosion, followed by a sea level rise (fig. 2).

Zane P5

Zone P5 marks the interval from the last appearance of *G. pseudomenardii* to the last appearance of *M. velascoensis* and at Elles spans the interval between 35 m and 51.5 m (fig. 3). In the lower part of this zone (from 34.3 m to 41.5 m) planktic foraminifera are rare and poorly preserved. Between 41.5 m and 44.2 m, samples are barren due to dissolution. The upper part of Zone P5 contains increasingly abundant and well preserved planktic foraminifera. Characteristic assemblages in Zone P5 include abundant morozovellids (*M. velascoensis*, *M. subbotina*, *M. apanthesma*, *M.*

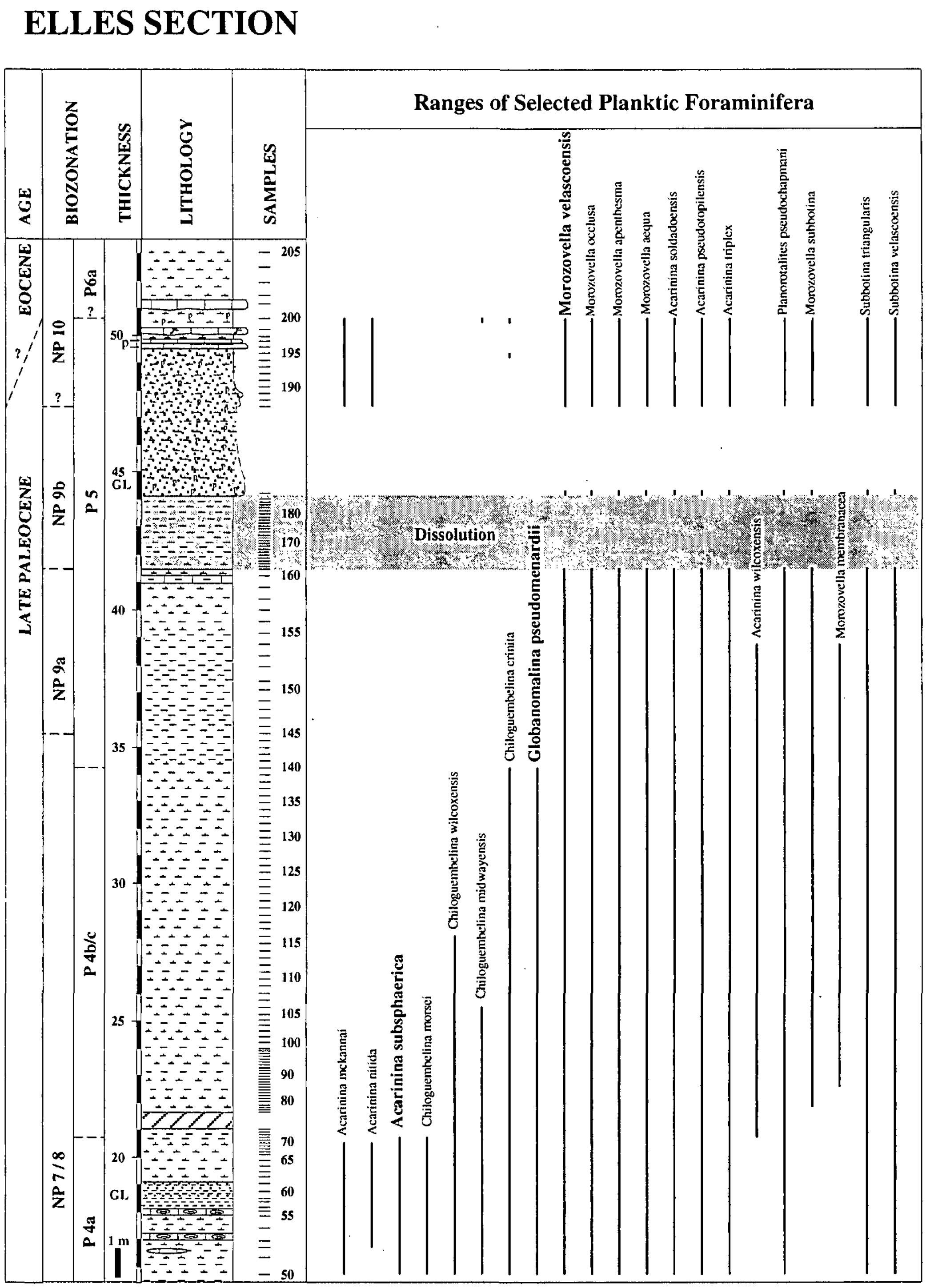

FIG. 3. – Range chart of critical planktic foraminifera at Elles.

FIG. 3. – *Charte de répartition des espèces critiques de foraminifères planctoniques à Elles.*

aequa, *M. occlusa*), large acarininids (*A. soldadoensis*, *A. pseudotopilensis*), and common biserial taxa (*Chiloguembelina crinita*) (fig. 3). High abundance of these taxa is characteristic of the generally warm climate following the ^{13}C shift and benthic extinction event [Pardo *et al.*, 1997], suggesting that the P/E event is likely within the dissolution interval below. In many sections, the P/E event is marked by strong carbonate dissolution, reduction of primary productivity and/or dilution by detrital minerals [Lu *et al.*, 1996; Bolle *et al.*, 1998].

Zone P6a

This zone is defined by the stratigraphic interval from the last appearance of *M.velascoensis* to the first occurrence of *M. formosa* and/or *M. lensiformis*.

Calcareous nannofossils

With the exception of rare, small and not identifiable reticulofenestrids in the uppermost thick bed, no calcareous nannofossils were found in the Thelja Formation of the

TABLE I. – Distribution chart of calcareous nannofossils identified at Elles and Foum Selja.

TABL. I. – *Charte de distribution des nannofossiles calcaires identifiés à Elles et Foum Selja.*

Calcareous nanno-fossils at Foum Selja and Elles	Abundance	Preservation	Bientholithus sp.	Biscutum sp.	Braarudosphaera bigelowii	Campylosphaera (eo)dela	Chiasmolithus cf. C. bidens	Chiasmolithus sp.	Chiasmolithus solitus	Coccolithus eopelagicus	Coccolithus pelagicus	Cruciplacolithus latipons	Cruciplacolithus sp. 10μ	Discoaster anartios	Discoaster binodosus	Discoaster bramlettei	Discoaster delicatus (4-8μ)	Discoaster diastypus	Discoaster lelcatus	Discoaster lenticularis	Discoaster mediosus	Discoaster megastypus	Discoaster mohleri
FS 88	vR	P						X			X				?								
FS 79	R	P																					
FS 71	+	vP									X												
FS 52	+	vP									?												?
FS 48	F	M					X	X			X												X
FS 48	R	P									X												
FS 31	F	P	X	X							X	X											
FS 28	+	vP									X												
EL195	R	Pm																					
EL194	F	Pm				X		X		X	X												
EL187	F	P								X	X		X					X					
EL183	+	P									X												
EL181	+	P									X												
EL179	+	P								X	X												
EL177	R	P									X												
EL175	vR	P									X								X				
EL173	vR	P									X												
EL171	R	P									X												
EL169	R	P									X												
EL167	Fc	Pm	?						X	X	X		X										
EL163	F	Pm								X	X			?						X		X	
EL161	Cf	Mp				X		X		X	X	?								X			
EL156	FC	M					X			X	X												
EL151	C	M					X	X	X	X	X	X	X				X						
EL145	Fc	M							X	X	X	X				X			X	X			X
EL139	A	Gm					X	X	X	X	X	X	X			?	X					?	
EL129	Fc	M									X		X										X
EL122	C	M						X		X	X		X										X
EL105	A	Gm						X		X	X	X	X							?	?		X
EL101	A	G						X		X	X	X	X	?									X
EL32	C	M			X			X		X	X	X	X		?								X

Calcareous nanno-fossils at Foum Selja and Elles	Discoaster multiradiatus	Discoaster s. 6 arms	Discoaster sp. 8 arms	Discoaste rsp. 9 arms	Ellipsolithus distichus	Ellipsolithus macellus	Ericsonia robusta	Ericsonia subpertusa/formosa	Fasciculithus magnicordis	Fasciculithus involutus	Fasciculithus? sp.	Fasciculithus schaubii	Fasciculithus sidaraus	Fasciculithus tympaniformis	Fasciculithus sp.	Fasciculithus/Heliolithus? sp.	Heliolithus kleinpellii	Hornibrookina sp.	Markalius variabilis	Markalius sp.	Micrantolithus sp.	Neochiastozygus distentus	Neochiastozygus sp.	Neochiastozygus junctus	Neochiastozygus c.f N. perfectus	Neococcolithes protenus	Neocrepidolithus sp.	Placozygus sigmoides	Pontosphaera rimosa	Pontosphaera sp.
FS 88	X																													
FS 79	?																													
FS 71	?																													
FS 52						?																								
FS 48								X	X					X			?	?						?	X	X	X	X		
FS 48								X									X								X					
FS 31								X										X									X	X		
FS 28								X			X																			
EL195																														
EL194	X					X		X														X		X						X
EL187																	X						X							
EL183														X																
EL181										X				X																
EL179	X									X	X			X																
EL177	X											X																		
EL175	X									X				X																
EL173	X													X																
EL171	X																													
EL169	X		X											X																
EL167	X			X	X					X				X														X		
EL163	X	X										X	X	X						?										
EL161	X							X		X				X																
EL156	X													X														X		
EL151	X				X	X	X	X		X				X	X					X			X	X	X			X		
EL145	X				X	X				X				X									X	X						
EL139					X	X	X	X		X	X			X	X	X				X		X	X	X	X			X		
EL129								X						X																X
EL122							X	X		X				X				X		X		X	X		X		X			
EL105					X	X	X	X		X				X	X	X	X	X	X			X	X		X	X	X		X	
EL101					X	X	X	X		X				X	X	X		X					X		X		X		X	X
EL32					X		X	X		X				X	X			X			X	X	X		X			X		

Calcareous nanno-fossils at Foum Selja and Elles	Prinsius bisulcus	Prinsius martinii	Rhomboaster cuspis	Scampanella sp.	Scapholithus fossilis	Scapholithus rhombicus	Semihololithus biskayae	Sphenolithus anarrhopus	Sphenolithus sp.	Sphenolithus cf. S. radians	Sullivania consueta	Sullivania 'maxi' >15μ	Sullivania sp. MINI	Thoracosphaera sp.	Toweius craticulus	Toweius eminens	Toweius occultatus	Toweius sp.	Zygodiscus bramlettei	Zygodiscus herlynii	Zygrhablithus bijugatus	Zygodiscus adamas	NP, Martini, 1971
FS 88																		X					10
FS 79																							?
FS 71																							9
FS 52									X														
FS 48		X							X		X		X	X	X	X		X					7/8
FS 48		X												X	?			X					6
FS 31	X	X														X		X					4/5
FS 28																							
EL195																							
EL194		X												X				X			X		10
EL187		X							X					X	X	X							
EL183																							
EL181																							
EL179																							
EL177									X							X					X		
EL175									X		X						X						
EL173									X														
EL171									X							X		X					9b
EL169																		X					
EL167									X					X		X		X			X		
EL163		X							X														
EL161		X	?				X		X						X			X		X			
EL156									X							X							
EL151		X				X			X		X		X	X	X	X		X	X	X		X	9a
EL145						X			X		X			X		X				X			
EL139		X				X			X		X		X	X	X	X		X		X			
EL129		X									X												
EL122		X							X	X	X		X	X	X	X		X		X		X	
EL105		X			X	X		?	X		X		X	X	X	X		X		X		X	7/8
EL101		X		X	X	X			X		X	X		X	X	X		X		X	X	X	
EL32	X	X				X			X		X	X	X	X	X	X		X		X	X		

Reworked Calcareous nanno-fossils at Foum Selja and Elles	Arkhangelskiella cymbiformis	Biscutum sp.	Cretarhabdus crenulatus	Cribrosphaera ehrenbergii	Eiffellithus turriseiffelii	Lithastrinus grillii	Lucianorhabdus cayeuxii	Microrhabdulus attenuatus	Micula decussata	Micula prinsii	Micula swastica	Quadrum sp.	Prediscosphaera cretacea	Watznaueria barnesae
FS 86														
FS 79									X		X	X		X
FS 71														
FS 52														
FS 48														X
FS 46					X			X						
FS 31			X			?			X				X	
FS 28														
EL195														
EL194														X
EL187														
EL183														
EL181														
EL179									X					
EL177														
EL175														
EL173									X					
EL171									X					
EL169														
EL167									X					
EL163									X					
EL161														
EL156									X					
EL151	X													
EL145														
EL139														
EL129														
EL122														
EL105														
EL101														
EL32					X									X

Abundance
A = abundant
C = common
F = few
R = rare
X = present
X = marker species

Preservation
G = good
M = moderate
P = poor

Foum Selja section. In samples 6.2 and 6.3, however, reddish spherules with a diametre of about 5 µ are quite common. Such spherules are not unusual in sediments where no coccoliths are found. The spherules could represent pseudomorphs after coccospheres of very small coccoliths such as *Neobiscutum* or *Prinsius* (Lower Danian), *Prinsius dimorphosus* (Lower Danian) or other, younger very small coccospheres. The first, very rare and poorly preserved calcareous nannofossils appear towards the top of the lowermost marly interval of the Chouabine Formation (fig. 2 and table I). The presence, in sample 28, of *Coccolithus pelagicus*, *C.* cf. *C. robustus* and *Fasciculithus* sp. indicates an age not older than the upper part of Zone NP4, more likely Zone NP5 of Martini [1971]. The presence of *Heliolithus cantabriae* and specimens between *H. cantabriae* and *H. kleinpellii* suggest the upper part of Zone NP5 in sample 31, which also contains an unusually high abundance of *Hornibrookina* cf. *H. teuriensis*. The very poor assemblage of sample 52 contains the first specimen of the genus *Discoaster*, possibly *D. mohleri*, and thus can tentatively be assigned to Zone NP7 or younger. In samples 71 and 79, poorly preserved parts of what are probably *Discoaster multiradiatus* were found. This suggests that the upper part of the Chouabine Formation belongs to Zone NP9 (or Zone NP10). No classical markers of calcareous nannofossil zones younger than Zone NP9 were found in sample 86 which includes very rare *Discoaster multiradiatus*, *D. binodosus*, *Chiasmolithus* cf. *C. solitus* and *Toweius* sp. (tab. I). The number of rays in *D. multiradiatus* is around 18, the size about 13 µ. Such small forms with few rays usually occur in Zone NP10 rather than Zone NP9 [Wei, 1992].

At Elles, calcareous nannofossils are rare to common and poorly to moderately-well preserved. *Discoaster mohleri* was found from the lowermost samples studied, thus Zone NP7 includes the base of the section. The marker for the base of Zone NP8, *Heliolithus riedelii*, was not found – a not uncommon situation, which has led to the combining of the two zones in many regions of the world. At the base of Zone NP9, the first occurrence (FO) of *Discoaster multiradiatus*, was observed in sample 145 and the presence of the upper part of Zone NP9 (NP9b) is indicated by *Campylosphaera eodela* in sample 161 (tab. I). Above this level, one would expect the successive appearances of the genera *Rhomboaster* and *Tribrachiatus*, which usually serve to subdivide Zone NP10. Neither genus was found and thus Zone NP10 could not be recognized with the original marker. On the other hand, the FO of *Discoaster diastypus* is often used to approximate the lower boundary of Zone NP10, and its lowermost occurrence is in sample 187. At this level, no more species of the genus *Fasciculithus* were found (tab. I). The genus usually becomes extinct in the lower part of Zone NP10. At Elles, the stratigraphically highest specimens were encountered in the shales which represent the P/E boundary interval. These are the very rare calcareous nannofossils which resisted dissolution, in addition to *Discoaster multiradiatus*.

Reworked flora from the upper Cretaceous were found in several samples from both Foum Selja and Elles (tab. I). Reworking from sediments of this age thus occurred repeatedly during the deposition of the Chouabine Formation. At Elles, reworking seems to have been most common before and after the P/E event. At Foum Selja, reworking is especially evident in sample 79, where the reworked Upper Cretaceous calcareous nannofossils *Micula decussata*, *M. swastica*, *Quadrum* sp. and *Watznaueria barnesae* are more abundant than the very rare, probably in situ, forms.

The abundance relationship between the families of the *Coccolithaceae* and *Prinsiaceae* changes across the P/E boundary interval both in the northern and southern Tethys and in the Pacific [Von Salis *et al.*, 1998]. From a predominance of small and middle sized forms of *Prinsiaceae* below the P/E boundary interval a near total disappearance of the *Prinsiaceae* can be observed and their return occurs well after the P/E boundary interval. At Elles, this shift can be observed in NP9b, below the barren interval. Upsection where coccolith assemblages are again preserved (sample 187), the *Prinsiaceae* are again dominant over the *Coccolithaceae*. The *Prinsiaceae* are coccolithophorids which today take advantage of high nutrient supply whereas other families are more abundant at lower nutrient levels. This relationship may suggest that nutrients were relatively scarce at the P/E boundary at this locality.

Mineralogy

Bulk rock

Bulk rock variations reflect changes in sediment source that reflect variable intensity of weathering and erosion under arid and humid climates and the variable influx of terrigenous sediments into the oceans during sea level fluctuations. Bulk rock compositions were analyzed in the marine sediments of the Elles and Foum Selja sections to evaluate sediment sources, proximity to terrigenous sediments and intensity of erosion and transport associated with sea level changes.

Foum Selja

In this section, bulk rock analysis shows variable mineralogy (fig. 4). In the first 25 metres of the Thelja Formation, dolomite averages 50 % in shaly beds and alternates with calcite-rich shelly beds (60-90 %), with the remaining constituents phyllosilicates. From 25 m to 56.5m, dolomite predominates, averaging 75 % though decreasing near the top to 55 % (fig. 4), with phyllosilicates increase. The presence of gypsum and halite reflects enhanced evaporation. The low detritus/carbonate ratio in the Thelja Formation suggests reduced terrigenous input into the shallow restricted Gafsa Basin during the formation of evaporites. In the Chouabine Formation phyllosilicates dominate (71 %) in the lower part. In this interval, first phosphate deposits appear and calcite is highly variable from bed to bed ranging from near 0 to 80 %. The phosphatic layer consists of a carbonate fluoroapatite, francolite [Lucas *et al.*, 1979]. Phosphate can reach a maximum of 93 %. This enrichment is interpreted to be a result of the low sedimentation rate leading to episodes of phosphatogenesis [Sassi, 1974]. In the Kef Eddour Formation, carbonates (calcite and dolomite) are dominant, varying between 10 % and 80 %. In this interval, francolite and phyllosilicates decrease to a mean value of 10 % and 36 % respectively (fig. 4). Minor components of this section include detritus (the combination of quartz, K-feldspar and plagioclase). The low detritus/carbonate ratio and high francolite content indicate decreased detrital input during periods of phosphate deposition.

Elles

The major components of the bulk rock are phyllosilicates, which average 68 % in the first 45 metres of the section and decrease to 20 % in the last 9 metres (fig. 5). Calcite content is variable and reaches 70 % in calcareous beds of the lower and top parts of the section, but generally averages less than 25 %. Phosphate reaches 16 % in the upper part of the section and coincides with a decrease in phyllosilicates to 25 %. Detrital minerals are less common and include primarily quartz, some plagioclase and K-feldspar. Quartz averages 5 % throughout the section.

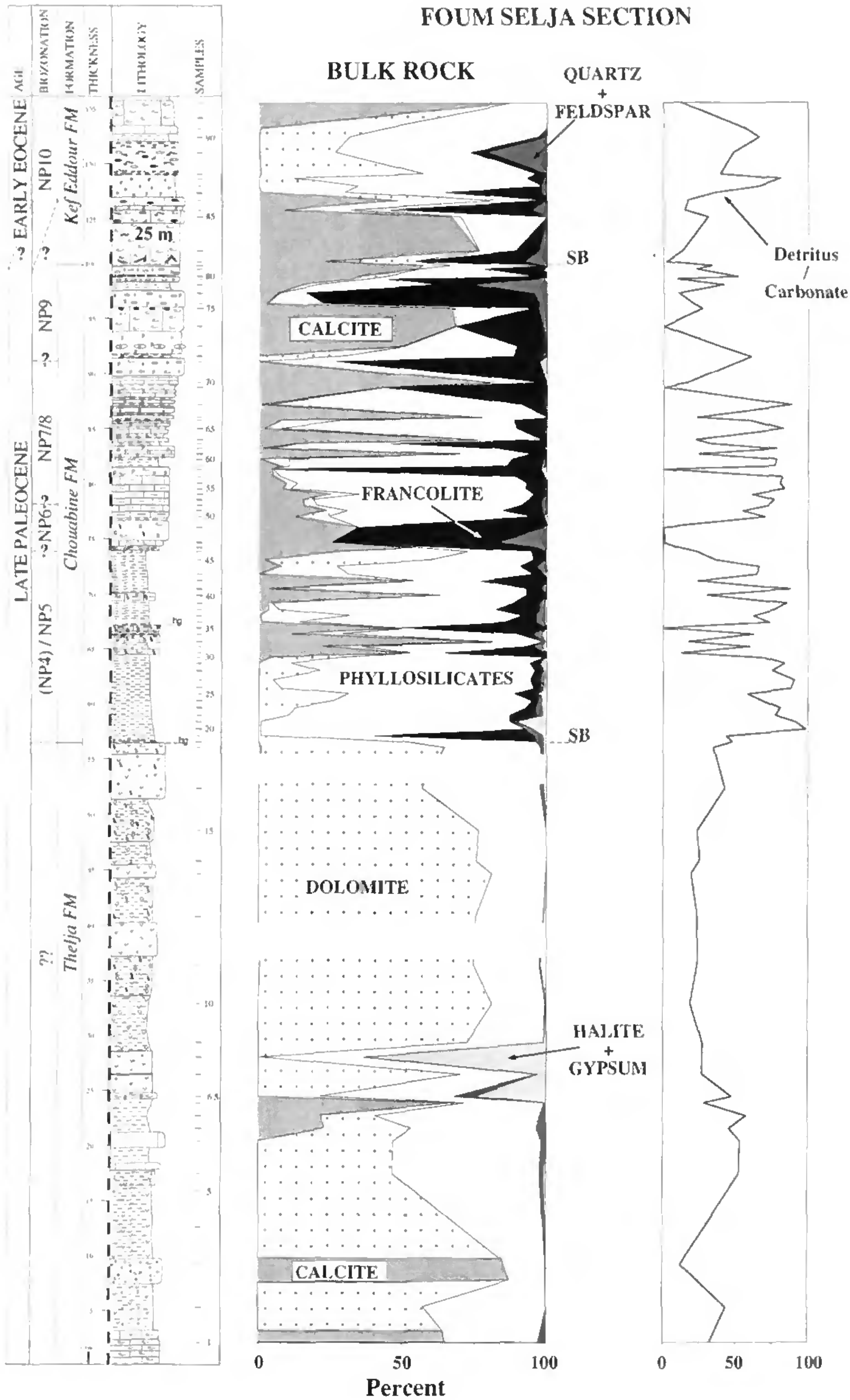

FIG 4. – Bulk rock mineral compositions and the detritus/carbonate ratio at Foum Selja. The label detritus includes quartz, plagioclase, K-feldspar and phyllosilicates. The ratio is calculated from XRD mineral peak data in counts per minute.

FIG. 4. – *Composition minéralogique de la roche totale et rapport détritique/carbonate à Foum Selja. Le label détritique inclus le quartz, le plagioclase, le feldspath potassique et les phyllosilicates. Le rapport est exprimé en intensités brutes (coups par minute).*

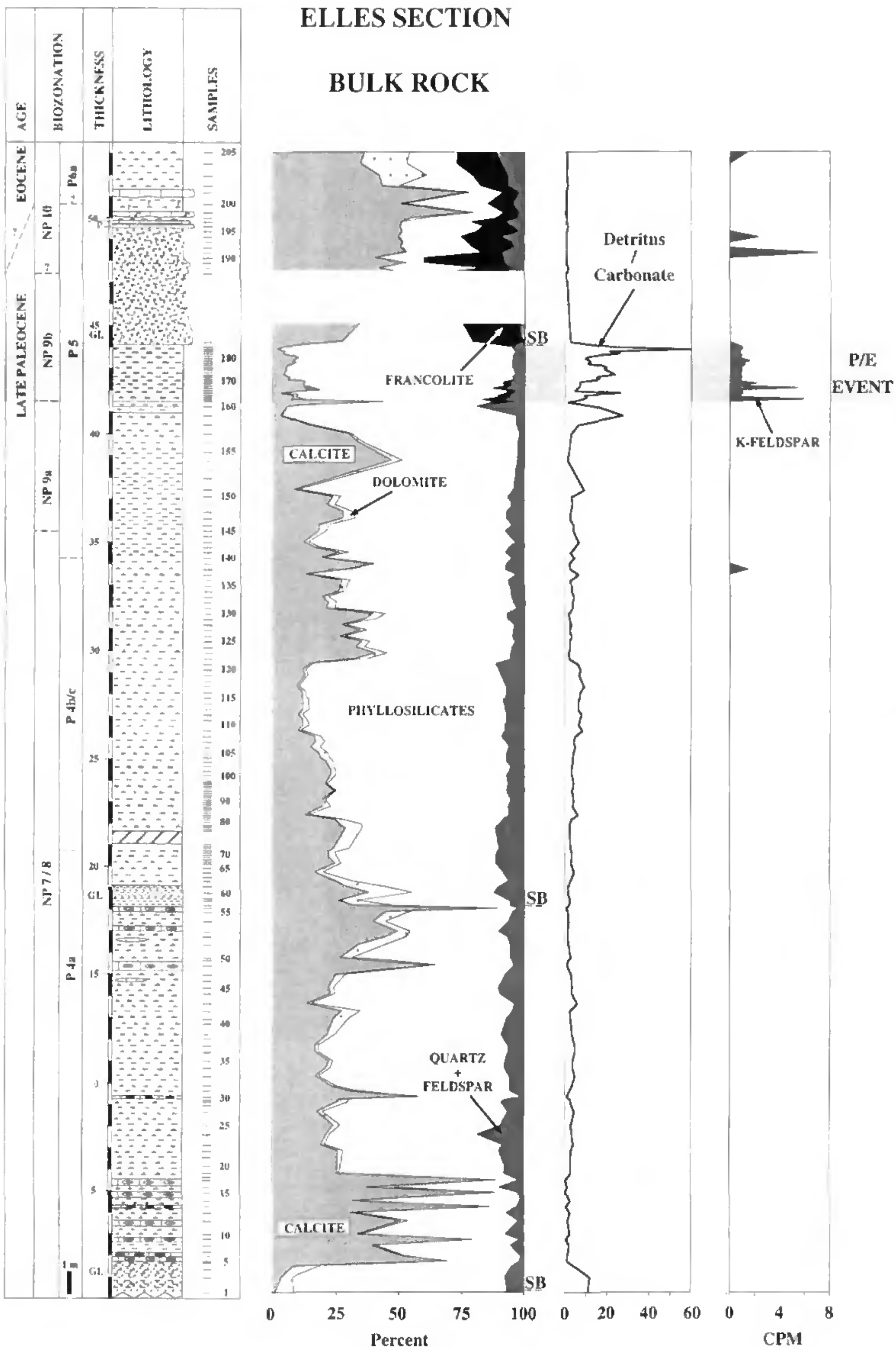

FIG. 5. – Bulk rock mineral compositions and the detritus/carbonate ratio at Elles. Ratio is calculated from XRD mineral peak data in counts per minute.

FIG. 5. – *Composition minéralogique de la roche totale et rapport détritique/carbonate à Elles. Le rapport est exprimé en intensités brutes (coups par minute).*

The clay interval (P/E transition event) is marked by a drastic decrease in calcite from 30 % to 7 %, an increase in phyllosilicates to 85 %, the occurrence of K-feldspar (1 to 6 %). The restricted presence of K-feldspar and the high detritus/carbonate ratio in this interval suggest an increase in terrigenous influx at this time. These mineralogical changes may reflect decreased primary productivity and/or dissolution and increased erosion.

The main mineralogical differences between the Foum Selja and the Elles sections include the higher quartz content at Elles (5 %) as compared with Foum Selja (1.5 %) and the dominance of phyllosilicates at Elles versus calcite and dolomite at Foum Selja. In addition, glauconite is abundant at Elles whereas francolite is abundant at Foum Selja. The onset of phosphate deposition is diachronous in the two sections. At Elles, phosphatic minerals first appear in Zone NP9 at the base of the P/E event and increase strongly above it, whereas at Foum Selja, francolite is already present in Zone NP4 or NP5.

In the two sections, sequence boundaries (SB) and transgressive surfaces (TS) are marked by bulk rock composition changes. In a sequence-stratigraphic context, phosphate deposits preferentially occur along transgressive and maximum flooding surfaces [Föllmi, 1996]. Thus at Foum Selja, high francolite contents underline the transgressive surfaces and consequently the sequence boundaries below (fig. 2). At Elles, sequences boundaries are essentially marked by the presence of glauconite. Nevertheless in this section, bulk rock composition changes characterize mainly the P/E interval, reflecting processes other than erosion, reduced sedimentation or reworking (fig. 5).

Clay-minerals

Foum Selja

In this section, the clay mineral content (< 2 µm fraction) is highly variable (fig. 6). Kaolinite is the major component in the first 23 metres (11 to 77 %). The dramatic decrease in kaolinite coincides with an increase in smectite (34 to 75 %) and increased mica (20 to 50 %) in the uppermost 22 metres of the Thelja Formation. The Chouabine Formation is characterized by high amounts of smectite (37 to 95 %), the presence of mica (1 to 25 %) and the occurrence of palygorskite and sepiolite (2 to 40 %). Kaolinite is only present (1 to 30 %) in the basal 5 metres of the Chouabine Fm. The mineralogical composition of the Kef Eddour Formation is very similar to that of the Chouabine Fm, though palygorskite reached peak abundance of 60 % and smectite decreased.

Elles

Smectite is the major component in Zone P4a with an average of 74 %. Kaolinite (9 %), mica and chlorite are minor components and average respectively 11 % and 6 % (fig. 7). The Zone P4b/c interval is marked by increased smectite (78 %), kaolinite (12 %) and decreased mica (8 %) and chlorite (3 %). The lower part of Zone P5 is characterized by increased kaolinite, with maximum values (16-48 %) coinciding with decreased smectite from 78 to 58 % across the P/E transition. The upper part of Zone P5 (45 m to 52 m) and lower part of Zone P6a lack kaolinite. Its absence corresponds with an increase in smectite to 92 % and an increase in mica from 4 % to 7 %.

Stable Isotopes

Elles

Below the 2.7 metres thick clay layer which biostratigraphically corresponds to the P/E transition, $\delta^{13}C$ values gradually decrease from 1.25 to – 0.4 ‰ (fig. 8 and table II). Within the clay layer, $\delta^{13}C$ values decrease by 1.3 ‰ and reach minimum values (– 1.7‰) between 42.8 and 44.6 m. Above the P/E interval, in the glauconite enriched-phosphate sandstone, $\delta^{13}C$ values drop to a minimum of – 2.5‰. In this sandstone $\delta^{18}O$ values are also very negative (– 3.8 to – 2.95‰). High carbonate fluorapatite (francolite) content generally coincides with the negative $\delta^{13}C$ and $\delta^{18}O$ values measured above the P/E interval (fig. 8 and tab. II).

TABLE. II. – Elles section : analyses of stable isotopes ($\delta^{13}C$ and $\delta^{18}O$) and francolite content.

TABL. II. – *Profil d'Elles : analyses isotopiques ($\delta^{13}C$ and $\delta^{18}O$) et minéralogiques.*

Elles section

Samples	δ 13 C	δ 18 O	Apatite
	(‰)		(%)
86	1.25	-2.97	0
102	0.69	-1.49	0
115	-0.44	-1.05	0
122	0.32	-1.38	0
130	0.16	-2.43	0
137	0.10	-1.44	0
143	-0.16	-1.11	0
149	-0.93	-1.26	0
153	-0.12	-0.97	0
156	-0.86	-2.03	0
160	-0.41	-1.34	0
162	-0.71	-1.51	8.45
164	-0.55	-1.50	7.39
166	-1.25	-1.51	3.3
168	-1.05	-1.52	2.83
170	-1.71	-1.69	2.19
172	-0.67	-1.29	0
175	-0.78	-1.11	0
178	-0.86	-1.50	0
180	-1.31	-1.68	0
183	-1.34	-1.28	0
185	-0.90	-1.45	0
186	-2.63	-3.82	19.92
189	-1.85	-3.14	31.95
193	-1.46	-2.95	18.08
198	-0.99	-2.74	8.59
202	-1.17	-2.47	11.1
205	-1.56	-2.24	15.42

Foum Selja

The very negative $\delta^{13}C$ (between –2 and –12‰) and $\delta^{18}O$ (between –0.7 and –5.5‰) values coincide generally as in the Elles section with high francolite content (fig. 8 and table III).

The presence of francolite, formed during early diagenesis and characterized by very "light" $\delta^{13}C$ (– 12‰) and $\delta^{18}O$ (– 11‰) values [Kastner *et al.*, 1984; Mertz, 1984] probably obscurs or overprints the original marine isotopic signals in both sections.

TABLE III. – Foum Selja section : analyses of stable isotopes ($\delta^{13}C$ and $\delta^{18}O$) and francolite content.

TABL. III. – *Profil de Foum Selja : analyses isotopiques ($\delta^{13}C$ and $\delta^{18}O$) et minéralogiques.*

Foum Selja Section

Samples	δ 13 C	δ 18 O	Apatite
	(‰)		(%)
60	-5.55	-0.70	10.99
65	-4.98	-1.31	9.35
69	-10.57	-5.37	56.74
70	-12.77	-1.48	1.84
72	-8.45	-1.02	9.93
73	-9.55	-3.34	10.29
74	-2.64	-3.36	30.57
75	-1.96	-3.51	2.60
78	-6.69	-2.84	12.23
80	-8.44	-3.38	4.33
82	-8.70	-3.50	0
84	-2.21	-4.89	8.30

FIG. 6. – Clay mineral composition, smectite/mica + chlorite ratio and inferred climatic conditions at Foum Selja. Ratio is calculated from XRD mineral peak data in counts per minute.

FIG. 6. – *Nature des minéraux argileux, rapport smectite/mica + chlorite et évolution climatique à Foum Selja. Le rapport est exprimé en intensités brutes (coups par minute).*

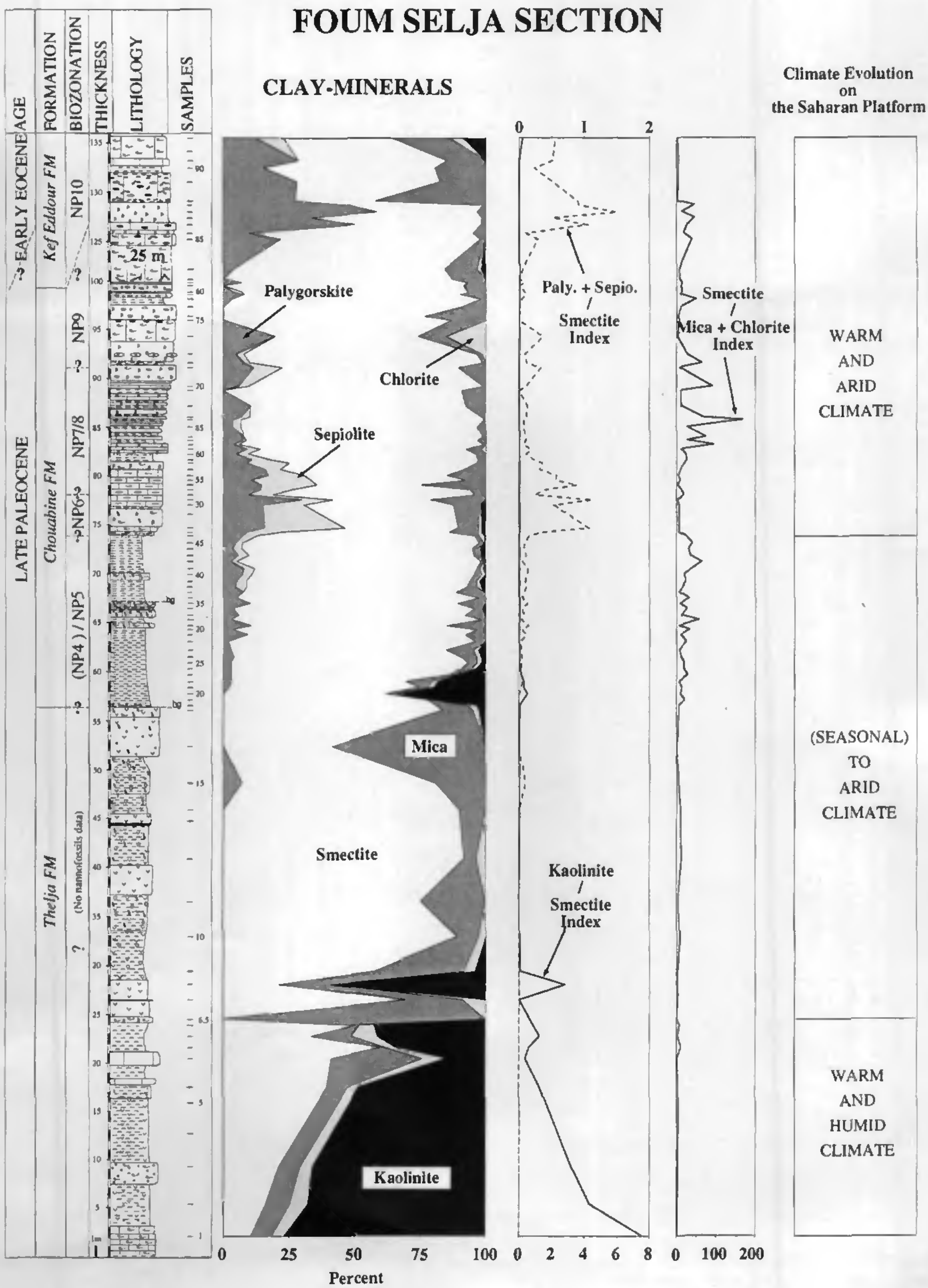
FOUM SELJA SECTION
CLAY-MINERALS
Climate Evolution on the Saharan Platform
AGE
FORMATION
BIOZONATION
THICKNESS
LITHOLOGY
SAMPLES
EARLY EOCENE
LATE PALEOCENE
Kef Eddour FM
Chouabine FM
Thelja FM
NP10
NP9
NP7/8
NP6
(NP4) / NP5
(No nannofossils data)
25 m
Palygorskite
Chlorite
Sepiolite
Mica
Smectite
Kaolinite
Paly. + Sepio. / Smectite Index
Smectite / Mica + Chlorite Index
Kaolinite / Smectite Index
WARM AND ARID CLIMATE
(SEASONAL) TO ARID CLIMATE
WARM AND HUMID CLIMATE
0 25 50 75 100
Percent
0 1 2
0 2 4 6 8
0 100 200

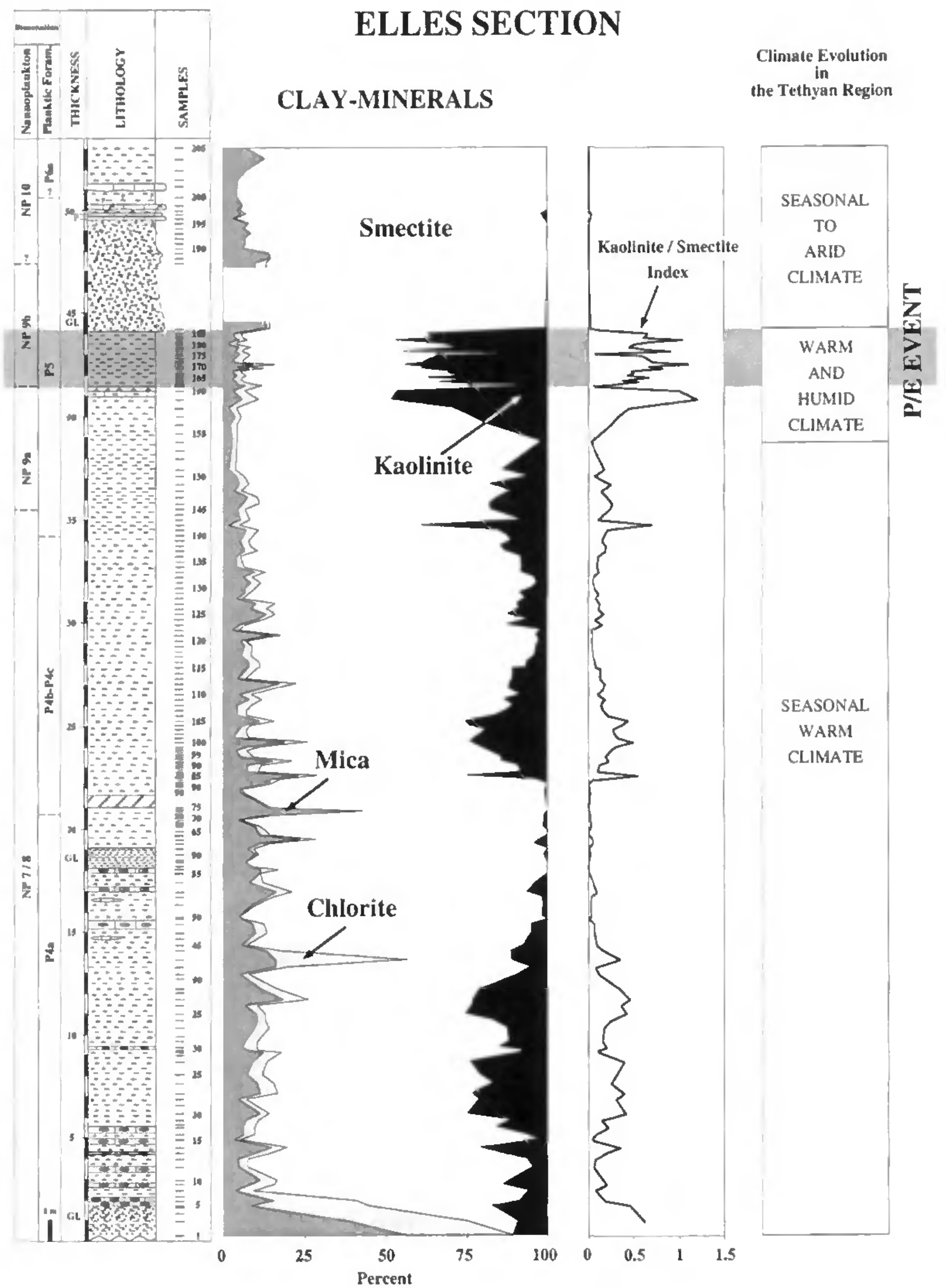

FIG. 7. – Clay mineral composition, kaolinite/smectite ratio and inferred climatic conditions at Elles. Ratio is calculated from XRD mineral peak data in counts per minute.

FIG. 7. – *Nature des minéraux argileux, rapport kaolinite/smectite et évolution climatique à Elles. Le rapport est exprimé en intensités brutes (coups par minute).*

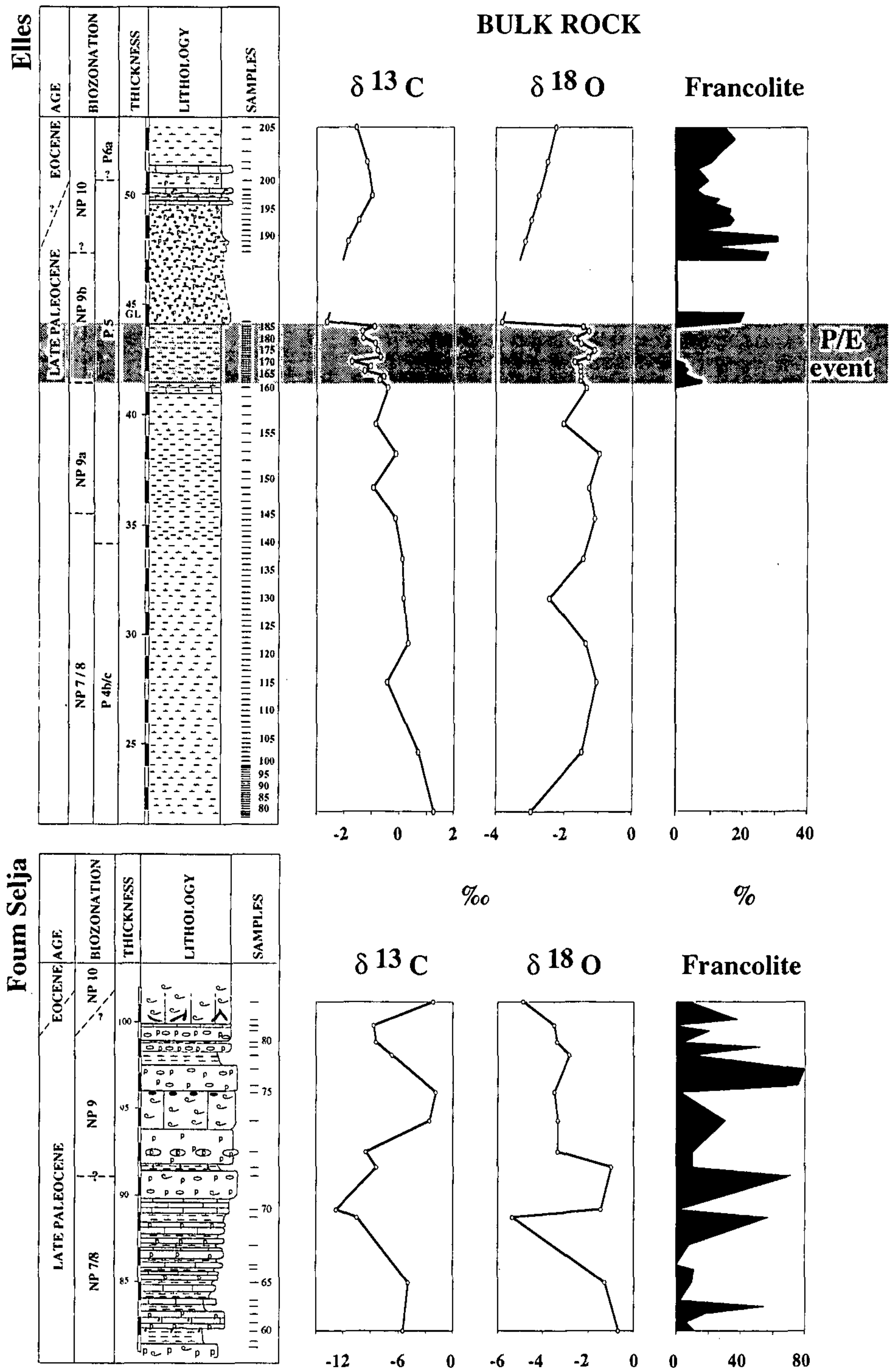

FIG. 8. – Stable isotopic bulk rock analysis ($\delta^{13}C$ and $\delta^{18}O$) correlated with francolite across the Paleocene-Eocene transition at Elles and Foum Selja.

FIG. 8. – *Variations des valeurs des isotopes stables ($\delta^{13}C$ and $\delta^{18}O$) mesurés sur la roche totale corrélées avec la teneur en francolite à Elles et à Foum Selja.*

DISCUSSION

Paleocene-Eocene transition

The P/E transition is globally characterized by a mass extinction in benthic foraminifera, turnover in planktic foraminifera and calcareous nannoplankton, an abrupt negative $\delta^{13}C$ excursion, decreased calcite and increased detrital minerals. At Elles, the P/E transition identified by fauna, mineralogical bulk rock and isotopic analyses corresponds to a 2.70 m thick clay layer as also observed at Zumaya and Trabakua [Canudo *et al.*, 1995; Bolle *et al.*, 1998] in northern Spain (Atlantic Realm) and at Alamedilla [Lu *et al.*, 1998] and Caravaca [Canudo *et al.*, 1995] in southern Spain (Tethyan Realm). These characteristic trends cannot be identified at Foum Selja where sediments were deposited in the shallow restricted Gafsa Basin which bordered the Saharan Platform to the south.

Phosphate deposits which obliterate the original isotopic signal, strong dissolution of the planktic fauna and flora in these phosphatic layers, and the presence of a condensed interval just after this event, all are criteria that prevent the choice of the Elles section as a potential GSSP candidate for the P/E boundary.

Clay minerals : Climatic signal?

Clay minerals and their relative abundance may record informations on climate, eustasy, burial diagenesis, or reworking. The constant but variable presence of smectite and the high kaolinite content observed at the base of Foum Selja and during the P/E interval at Elles suggest that the sediments of the two sections did not suffer a deep burial diagenesis. This implies that clay minerals may come from detrital or authigenic sources. Authigenic smectite, palygorksite and sepiolite can form locally in deep-sea environments during hydrothermal weathering of volcanic rocks [Karpoff *et al.*, 1989; Chamley, 1998] or through the alteration of clay minerals at the water/sediment interface [Thiry and Jacquin, 1993; Pletsch, 1998]. However, from the Paleocene to early Eocene the southern Tethyan margin corresponded to a relatively stable period, with no hydrothermal and submarine volcanic activity [Oberhänsli, 1992] suggesting a detrital origin for these minerals which can thus be used as markers of past continental climates. Smectite reflects generally a warm climate, with seasonally alternating wet and dry conditions whereas palygorksite and sepiolite form mainly on warm but arid land masses associated with enhanced evaporation [Robert and Chamley, 1991].

Kaolinite results either from increased runoff, which could be caused by sea level lowering, or by increased rainfall. This mineral may develop in tropical soils characterized by warm, humid climate, well-drained areas with high rainfall and accelerated leaching of parent rocks [Robert and Chamley, 1991; Robert and Kennett, 1994]. Nevertheless, kaolinite may be introduced in significant amounts into oceanic sediments through the erosion of older sediments and soils during sea level transgressions [Thiry, 1989; Chamley, 1998].

The P/E interval is marked in South Atlantic and Antarctica [Robert and Chamley, 1991; Robert and Kennett, 1992, 1994], in North Atlantic [Gibson *et al.*, 1993; Knox, 1996; Gawenda *et al.*, 1999] and in some Tethyan sections [Adatte and Lu, 1995; Lu *et al.*, 1998] by the appearance or a strong increase in kaolinite. This high kaolinite content has been interpreted as marker of humidity. Even if at Elles, kaolinite is partly reworked, the general trend of this mineral is in agreement with those observed in many P/E sections. In this section, the strong increase of kaolinite may be related to the humid climatic episode which affected many regions during the P/E transition. At Foum Selja, the disappearance of kaolinite before Zone NP4-5, during a relatively stable high sea level, its absence during the P/E transgression [Haq *et al.*, 1988] and the appearance of different minerals such as palygorskite and sepiolite confirm that the detrital clay mineral distribution record minors regional qualitative climatic changes. Thus, the kaolinite/smectite index reflects climate variations from humid/warm to more seasonal conditions. The increase of the palygorskite-sepiolite/smectite index indicates changes from seasonal to warm and arid climatic conditions. However, at Foum Selja, the reappearance in few amounts of kaolinite, restricted to the first 3 metres of the Chouabine Formation (fig. 6) is probably rather due to reworking accelerated during the sea level rise which marks the base of the phosphatic sequence than to a brief warm and humid pulse (fig. 2).

Climatic Evolution

Clay mineral variations in the sediments of Foum Selja and Elles reveal the climatic and environmental evolution of the Gafsa and El Kef Basins during late Paleocene to early Eocene. The two sections are located in two different palaeogeographic areas separated by Kasserine Island and their mineral composition suggests different climatic conditions. At Foum Selja, sediment deposition occurred in the shallow restricted Gafsa Basin which was generally cut-off from the open marine environment to the north during low sea level intervals. The principal sediment source for the Gafsa Basin was the adjacent Saharan Platform. The high kaolinite/smectite ratio observed before Zone NP4-5 indicates a warm and humid climate on the Saharan Platform (fig. 6). This climatic trend is in agreement with the generally humid and warm climate that marked the end of the Cretaceous and the early Danian (P1a to P1c) in this region [Keller *et al.*, 1998]. The disappearance of kaolinite and high amount of smectite suggest a seasonal to arid climate with enhanced evaporation on the adjacent coastal areas, as indicated by the presence of evaporites. Arid climatic conditions developed on the Saharan Platform in nannofossil Zone NP6, reaching maximum aridity in Zone NP 10 indicated by the high ratio of palygorskite-sepiolite/smectite. Similar climatic conditions have been observed in the coastal basins and peri-marine environments of West Africa, from Morocco to Benin, where palygorskite deposition increased during the late Paleocene, indicating that low-latitudes and especially their coastal areas, were subjected to intensive dryness and evaporation [Robert and Chamley, 1991].

Sediment deposition at Elles occurred in an open marine environment connected to the Tethys. The sediment source was primarily from the Tethyan region. The low kaolinite content and the abundance of smectite suggest a seasonal warm climate in the late Paleocene (Zones P4, NP7-8) whereas the very high kaolinite/smectite ratio implies a warm and humid climate across the P/E transition (Zones P5, NP9). The development of arid to seasonal climatic conditions in the Tethyan region after the P/E event is suggested by the disappearance of kaolinite and the increase of mica and smectite (fig. 7).

Similar climatic variations have been observed in the Atlantic and the northern part of the Tethyan Realms. At Zumaya in northern Spain, kaolinite was deposited during the early Paleocene (Zones NP1 to NP4), and just before the P/E interval (Zone NP9) reaching a maximum of 45% within this interval [Gawenda *et al.*, 1999]. The early Eocene (Zone NP10-11) is marked by decreased kaolinite and corresponding increase in smectite. Gawenda *et al.* [1999] interpreted the re-appearance of kaolinite as indicating a climatic change from warm, seasonally wet conditions to very warm, perennially humid conditions during the P/E transition. Seasonal conditions dominated again in the NP11 zonal interval. In the central North Sea, the P/E transition was marked by the influx of kaolinite, which persisted into Zone NP10 [Knox, 1996] indicating increased warm and humid conditions in the source areas in the northwestern part of Europe. Kaolinite increases several metres below the P/E transition at Alamedilla and Caravaca, in southern Spain [Adatte and Lu, 1995; Lu *et al.*, 1998] and at Elles (Tethyan Realm, fig. 9). The abundance of smectite observed above the P/E event in these sections indicates increased aridity in the Tethyan region at the end of Zone NP9. Except the southern Tethyan margin where very arid climatic conditions prevailed during the P/E transition, both Tethys and Atlantic Realms were marked by increased precipitation. This humid climate was recorded several metres below the P/E interval, reaching a paroxysm within it. Du-

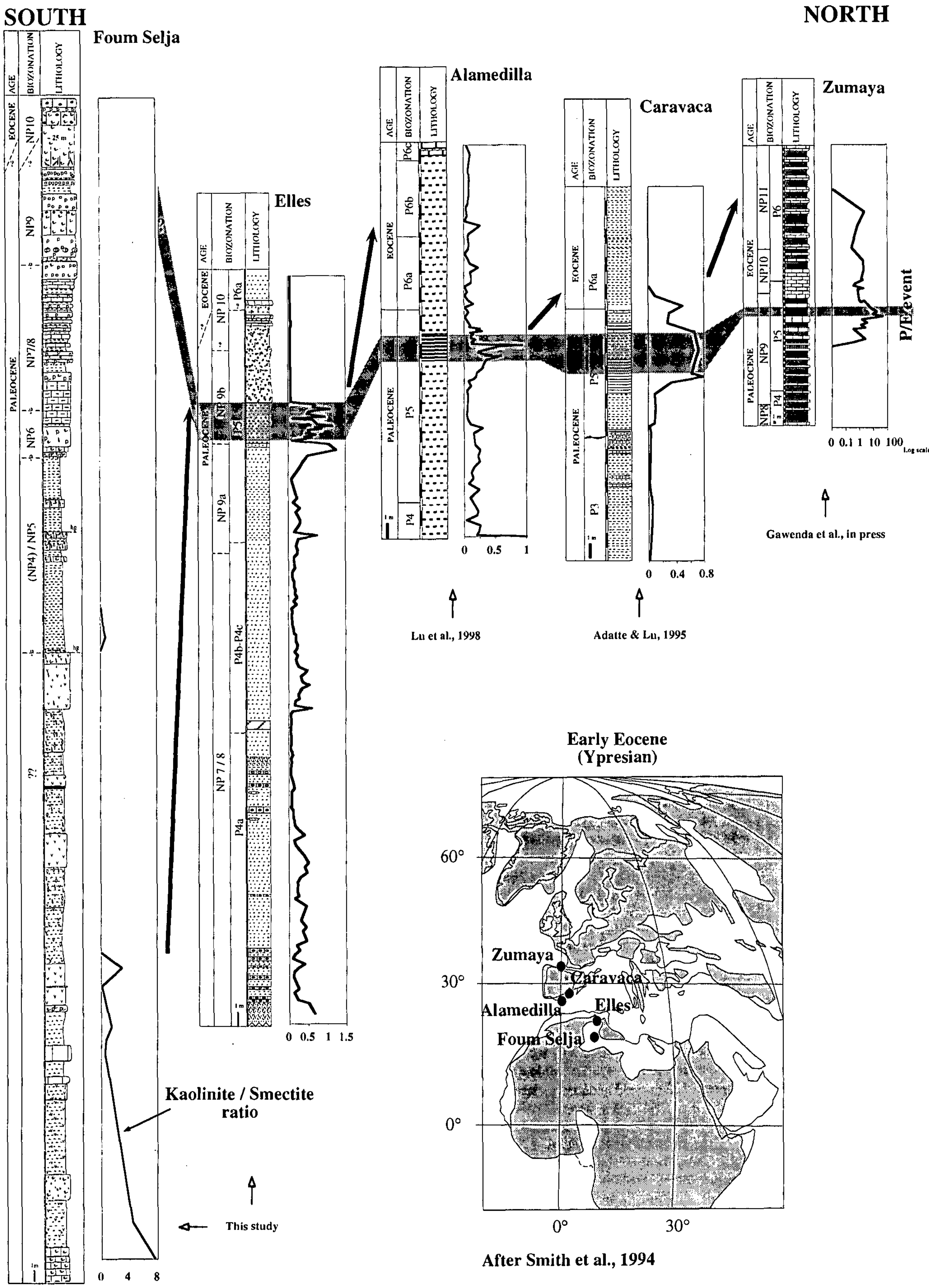

FIG. 9. – Variations in the kaolinite/smectite ratios with the palaeogeographical location of the studied sections. Ratios are calculated from XRD mineral peak data in counts per minute.

FIG. 9. – *Variations des rapports kaolinite/smectite et situation paléogéographique des profils étudiés. Les rapports sont exprimés en intensités brutes (coups par minute).*

ring the early Eocene (end of Zones NP9-NP10), seasonal to arid climatic conditions developped in the Tethys whereas the Atlantic Realm was always submitted to humid conditions. From Africa to northern Europe kaolinite disappeared diachronously, before Zone NP4-5 at Foum Selja (southern marginal Tethys), in Zone NP9 at Elles (Zone P5) and Caravaca (early part of Zone P6a) and in Zone NP11 (later part of Zone P6a) at Zumaya (fig. 9). At Alamedilla, very low kaolinite contents persisted into the early Eocene. This diachronous disappearance of kaolinite suggests a latitudinal shift in the source area of kaolinite and consequently in the climatic zones, from lower to higher latitudes (fig. 9).

Environmental changes

At Elles, sea level changes are suggested by two glauconitic sandstones (Zones NP7-8) and a more phosphatic sandstone (Zone NP9b). In an open marine environment the presence of glauconite indicates condensed sedimentation and reworking. Allochthonous reworking is also suggested by the coexistence of phosphatic grains and glauconite, two minerals which form in different open marine environments. An abrupt change in the faunal assemblage above the second glauconitic bed (20 m) and maximum reworking between 19 m and 20 m, all point towards a sea level fall and erosion probably below this glauconitic level, followed by a sea level rise. The Elles section shows three sequence boundaries (SBa,b,c) associated with unconformities and some minor fluctuations (fig. 2). The two lower sequence boundaries identified in the NP7-8 zonal interval and the third one at the top of Zone NP9 appear to represent major sequences with probably tectonic enhancement. The smaller sequence boundaries related to minor sea level fluctuations are difficult to identify in this relatively deep water section because no major facies changes occurred.

The shallower Foum Selja section should record facies changes at essentially all sea level fluctuations but since the deposits very shallow, the section must be expected to be incomplete. Local tectonic activity (e.g the uplift of Kasserine Island) associated with an alkaline explosive volcanism of which traces have been observed in the phosphate deposits of the Upper Paleocene [Beji Sassi *et al.*, 1996] could be one of the major mechanisms behind the sea level fluctuations observed at Elles and more particularly at Foum Selja.

The Thelja Formation corresponds to a period of relatively low sea level marked by reduced terrigenous input, during which the seaway between the Gafsa Basin and the open sea to the north was nearly closed. This restricted marine setting (littoral-lagoonal) under warm and arid climatic conditions favoured the formation of primary evaporites (gypsum and halite) (figs. 2 and 4). Upsection (Chouabine Formation) a change to phosphate-rich sedimentation suggests a sea level rise and hence a more open seaway to the north. During time of climate warming, rising sea levels and increased nutrient-rich oceanic water influx, phosphate deposition accelerated, taking place preferentially along the transgressive surfaces [Föllmi *et al.*, 1992; Föllmi, 1996]. Reworked floras from the upper Cretaceous seem to be at a maximum (e.g. sample 79, see p. 9) near the transgressive surfaces (TS) defined by the high apatite content. It has also been shown that maximum amounts of smectite frequently coincide with long-term or short-term high sea levels [Adatte and Rumley, 1989; Chamley *et al.*, 1990; Debrabant *et al.*, 1992; Deconinck, 1992]. The high smectite/mica and chlorite ratio from the upper part of Zone NP4-5 confirms that the Chouabine Formation corresponds to a period of relatively high sea level with probably a maximum of rise in Zone NP7-8 where the ratio is highest (fig. 2 and 4). The base of this interval is marked by a major lithological change from evaporite to phosphate deposits and the presence of a phosphatized hard ground (Hg, fig. 2) which indicates a period of non-deposition and/or erosion. A second phosphatized hard ground is observed in the NP4-5 zonal interval (fig. 2). The base of the Kef Eddour Formation shows a lithological change from phosphate deposits to shelly limestones with the two basal metres highly bioturbated (Thalassinoides) and phosphatized. The nature of the facies indicates in this uppermost interval a return to more restricted environmental conditions. Based on these observations, the Foum Selja section appears to have three sequence boundaries associated with unconformities and some sea level changes without unconformities. Smaller sequence boundaries related to minor sea level fluctuations were identified because major facies changes occurred (fig. 2).

Without more appropriate investigations we can only attempt to correlate the relatively deep sequences of Elles with the shallower sequences of Foum Selja. Based only on the biostratigraphic data, the two lower sequence boundaries (SBa and SBb) observed at Elles should correlate with the Zone NP7-8 of the Chouabine Formation of Foum Selja. However because of the condensation of this interval, their identification is difficult and we cannot determine with precision the correspondance between SBa and SBb observed at Elles and the small sequence boundaries of Foum Selja. At least the sequence boundary (SBc) identified above the P/E event at Elles could correspond with the boundary between the Chouabine and the Kef Eddour Formations of Foum Selja (fig. 2).

Intermittent upwelling episodes which is one of the best known and most efficient ways of supplying nutrients [Lucas and Prévôt-Lucas, 1997] must have affected the southern Tethyan margin particularly from the late Paleocene to the early Eocene (Zones NP5 to NP10), a period of time marked by repeated occurrences of phosphate deposits linked to rising sea level. However, in addition to high organic productivity, some conditions such as no or very few detrital input, a shelf fringing an arid continent and the dominance of organisms without carbonate shells in an environment which does not favour the precipitation of biogenic carbonate are required to favour the accumulation of phosphates [Lucas and Prévôt-Lucas, 1997]. At Foum Selja, phosphate deposition coincides with arid climatic conditions onto the Saharan Platform and subsequent reduced detrital sediment supply into the Gafsa Basin (figs. 4 and 6). The episodes of phosphate accumulation reflect probably the invasion of nutrient-rich upwelling waters into this shallower basin. At Elles, the increase of the aridity in the Tethyan region and subsequent very low detrital input into the El Kef Basin only after the P/E event (figs. 5 and 7) could be the main causes for the late accumulation of phosphates (in Zone NP9) compared to Foum Selja (in Zone NP4-5).

The occurrence of phosphate deposits related to climate change and consequently reduced detrital influx suggests a change in palaeoceanic and/or palaeoatmospheric circulation on the southern Tethyan margin from the upper Paleocene (Foum Selja) through the Paleocene-Eocene transition (Elles).

CONCLUSIONS

During the early Paleocene, the Saharan Platform experienced a warm and humid climate that changed to warm and very arid climatic conditions during the late Paleocene to early Eocene. In contrast, the Tethyan region was marked by a seasonal warm climate in the late Paleocene changing to a warm and humid climate across the P/E transition and to arid/seasonal conditions in the early Eocene. From south to north, the disappearance of kaolinite is diachronous suggesting a latitudinal shift in the kaolinite source and consequently in the climatic zones, from lower to higher latitudes.

The Elles section shows three major sequence boundaries associated with unconformities. The two lower identified in the NP7-8 zonal interval should correlate into the Chouabine Formation of Foum Selja. However, because of the condensation in this interval, their identification is difficult. The third sequence boundary identified above the P/E interval at Elles corresponds to the boundary between the Chouabine and Kef Eddour Formations at Foum Selja.

Arid climatic conditions and consequently reduced detrital influx are consistent with phosphate deposits which are associated with intermittent upwelling episodes, suggesting palaeoceanic and/or palaeoatmospheric circulation changes in the southern Tethys from the upper Paleocene to the early Eocene.

At Elles, fauna, bulk rock mineralogic and isotopic analyses identified the P/E event interval which corresponds to a 2.7 m thick clay layer. These characteristic trends cannot be identified at Foum Selja where sediments were deposited in the shallow restricted Gafsa Basin which bordered the evaporite Saharan Platform to the south.

Phosphate deposits which obliterate the original isotopic signal, strong dissolution of the planktic fauna and flora in these phosphatic layers and the presence of a condensed interval just after this event, all are criteria that prevent the choice of the Elles section as a potential GSSP candidate for the P/E boundary.

Acknowledgments. – The authors thank Dalila Turki from the University of Tunis for guiding us in the field and José Richard for conducting X-ray preparations at the laboratory of mineralogy and petrology, University of Neuchâtel, Switzerland. This study was supported by the Swiss National Foundation, N° 2100-043450.95/1.

References

ADATTE T. & LU G. (1995). – Clay mineral correlation across the Paleocene-Eocene boundary : evidence for global turnover from western to eastern Tethys. – *GSA 1995, annual meeting,* New Orleans, USA, Abstract p. 405.

ADATTE T. & RUMLEY G. (1989). – Sedimentology and mineralogy of Valanginian and Hauterivian in the stratotype region (Jura mountains, Switzerland). *In* : J. WIEDEMANN, Ed., Cretaceous of the western Tethys. – *Proc. 3rd Intern. Cretaceous Symposium*, Tuebingen, 329-351.

ADATTE T., STINNESBECK W. & KELLER G. (1996). – Lithostratigraphic and mineralogic correlations near K/T boundary clastic sediments in northeastern Mexico : Implications for origin and nature of deposition. – *Geol. Soc. Amer. sp. paper*, **307**, 211-226.

AXELROD D.I. (1984). – An interpretation of Cretaceous and Tertiary biota in polar regions. – *Palaeogeogr. Palaeoclimatol. Palaeoecol.*, **45**, 105-147.

BEJI-SASSI A. (1985). – Pétrographie, minéralogie et géochimie des sédiments phosphatés de la bordure orientale de l'île de Kasserine (Tunisie). – Thèse de Doctorat, Univ. Orléans, 230 p.

BEJI-SASSI A., OUAZAA LARIDHI N. & CLOCCHIATI R. (1996). – Témoignage d'un volcanisme alcalin d'âge paléocène supérieur-éocène dans les sédiments phosphatés de la Tunisie méridionale. – *17th Regional African European Meeting of Sedimentology*, Sfax, Tunisia, abstract p. 23.

BERGGREN W., KENT D., SWISHER C. & AUBRY M.-P. (1995). – A revised Cenozoic geochronology and chronostratigraphy. *In* : W. BERGGREN *et al.*, Eds, Geochronology, time scale and global stratigraphy correlation. – *SEPM sp. publ.*, **54**, 129-212.

BERTHON L. (1928). – Les réserves de la Tunisie en acide phosphorique. *In* : Les réserves mondiales en phosphates . – S.A Graficas Reunidas, Madrid, 615-658.

BOLLE M.-P., ADATTE T., KELLER G., VON SALIS K. & HUNZIKER J. (1998). – Stratigraphy, mineralogy and geochemistry of the Trabakua Pass and Ermua sections in Spain : Paleocene-Eocene Transition. – *Eclogae geol. Helv.*, **91**, 1-25.

BUROLLET P.F. (1956). – Contribution à l'étude stratigraphique de la Tunisie centrale. – *Ann. Mines Géol., Tunis*, **18**, 350 p.

BUROLLET P.F. (1967). – General geology of Tunisia. *In* : L. MARTIN Ed., Guidebook to the geology and history of Tunisia. – *Petrol. Explor. Soc. Libya, 9th Ann. Field. Conf.*, 67 p.

CANUDO J., KELLER G., MOLINA E. & ORTIZ N. (1995). – Planktic foraminiferal turnover and $\delta^{13}C$ across the Paleocene-Eocene transition at Caravaca and Zumaya, Spain. – *Palaeogeogr. Palaeoclimatol. Palaeoecol.*, **114**, 75-100.

CHAMLEY H. (1998). – Clay mineral sedimentation in the ocean. *In* : H. PAQUET and N. CLAUER, Eds, Soils and sediments (mineralogy and geochemistry). – Springer-Verlag, Berlin, 269-302.

CHAMLEY H., DECONINCK J.F. & MILLOT G. (1990). – Sur l'abondance des minéraux smectitiques dans les sédiments marins communs déposés lors des périodes de haut niveau marin du Jurassique supérieur au Paléogène. – *C.R. Acad. Sci.*, Paris, (II), **311**, 1529-1536.

DEBRABANT P., FAGEL N., CHAMLEY H., DECONINCK J.F., RECOURT P. & TROUILLET A. (1992). – Clay sedimentology, mineralogy and chemistry of Mesozoic sediments drilled in the northern Paris Basin. – *Sci. Drilling*, **3**, 138-152.

DECONINCK J.F. (1992). – Sédimentologie des argiles dans le Jurassique-Crétacé d'Europe occidentale et du Maroc. – Mém. Habilit., Univ. Lille 1, 226 pp.

DICKENS G., CASTILLO M. & WALKER J.C. (1997). – A blast of gas in the latest Paleocene : Simulating first-order effects of massive dissociation of oceanic methane hydrate. – *Geology*, **25**, (3), 259-262.

DICKENS G., O'NEIL J., REA D. & OWEN R.M. (1995). – Dissociation of oceanic methane hydrate as a cause of the carbon isotope excursion at the end of the Paleocene. – *Paleoceanography*, **10**, 965-971.

ESTES R. & HUTCHISON J.H. (1980). – Eocene lower vertebrates from Ellesmere Island, Canadian Arctic Archipelago. – *Palaeogeogr. Palaeoclimatol. Palaeoecol.*, **30**, 325-347.

FERRERO J. (1966). – Nouvelle méthode empirique pour le dosage des minéraux par diffraction RX. – Rapport C.F.P. (Bordeaux), inédit, **26**.

FÖLLMI K. (1996). – The phosphorus cycle, phosphogenesis and marine phosphate-rich deposits. – *Earth Sci. Rev.*, **40**, 55-124.

FÖLLMI K., GARRISON R., RAMIREZ P., ZAMBRANO-ORTIZ F., KENNEDY W. & LEHNER B. (1992). – Cyclic phosphate-rich successions in the Upper Cretaceous of Colombia. – *Palaeogeogr. Palaeoclimatol. Palaeoecol.*, **93**, 151-182.

FOURNIÉ D. (1980). – Nomenclature lithostratigraphique des séries du Crétacé supérieur au Tertiaire en Tunisie. – *Bull. Centr. Rech. Explor. Prod., Elf Aquitaine*, **2**, (1), 97-148.

GAWENDA P., WINKLER W., SCHMITZ B. & ADATTE T. (1999). – Climatic and bioproductivity control on carbonate turbidite sedimentation (Paleocene to earliest Eocene Gulf of Biscay, Zumaia). – *J. Sed. Res.* (in press).

GIBSON T.J., BYBELL L.M. & OWENS J.P. (1993). – Latest Paleocene lithologic and biotic events in the neritic deposits of southwestern New Jersey. – *Paleoceanography,* **8**, 495-514.

HAQ B.U., HARDENBOL J. & VAIL P.R. (1988). – Mesozoic and Cenozoic chronostratigraphy and cycles of relative sea-level change. *In* : C.K. WILGUS *et al.*, Eds., Sea-level changes : An integrated approach. – *SEPM, sp. publ.*, **42**, 71-108.

KARPOFF A.M., LAGABRIELLE Y., BOILLOT G. & GIRARDEAU J. (1989). – L'authigenèse océanique de palygorskite par halmyrolyse de péridotites serpentinisées (marge de Galice) : ses implications géodynamiques. – *C.R. Acad. Sci.*, Paris, (II), **308**, 647-654.

KASTNER M., MERTZ K., HOLLANDER D. & GARRISON R. (1984). – The association of dolomitite-phosphorite-chert : cause and possible diagenetic sequences. *In* : R. GARRISON *et al.*, Eds, Dolomites of the Monterey Formation and other organic-rich units, Pacific Section. – *SEPM publ.*, **41**, 75-86.

KELLER G., ADATTE T., STINNESBECK W., STUBEN D., KRAMAR U., BERNER Z., LI L. & VON SALIS K. (1998). – The Cretaceous-Tertiary transition on the shallow Saharan Platform of southern Tunisia. – *Geobios*, (7), **30**, 951-975.

KENNETT J.P. & STOTT L.D. (1990). – Proteus and Proto-Oceanus : Paleogene oceans as revealed from Antartica stable isotopic results. – *Proc. ODP, Sci. Results*, **113**, 865-879.

KENNETT J.P. & STOTT L.D. (1991). – Abrupt deep-sea warming, palaeoceanographic changes and benthic extinctions at the end of the Paleocene. – *Nature*, **353**, 225-229.

KLOOTWIJK C.T., GEE J.S., PEIRCE J.W., SMITH G.M. & MCFADDEN P.L. (1992). – An early India-Asia contact : Paleomagnetic constraints from Ninetyeast Ridge, ODP Leg 121. – *Geology*, **20**, 395-398.

KNOX R.W. (1996). – Correlation of the early Paleogene in northwest Europe : an overview. *In* : R. KNOX *et al.*, Correlation of the Early Paleogene in Northwest Europe, – *Geol. Soc., sp. publ.*, London, **101**, 1-11.

KÜBLER B. (1983). – Dosage quantitatif des minéraux majeurs des roches sédimentaires par diffraction X. – *Cahiers de l'Institut de Géologie de Neuchatel*, Série AX N° 1.1 and 1.2.

KÜBLER B. (1987). – Cristallinité de l'illite, méthodes normalisées de préparations, méthodes normalisées de mesures. – *Cahiers de l'Institut de Géologie de Neuchatel*, Série ADX, 1-8.

LU G., ADATTE T., KELLER G. & ORTIZ N. (1998). – Abrupt climatic, oceanographic and ecologic changes near the Paleocene-Eocene Transition in the Deep Tethys Basin : The Alamedilla Section, southern Spain. – *Eclogae geol. Helv.*, **91**, 293-306.

LU G., KELLER G., ADATTE T., ORTIZ N. & MOLINA E. (1996). – Long-term (10^5) or short-term (10^3) $\delta^{13}C$ excursion near the Paleocene-Eocene transition : evidence from the Tethys. – *Terra Nova*, **8**, (4), 347-355.

LUCAS J., CHAABANI F. & PRÉVÔT L. (1979). – Phosphorites et évaporites : deux formations de milieux sédimentaires voisins étudiés dans la coupe du Paléogène de Foum Selja (Metlaoui, Tunisie). – *Sci. Géol., Bull.*, **32**, (1-2), 7-19.

LUCAS J. & PRÉVÔT-LUCAS L. (1997). – On the genesis of sedimentary apatite and phosphate-rich sediments. *In* : H. PAQUET and N. CLAUER, Eds, Soils and sediments (mineralogy and geochemistry). – Springer-Verlag, Berlin, 249-268.

MARTINI E. (1971). – Standard Tertiary and Quaternary calcareous nannoplankton zonation. *In* : A. FARINACCI Ed., Proc. 2nd Planktonic Conference Roma. – *Tecnoscienza*, 739-785.

MERTZ K.A. (1984). – Diagenetic aspects, Sandholdt Member, Miocene Monterey Formation, Santa Lucia Mountains, California : Implications for depositional and burial environments, *In* : R. GARRISON *et al.*, Eds, Dolomites of the Monterey Formation and other organic-rich units, Pacific Section. – *SEPM publ.*, **41**, 49-74.

OBERHÄNSLI H. (1992). – The influence of the Tethys on the bottom waters of the early Tertiary ocean. *In* : J.P. KENNETT Ed., The Antarctic paleoenvironment : A perspective on global change, **56**, 167-184.

OBERHÄNSLI H. & HSÜ K.J. (1986). – Paleocene-Eocene paleoceanography. *In* : Mesozoic and Cenozoic Oceans. – *Geodynamic Series*, **15**, 85-100.

PARDO A., KELLER G., MOLINA E. & CANUDO J.I. (1997). – Planktic foraminiferal turnover across the Paleocene-Eocene transition at DSDP Site 401, Bay of Biscay, North Atlantic. – *Mar. Micropal.*, **29**, 129-158.

PLETSCH T. (1998). – Origin of Lower Eocene palygorskite claystones on the Côte d'Ivoire-Ghana Margin (Leg 159, eastern Equatorial Atlantic). – *Proc. ODP, Sci. Res.*, **159**, in press.

REGAYA K., LAATAR S., CHAOUACHI, A., ZARGOUNI F. & BENSALEM H. (1991). – Carte géologique de la Tunisie, N° 65, Metlaoui.

ROBERT C. & CHAMLEY H. (1991). – Development of early Eocene warm climates, as inferred from clay mineral variations in oceanic sediments. – *Palaeogeogr. Palaeoclimatol. Palaeoecol.*, **89**, 315-332.

ROBERT C. & KENNETT J.P. (1992). – Paleocene and Eocene kaolinite distribution in the South Atlantic and Southern Ocean : Antarctic climatic and paleoceanographic implications. – *Mar. Geol.*, **103**, 99-110.

ROBERT C. & KENNETT J.P. (1994). – Antarctic subtropical humid episode at the Paleocene-Eocene boundary; clay-mineral evidence. – *Geology*, **22**, 211-214.

SAID R. (1978). – Etude stratigraphique et micropaléontologique du passage Crétacé-Tertiaire du synclinal d'Elles (région Siliana-Sers), Tunisie centrale. – Thèse de Doctorat, Univ. P. et M. Curie, Paris, 57 p.

SASSI S. (1974). – La sédimentation phosphatée au Paleocène dans le Sud et le Centre-Ouest de la Tunisie. – Thèse de Doctorat ès-Sciences, Université Paris-Sud, Orsay, 292 p.

SASSI S. (1980). – Contexte paléogéographique des dépôts phosphatés de l'Eocène de Tunisie. *In* : Géologie comparée des gisements de phosphate et de pétrole. – BRGM, Orléans, 83-167.

SASSI S., BELAYOUNI H. & CHAABANI F. (1987). – Paleocene-Eocene phosphorites and associated facies in Gafsa Basin. – *Geological Field Guide of IAS, 8th regional meeting of sedimentology*, 219-252c.

SMITH A., SMITH D. & FUNNELL B. (1994). – Atlas of Mesozoic and Cenozoic coastlines. – Cambridge University Press, 99 p.

SPEIJER R.P. (1994). – Extinction and recovery patterns in benthic foraminiferal paleocommunities across the Cretaceous/Paleogene and Paleocene/Eocene boundaries. – Ph. D. thesis, Universiteit Utrecht. – *Geol. Ultraiectina*, **124**, 191 p.

SVOBODA K. (1983). – Fosfaty Tuniska (Tunisian Phosphates). – *Geol. Pr., Prague*, **10**, 285-291.

SVOBODA K. (1985). – Nerostne suroviny Tuniska (Raw material of Tunisia). – *Geol. Pr., Prague*, **10**, 285-291.

SVOBODA K. (1989). – The Lower Tertiary phosphate deposits of Tunisia. *In* : A. NOTHOLT *et al.*, Eds, Phosphate deposits of the world. – Cambridge University Press, 285-288.

THIRY M. (1989). – Geochemical evolution and paleoenvironments of the Eocene continental deposits in the Paris Basin. – *Palaeogeogr. Palaeoclimatol. Palaeoecol.*, **70**, 153-165.

THIRY M. & JACQUIN T. (1993). – Clay minerals distribution related to rift activity, sea level changes and paleoceanography in the Cretaceous of the Atlantic Ocean. – *Clay minerals*, **28**, 61-84.

THOMAS E. (1990). – Late Cretaceous through Neogene deep-sea benthic foraminifers (Maud Rise, Weddell Sea, Antarctica). – *Proc. ODP. Sci. Results*, **113**, 571-594.

THOMAS E. & SHACKLETON N.J. (1996). – The latest Paleocene benthic foraminiferal extinction and stable isotope anomalies. – *J. Geol. Soc. London*, **101**, 421-441.

VISSE L.D. (1952). – Genèse des gîtes phosphatés du Sud-Est Algéro-Tunisien. – *19th int. geol. Congr. Alger, Monogr. rég.*, **27**, 58 p.

VISSE L.D. (1973). – Contributions des gisements tunisiens à la connaissance du faciès phosphaté. – *Ann. Mines Géol., Tunis*, **26**, 353-458.

VON SALIS K., OUDA K., SAAD EL DIN M., TANTAWY A. & BERNASCONI S. (1998). – Calcareous nannofossils, foraminifera and stable isotope studies from P/E boundary sections in Egypt. – *Strata*, 1, 9, 113-115.

WEI W. (1992). – Biometric study of *Discoaster multiradiatus* and its biochronological utility. – *Mem. Scienze geol.*, **XLIII**, 219-235.

WOLFE J.A. (1980). – Tertiary climates and floristic relationships at high latitudes in the northern hemisphere. – *Palaeogeogr. Palaeoclimatol. Palaeoecol.*, **30**, 313-323.

ZACHOS J., STOTT L. & LOHMANN K. (1994). – Evolution of early Cenozoic marine temperatures. – *Paleoceanography*, **9**, (2), 353-387.

Journal of the Geological Society, London, Vol. **157**, 2000, pp. 929–941. Printed in Great Britain.

Climatic evolution on the southeastern margin of the Tethys (Negev, Israel) from the Palaeocene to the early Eocene: focus on the late Palaeocene thermal maximum

M. P. BOLLE[1], A. PARDO[2], T. ADATTE[1], K. VON SALIS[3] & S. BURNS[4]
[1]*Institut de Géologie, Emile-Argand 11, Université de Neuchâtel, 2000 Neuchâtel, Switzerland (e-mail: marie-pierre.bolle@geol.unine.ch)*
[2]*Departamento de Ciencas de la Tierra, Universidad de Zaragoza, 50009 Zaragoza, Spain*
[3]*Geologisches Institut, ETH-Zentrum, 8092 Zürich, Switzerland*
[4]*Geologisches Institut, Balzerstrasse, Universität Bern, Switzerland*

Abstract: During the early Palaeocene (zones P1 to P2), the southeastern Tethyan margin experienced a warm and humid climate with high rainfall as indicated by the abundance of kaolinite within marine sedimentary rocks. Subsequently, in Zone P2, arid climatic conditions evolved in the coastal basins of the southern Tethys margin as indicated by the gradual disappearance of kaolinite and the increased abundance of palygorskite and sepiolite. Arid climatic conditions persisted during the Selandian and Thanetian (late Palaeocene) and reached a maximum in the Ypresian (early Eocene). During the late Palaeocene thermal maximum, warm climatic conditions were associated with increased aridity and led to sea surface warming, though not bottom water warming, as suggested by the planktic $\delta^{18}O$ excursion observed at the Zomet Telalim basin (Negev, Israel). Strongly reduced surface productivity accompanied by unusually light $\delta^{13}C$ are associated with the late Palaeocene thermal maximum in the Negev as well as globally.

Keywords: Israel, Palaeogene, climate, clay minerals, stable isotopes.

The late Palaeocene corresponds to a time of prominent climatic changes in Earth history with a warming of 6–8°C in deep and high-latitude surface waters (referred to as the late Palaeocene thermal maximum (Kennett & Stott 1991; Zachos *et al.* 1993). However, low-latitude surface water temperatures remained relatively unchanged (Bralower *et al.* 1995; Lu *et al.* 1995; Thomas & Shackleton 1996). This long-term warming is indicated by the presence of sub-tropical to temperate faunas and floras in subpolar regions of both hemispheres (Estes & Hutchison 1980; Wolfe 1980; Axelrod 1984) that coincides with warm-water pelagic marine organisms (Premoli-Silva & Boersma 1984; Kennett & Stott 1990; Lu & Keller 1993). The abundance of kaolinite in oceanic sediments indicates a time of high humidity with enhanced chemical weathering in the South Atlantic and Southern Ocean (Antarctica) (Robert & Chamley 1991; Robert & Kennett 1992, 1994). Such a period of warming and high rainfall has also been interpreted in the central North Sea (Knox 1996), New Jersey continental margin (Gibson *et al.* 1993) and northern Spain (Gawenda *et al.* 1999). In contrast, from the late Palaeocene to the early Eocene, West and North Africa and the Arabian peninsula are characterized by increased aridity and enhanced evaporation, as indicated by the occurrence of palygorskite and sepiolite and the presence of evaporites (Mélières 1977; Robert 1982; Robert & Chamley 1991; Oberhänsli 1992; Bolle *et al.* 1999).

In both high and low latitudes, the warm pulse coincides with a pronounced short-term negative $\delta^{13}C$ excursion (e.g. Kennett & Stott 1991; Koch *et al.* 1992; Pak & Miller 1992) that could have been caused by the release of methane hydrates during the late Palaeocene thermal maximum (Dickens *et al.* 1995, 1997). The $\delta^{13}C$ excursion is also associated with the extinction of 35–50% of deep-sea benthic foraminiferal species (Thomas 1990; Kennett & Stott 1991), the radiation of planktic foraminifera (Lu & Keller 1993, 1995; Lu *et al.* 1998*a*; Pardo *et al.* 1999) and terrestrial vertebrates and plants (Gingerich 1980; Axelrod 1984).

In this study, new clay mineral data are presented from two sections through the Palaeocene to lower Eocene, at Ben Gurion and Zomet Telalim, Israel, on the southern margin of the Tethys. We also present new carbon and oxygen isotope profiles from the upper Palaeocene to the lower Eocene at Zomet Telalim. The climatic evolution of this region is reconstructed on the basis of these two sections paying special attention to the late Palaeocene thermal maximum and the major climatic and oceanographic changes that affected the area during this period of time.

Materials and methods

The Ben Gurion I and II and Zomet Telalim sections are located in the Zin valley of the Negev (Israel), on the southern Tethyan margin (Fig. 1). The sections are 20 km apart, occupying identical structural positions but in different synclines (Benjamini & Eisenshtein 1995) (Fig. 1). Palaeogeographic reconstructions of the Negev area from the late Palaeocene to the early Eocene reveal the presence of emergent land masses between the Ben Gurion and Zomet Telalim basins and to the south and southeast of the studied area (Fig. 2; Arkin *et al.* 1972). During this time interval, the configuration of land masses remained essentially the same (Arkin *et al.* 1972). Based on the benthic foraminiferal assemblage, Speijer (1994) estimated the palaeodepth of the Ben Gurion section as between 500 and 700 m. The Zomet Telalim section was located in a more open but shallower basin (Benjamini & Eisenshtein 1995; Fig. 2). However, the minimum depth of deposition at Zomet Telalim would have been about 500 m, because of the abundant presence of *Nuttallides truempyi* (Van Morkhoven *et al.* 1986; Speijer 1994).

The Zomet Telalim section is about 9 m thick and spans the upper Palaeocene to lower Eocene nannofossil zones NP7/8 to NP11 and the planktic foraminiferal subzones P4a to P6b. Marly limestones

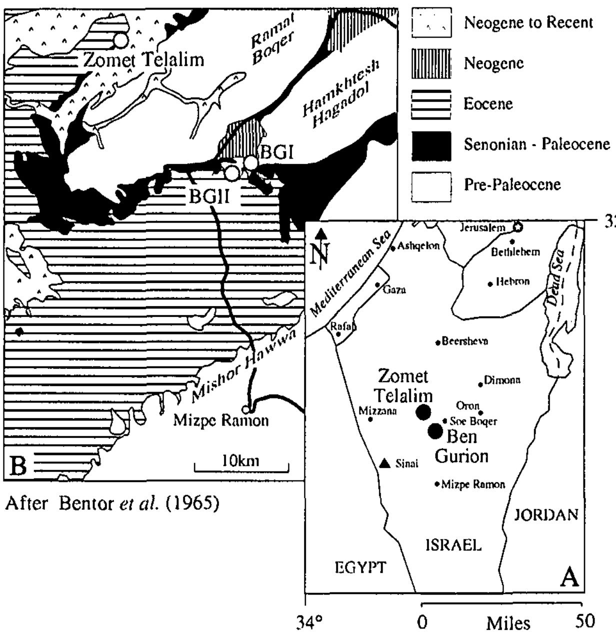

Fig. 1. (a) Geographical location of the Zomet Telalim and Ben Gurion sections. (b) Distribution of Palaeocene and Eocene sediments with the location of the studied sections after Bentor *et al.* (1965).

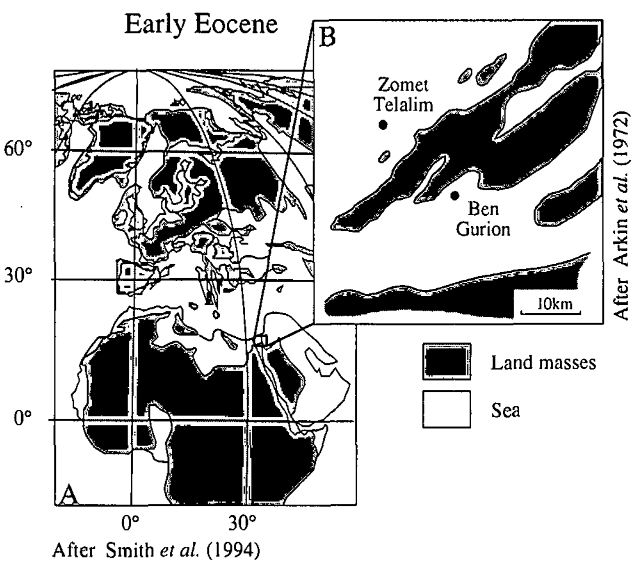

Fig. 2. (a) Worldwide palaeocoastline map during the early Eocene at 53 Ma after Smith *et al.* (1994). (b) Palaeogeographic map of the Negev area at the beginning of the Eocene after Arkin *et al.* (1972).

dominate the lower 3 m of the section, whereas the upper 6 m consists of alternating marls and shales (Fig. 3).

The Ben Gurion I outcrop is about 35 m thick and spans the planktic foraminiferal zones P1b to P4 (zonation of Berggren *et al.* 1995). The Ben Gurion II outcrop, located a few hundred metres east of Ben Gurion I, is about 19 m thick and spans Zone P4 (top) to Subzone P6b (Fig. 1). This composite section is dominated by shales, marls and calcareous marls throughout the Palaeocene to the lower Eocene (Figs 4 and 5). The biostratigraphy (Ben Gurion I and II), stable isotopes and mineralogical (bulk rock) records (Ben Gurion II) were previously published by Keller & Benjamini (1991), Benjamini (1992), Lu *et al.* (1995, 1998*b*) and Arenillas (1996).

A total of 84 samples from the Zomet Telalim section and 120 from the Ben Gurion section was collected by G. Keller and C. Benjamini. For the investigation of calcareous nannofossils, 29 smear-slides were prepared and studied with the light microscope at a magnification of $\times 1000$. Species concepts used are those of Perch-Nielsen (1985). Foraminiferal textural preservation was evaluated by binocular and scanning electron microscope. Oxygen and carbon isotope analyses were based on monospecific samples. Prior to analysis, foraminiferal tests were cleaned ultrasonically in order to remove adhering fine grained particles. The species *Morozovella subbotinae* (Fig. 6a) was used for planktic isotope analyses because of its surface dwelling habitat (Shackleton *et al.* 1985), and its presence throughout the studied interval. To minimize intraspecific variations, all planktic isotope analyses used 30 specimens from the 250–350 μm size fraction. Isotope analyses were performed on the benthic foraminifera *Nuttallides truempyi* (Fig. 6b). Each benthic isotope analysis used 40–50 specimens from the >125 μm size fraction. Analyses were conducted at the stable isotope laboratory of the University of Bern, Switzerland, using a VG Prism II ratio mass spectrometer equipped with a common acid bath (H_3PO_4). 44 foraminiferal samples of the Zomet Telalim section were analysed. The results were calibrated to the PDB scale with the standard errors of 0.1‰ for $\delta^{18}O$ and 0.05‰ for $\delta^{13}C$. X-ray diffraction (XRD) analyses of whole rock and clay mineral samples were conducted at the University of Neuchâtel, Switzerland, using a SCINTAG XRD 2000 Diffractometer with standard errors varying between 5 and 10% for the phyllosilicates and <5% for non-phyllosilicates (Adatte *et al.* 1991). Whole rock compositions were determined by XRD based on methods described by Ferrero (1966) and Kübler (1983). This method for semi-quantitative analysis of the bulk rock mineralogy used external standards. Clay mineral analyses followed the analytical method of Kübler (1987) described in Adatte *et al.* (1996). We present here data from the <2 μm fraction. Clay minerals are given in relative percent abundance and the clay mineral ratios are calculated from XRD mineral peak data in counts per minute.

Biostratigraphy

Planktic foraminifera

Planktic foraminiferal biostratigraphy of the Zomet Telalim section is based on the revised zonation by Berggren *et al.* (1995), and the subdivided Zone P5 into subzones P5a and P5b by Pardo *et al.* (1999). Preservation of planktic foraminiferal tests is generally good and surface textures and most morphological features are easily identifiable, though tests are partially to completely recrystallized (Figs 6 and 7).

Zone P4 is defined by the total range of *Globanomalina pseudomenardii* and divided into P4a, P4b and P4c subzones (Berggren *et al.* 1995). In the Zomet Telalim section, the lowermost 1 m corresponds to Subzone P4b, though the boundary between P4b and P4c could not be determined precisely because of dissolution between samples 120 and 124. *Muricoglobigerina soldadoensis*, the index species for subzone P4c, is present above this dissolution interval (Fig. 3). The top of Subzone P4c occurs about 4 m up from the base of the section. At Zomet Telalim the first appearance of *Morozovella subbotinae* predates the last appearance of *G. pseudomenardii*. In many sections, the first appearance of *M. subbotinae* occurs at or after the last appearance of *G. pseudomenardii* and this datum is commonly used to mark the base of P5 (Blow 1979; Berggren & Miller 1988).

Zone P5 is defined by the last appearance of *G. pseudomenardii* at the base and the last appearance of *Morozovella velascoensis* at the top (1.2 Ma duration; Berggren *et al.* 1995). Zone P5 is divided into two subzones based on the first appearance of *Acarinina sibaiyaensis* and/or *A. africana* (Pardo

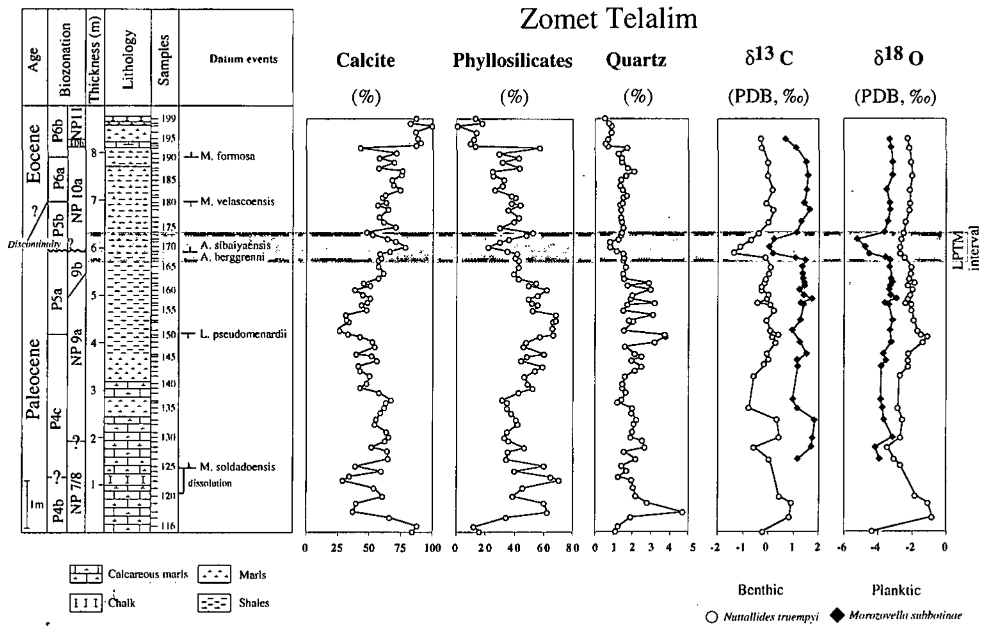

Fig. 3. Mineralogical and stable isotopic trends at Zomet Telalim in Israel. Stratigraphy is based on foraminiferal and nannofossil studies. Stable isotope analyses were conducted on the planktic foraminifera *Morozovella subbotinae* and the benthic foraminifera *Nuttallides truempyi*. The late Palaeocene thermal maximum (LPTM) interval occurs at the level of the negative $\delta^{13}C$ and $\delta^{18}O$ excursions at 5.91 m.

et al. 1999). The first appearance of these two short-ranging acarininid taxa coincide in other Tethys sections with the benthic foraminiferal extinction event, the negative carbon shift and the planktic foraminiferal diversification which characterize the late Palaeocene thermal maximum (Lu *et al.* 1998*a*; Pardo *et al.* 1999).

At Zomet Telalim, Subzone P5a spans from sample 150 to 168 (*c.* 1.8 m). The range of *A. sibaiyaensis* is truncated by a discontinuity at the top and a lithological change from clays to marls; the maximum of the negative carbon isotope excursion coincides with the occurrence of *A. sibaiyaensis* (Fig. 3). Subzone P5b has been identified by the occurrence of *A. sibaiyaensis* and *A. berggreni*, along with *M. velascoensis* and spans from sample 169 to 182 (*c.* 1 m) (Fig. 3). As noted above, a hiatus is present at the P5a–P5b boundary. As a result, the characteristic sudden increases of *A. sibaiyaensis* and *A. africana* are missing along with other subtropical acarininids, igorinids and morozovellids which generally occur at this interval in the Tethys (e.g. Arenillas & Molina 1996; Lu *et al.* 1998*a*; Pardo *et al.* 1999) and in the Pacific Ocean (Kelly *et al.* 1996; Bralower *et al.* 1995). It is unclear how much is missing at this hiatus. However, the absence of the peak abundance of acarininid species that commonly marks the late Palaeocene thermal maximum and the very low sedimentation accumulation rate of Zone P5 (estimated at 2.3 mm/ka^{-1}) suggest that much of this event is also missing.

Zone P6 is defined by the last appearance of *M. velascoensis* at the base and the first appearance of *M. aragonensis* at the top and can be divided into two subzones (Berggren *et al.* 1995). The subzone P6a–P6b boundary is defined by the first appearance of *M. formosa* (Berggren *et al.* 1995). At Zomet Telalim, Subzone P6a spans from sample 182 to sample 190 (*c.* 0.8 m) whereas Subzone P6b spans from sample 190 to the top of the section, though the top of this zone has not been recovered (Fig. 3).

Calcareous nannofossils

Only the calcareous nannofossils of the Zomet Telalim section were investigated in this study. All the 29 samples examined contained calcareous nannofossils; the abundance varying from rare (<1%) to abundant (>20%) (Table 1). The preservation is poor to moderate, some assemblages have suffered dissolution (Table 1).

The lowermost sample (115) studied contains *Discoaster mohleri*, the first appearance of which defines the base of Zone NP7 of Martini (1971). The marker of Zone NP8, *Heliolithus riedelii* was not found, neither was *Discoaster nobilis*, the marker of the base of Zone CP7 of Okada & Bukry (1980). NP7 and NP8 are often not separated due to the very short interval where *H. riedelii* is found.

Discoaster multiradiatus is present from sample 122 on upwards, thus indicating the presence of Zone NP9 or Zone CP8a, the *Discoaster multiradiatus* Zone, in most of the lower part of the section. A subdivision of Zone NP9/CP8a has been suggested by various authors based on the first appearance of *Campylosphaera eodela*. In the present material, very small forms of *C. eodela* (6–7 μm) are found as far down in Zone NP9 as sample 134. Bybell & Self-Trail (1995) showed the gradual increase in average size of this species from upper Zone NP9 through Zone NP14. A size increase is also observed in this study.

The base of Zone NP10, the *Rhomboaster bramlettei* Zone of Martini (1971), is defined by the first appearance of the nominate species. In recent papers there has been an unresolved controversy about the taxonomy of this species and whether it belongs to *Rhomboaster* or *Tribrachiatus*. *R. bramlettei* occurs very suddenly, together with other species of the genus in sample 169, suggesting an unconformity between this sample and the one below. The representatives of *Rhomboaster*/*Tribrachiatus* were found over most of the upper part of the section (Table 1)

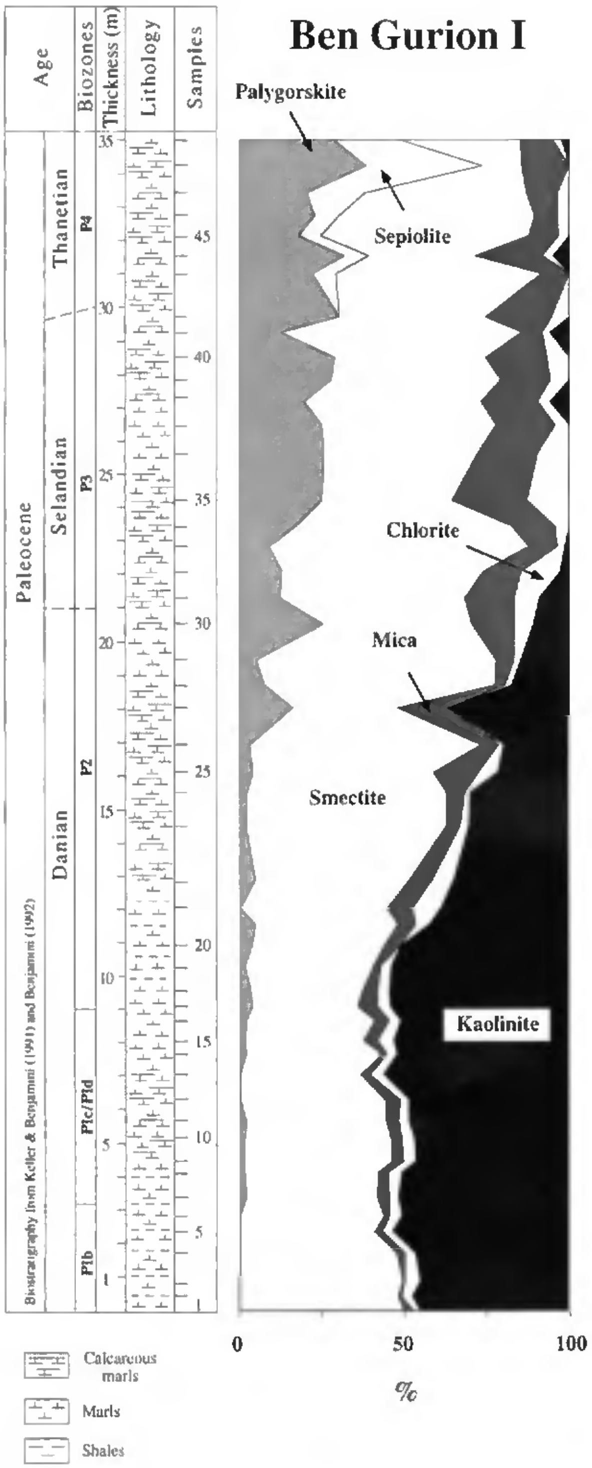

Fig. 4. Clay mineral composition at Ben Gurion I (size fraction <2 μm). Clay minerals are given in relative percent abundance.

and include *Rhomboaster* sp., *R. cuspis*, *R. bramlettei* and *R. spineus*.

The diversity within the genus *Fasciculithus* is known to decrease rapidly in Zone NP10 (Angori & Monechi 1996; Bybell & Self-Trail 1995), a phenomenon also observed at Zomet Telalim. The base of Zone CP9 is defined by the first appearance of *Discoaster diastypus*, a discoaster 'with two stems' that are not easy to distinguish under light microscopy. While the first appearance of *D. diastypus* was used by Okada & Bukry (1980) to mark the base of the Eocene, it is often found somewhat higher in Zone NP10, as in the present section.

Aubry (1996) has subdivided Zone NP10 based on the evolution of *Rhomboaster/Tribrachiatus*. This does not seem applicable in the present section due to the absence of *Tribrachiatus digitalis* in the samples studied. In the upper part of the section, *Tribrachiatus contortus* was only found in a single sample (192). Its last appearance defines the base of Zone NP11/CP9b.

Reworked Cretaceous coccoliths are very rare and include mainly relatively solution resistant forms. The presence of the Cretaceous species *Micula decussata* in most samples suggests very minor, but quite continuous, reworking of upper Cretaceous (Coniacian through Maastrichtian) sediments. Reworking is present between samples 148 and 162, where clastic sediment reaches higher values (Fig. 3). *Arkhangelskiella cymbiformis* forms part of the reworked assemblage in the upper interval of the section. *A. cymbiformis* is only common in upper Campanian and Maastrichtian sediments. No species clearly assignable to the lower Cretaceous or Jurassic were encountered.

Mineralogy

Bulk rock

Sedimentary rocks of the Zomet Telalim section are dominated by calcite and phyllosilicates (*c.* 95%) with minor quartz and k-feldspar (Fig. 3). Minimum calcite content marks the lower part of subzones P4b/c and P5a. These two calcite minima are preceded by a gradual decrease from 78% and 65% to 28% and 25% respectively in Zone P4 and Subzone P5a, whereas phyllosilicates increase from 30% to 78% (Fig. 3). Slight increases in quartz and an influx of feldspar are also observed in these intervals.

Above the subzone P5a calcite minimum, calcite increased gradually to a maximum of 78% in the late Palaeocene thermal maximum interval whereas phyllosilicates decreased from 65% to 20%. In the uppermost 2.3 m of the section, calcite increased from 50% to 90% and phyllosilicates decreased from 58% to 10%. In this interval quartz content is relatively constant with a mean value of 1%.

Clay minerals

At Ben Gurion I, kaolinite (50%) and smectite (42%) dominate the clay mineral fraction in the lowermost 11 m (Fig. 4). Between 11.5 m and 22.2 m, kaolinite gradually disappears. This decrease coincides with a gradual increase in smectite (40 to 60%), mica (3 to 6%) and palygorskite (1 to 8%). Between 22.2 m and 38.55 m, palygorskite increases to 35% and sepiolite is found at the base of Zone P4 (30.85 m). Smectite (49%), mica (14%) and chlorite (4%) complete this clay-mineral association.

Upsection at Ben Gurion II, between 38.55 m and 49 m, smectite increases, reaching a maximum of 85% above the late Palaeocene thermal maximum interval (Subzone P6a, Fig. 5). This increase coincides with a general decrease in other minerals (mica, chlorite, palygorskite and sepiolite). In the uppermost 6 m, smectite decreases to 50% coincident with increased palygorskite from 10% to 40%.

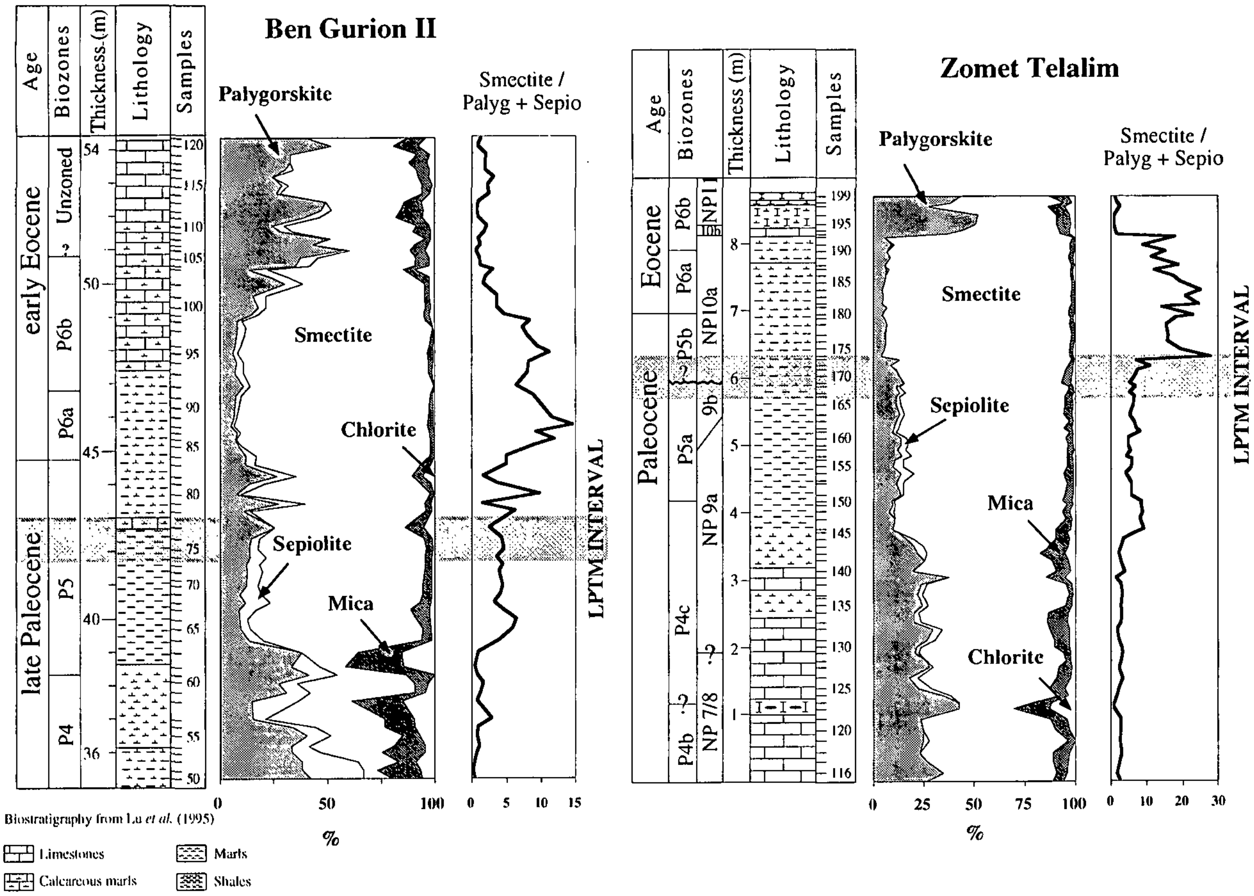

Fig. 5. Clay mineral compositions and smectite/palgygorskite+sepiolite ratios at Ben Gurion II and Zomet Telalim sections (size fraction <2 μm). Clay minerals are given in relative percent abundance and clay mineral ratios are calculated from XRD mineral peak data in counts per minute.

At Zomet Telalim, the clay mineral fraction is composed of smectite, palygorskite, sepiolite, mica and chlorite (Fig. 5). Between 0 and 8 m, palygorskite decreases gradually from 25% to 5%. At the same time, chlorite and mica decrease from 5% to near 0% and from 9% to 2% respectively. Smectite reaches a maximum of 90% above the late Palaeocene thermal maximum and decreases in the last metres of the section, whereas palygorskite increases strongly to 40%.

Clay minerals: climate signal?

Increased kaolinite either results from increased runoff, which could be caused by sea-level fall, or from increased rainfall (Robert & Kennett 1994). Kaolinite develops in equatorial to tropical soils characterized by a warm, humid climate, well-drained areas with high precipitation and accelerated leaching of parent rocks (Robert & Chamley 1991). Moreover, kaolinite can be introduced in significant amounts into oceanic sediments through erosion of older sedimentary rocks and soils during sea-level transgressions (Thiry 1989; Chamley 1998). However, the high kaolinite content (>50% of the clay fraction) observed in the lower Palaeocene of the Ben Gurion section is not the result of reworking; at this time period, kaolinite was deposited during a relatively stable high sea level (Haq *et al.* 1988). The high kaolinite content observed at Ben Gurion I therefore probably indicates that warm and humid conditions with high rainfall prevailed during the early Palaeocene in this region. This interpretation is consistent with a study of Arkin *et al.* (1972) who considered the presence of kaolinite in Danian sediments of the southeastern part of the Negev to be a climatic indicator. The source of the kaolinite was probably situated on a land mass, located to the east and SE, which had a moderate relief and a well developed soil cover (Arkin *et al.* 1972).

Palygorskite and sepiolite have three main origins. (1) These fibrous clay minerals can form during hydrothermal weathering of Mg-bearing rocks, especially those of volcanic origin (Karpoff *et al.* 1989). The Palaeocene to early Eocene corresponds to a relatively stable period at the southern Tethyan margin, with no tectonic, hydrothermal or volcanic activity (Oberhänsli 1992; Charisi & Schmitz 1995). (2) Palygorskite may also form along coastal or peri-marine environments where continental waters are concentrated by evaporation leading to solutions enriched in Si and Mg which favour the formation of palygorskite and/or smectite (Robert & Chamley 1991). This process of neoformation by chemical precipitation is accelerated in warmer temperature zones (Millot 1970; Chamley 1989). (3) Palygorskite and, to a much lesser extent sepiolite, are frequently found on land in calcareous pedogenic and calcrete soils in arid to semi-arid climatic zones (Chamley 1989; Robert & Chamley 1991). It is difficult to determine the origin of the palygorskite and sepiolite observed in the Negev area. Palaeogeographic maps established by Arkin *et al.* (1972) show the existence of restricted basins between emerged land areas (Fig. 2); such basins are favourable for the neoformation

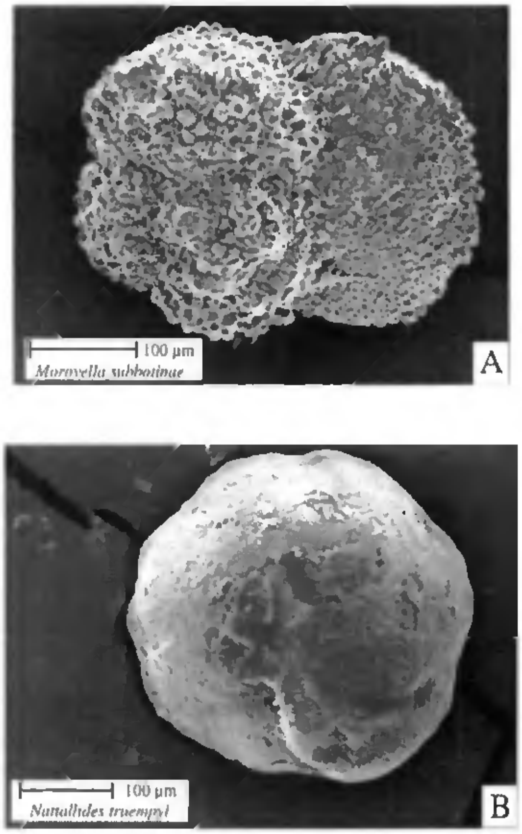

Fig. 6. Scanning electron microscope photos of (**a**) *Morozovella subbotinae*, (**b**) *Nuttallides truempyi*.

of palygorskite and sepiolite. This particular palaeogeographic setting suggests that most of these fibrous clay minerals observed at Ben Gurion and Zomet Telalim come from coastal basins. However, it can not be excluded that at least some of these clay minerals were formed in continental calcretes on the adjacent land areas around the peri-marine environments. Like smectite, fibrous clays may come from detrital or authigenic sources in marine environments (Chamley 1998). However, the simultaneous increases and decreases of mica and chlorite, two typically terrigenous species, with these fibrous clays (Figs 4 and 5), suggests a detrital origin for at least part of the palygorskite and sepiolite in the Ben Gurion and Zomet Telalim basins. Therefore, the occurrence of fibrous clays in these two basins, probably indicates warm conditions associated with major seasonal aridity with enhanced evaporation on adjacent land areas and in coastal basins where these minerals mainly formed.

Smectite in oceanic sediments can originate from volcanogenic, diagenetic and detrital sources. The sediments within the Israeli sections did not suffer deep burial diagenesis; a low burial diagenetic overprint throughout the Ben Gurion and Zomet Telalim sections is documented by the constant but variable presence of smectite, the absence of mixed-layer illite-smectite, the co-existence of smectite with high kaolinite content at the base of the Ben Gurion 400 section, and with palygorskite and sepiolite at Zomet Telalim and at Ben Gurion 500. Since clay minerals in the Israel sections were not affected by volcano-hydrothermal activity, the smectite is mainly considered to be detrital in origin and may be used as an indicator of warm climate, with seasonally alternating wet and dry conditions (Chamley 1998). The emerged areas present during

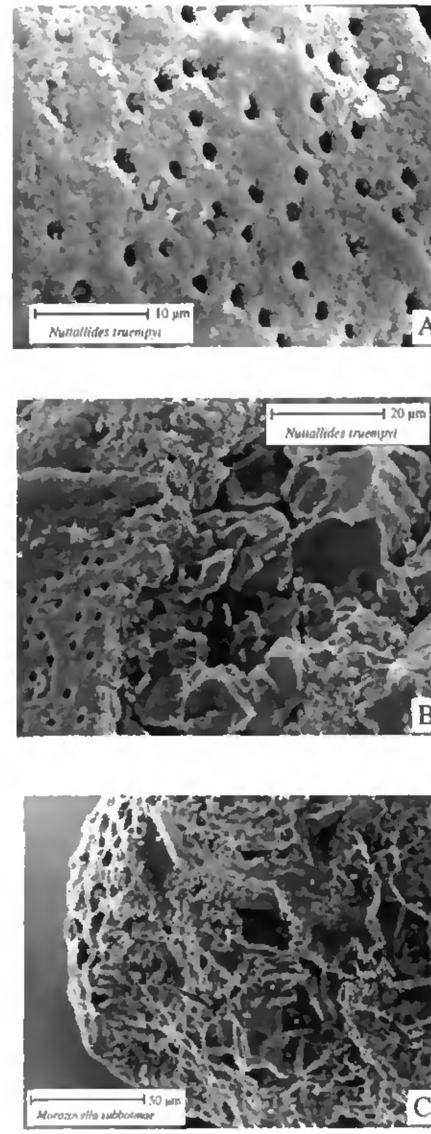

Fig. 7. Scanning electron microscope photos of *Nuttallides truempyi*. (**a**) Small pores that traverse test wall lack infillings. (**b**) Note that chambers are infilled by diagenetic calcite. (**c**) *Morozovella subbotinae* with fractured chamber infilled by diagenetic calcite.

the late Palaeocene and early Eocene in the Negev (Fig. 2) could have formed local source areas for detrital material (mica, chlorite, smectite). However, it has been shown that maximum amounts of smectite frequently coincide with long-term or short-term high sea levels (Debrabant *et al.* 1992; Deconinck 1992). Therefore the very high smectite/palygorskite-sepiolite ratio observed just above the late Palaeocene thermal maximum at Ben Gurion and Zomet Telalim in Zone P6a (Fig. 5) probably does not only indicate a major climatic change from arid to more seasonal conditions, but may be related to the short-lived transgression which took place in the *M. edgari* Zone (*c.* P6a) (Luger & Schrank 1987).

Stable isotopes

Foraminiferal preservation and diagenetic effects

Scanning electron microscope observations on fractured tests of foraminifera reveal that, although the small pores in the test

Table 1. *Distribution chart of calcareous nannofossils at Zomet Telalim, Israel*

Samples	115	122	134	145	148	151	155	158	160	161	162	163	164	165	166	167	168	169	170	171	174	177	180	183	186	188	192	195	199
Abundance	C	R	A	C	C	C	Cg	C	A	Cf	F	C	C	Rf	A	C	C	A	F	C	A	Cg	Cg	A	Cf	C	A	C	Fc
Preservation	Mp	P	G	Mp	Mp	Pm	Mp	Mp	Mg	Mp	Mp	M	M	P	Mg	Mp	M	G	P	Mg	M	M	M	Mp	M	P	Mg	Mp	Mp
Campylosphaera (eo)dela			?	?	?		?	?	x	x					?		x	x	x	x	x	x	x	x	x	x	x	x	x
Chiasmolithus cf. C. bidens	x				x	x	x					x	x		x		x	x	x	x		x	x		x	x	x	x	
Chiasmolithus sp.	x	x	x		x	x	x	x	x																				
Clausicoccus sp.						x														x	x								
Coccolithus eopelagicus	x	x	x	x	x	x	x	x	x	x	x	x	x	x	x	x	x	x	x	x	x	x	x	x	x	x	x	x	x
Coccolithus pelagicus	x	x	x	x	x	x	x	x	x	x	x	x	x	x	x	x	x	x	x	x	x	x	x	x	x	x	x	x	x
Cr. latipons	x			x												?		x	?	?									
Cruciplacolithus primus																					?			x					
Cruciplacolithus subrotundus	x																												
Cruciplacolithus sp. 10µ	x		x	x								X				X													
Cyclagelosphaera sp.									x	x																			x
Discoaster anartios																		x		x	x	?							
Discoaster araneus												?						x		?									
Discoaster binodosus						x											x				x	x	x	x	x	x	x	x	x
Discoaster bramlettei			x																										
Discoaster delicatus (4-8µ)					x	?	x	x	x	x	x	x			x	x	x	x		x	x		x		x				
Discoaster diastypus																					x	x	x	x	x				
Discoaster falcatus				x	x	x	?	x	x	x	x			x	x	x	x	x		x	x	x							
Discoaster kuepperi																							?	?				x	x
Discoaster lenticularis			x	x	x	x	x				x	x	x			x	x			x	x		x	x	x	x		?	
Discoaster mahmoudii																		?			x	x	x						
Discoaster mediosus		x							x	x																			
Discoaster megastypus			x	x				x	x						x														
Discoaster mohleri	x	x	x		x									?														?	
Discoaster multiradiatus		x	x		x	x	x	x	x	x	x	x	x	x	x	x	x	x	x	x	x	x	x	x	x	x	x		
Discoaster sp. 5 arms	x							x																					
Discoaster s. 6 arms	x			x					x											x									
Discoaster sp. 7 arms						x		x	x	x																			
Discoasts rsp. 8 arms			x		x	x	x	x	x			x									x								
Ellipsolithus distichus					x	x	x	x	x	x		x	x		x	x	x	x		x	x	x	x	x					
Ellipsolithus macellus			x	x	x										x	x				x		x		x	x	x	x	x	x
Ericsonia robusta	x	x	x		x							x	x	x	x	x		x		x									
Ericsonia subpertusa/formosa	x					x		x		x										x	x								
Fasciculithus alanii											x	x	x	x	x	x	x												
Fasciculithus bobii												x							x										
Fasciculithus clinatus	x	x	x									x			x	x	x	x				x	x	x					
Fasciculithus involutus	x	x	x		x	x	x	x	x	x	x		x	x	x	x	x	x		x	x	x							
Fasciculiths "low"												x			x	x	x	x			x	x	x	x					
Fasciculithus lillianae											x	x	x	x	x	x	x	x											
Fasciculithus mitreus											x			x		x	x	x											
Fasciculithus sidereus			x				x	x		x		x	x	x	x	x	x	x											
Fasciculithus richardii																x													
Fasciculithus tympaniformis	x	x	x		x	x	x	x	x	x	x	x	x	x	x	x	x	x	x	x	x	x	x	x		x			
Fasciculithus sp.											x	x															x		
Fasciculithus/Heliolithus? sp.	?													x															
Heliolithus kleinpellii									x				x				x												
Hornibrookina cf. H. australis																				x	x	x		x					
Lophodolithus nascens					x		x	x	x	x																			
Markalius apertus										x																			
Markalius sp.						x	x								x	x	x												
Neochiastozygus cearae																				x	x	x	x	x		x	x		
Neochiastozygus distentus	x		x				x		x							x	x	x	x	x	x		x	x					
Neochiastozygus junctus																		x				x	x	x	x	x			
Neochiastozygus c.f N. perfectus	x																												
Neococcolithes protenus																					x	x	x	x				x	x
Placozygus sigmoides	x		x			x	x	x	x	x										x	x	x	x	x	x		x		
Pontosphaera rimosa									x									x	x			x		?	x				
Prinsius bisulcus	?									?										x									
Prinsius sp. round 5µ																				x									
Rhabdolithus solus																		x	?		x	x	x	x					
Rhomboaster bramlettei																		x		x	x	x	x			x			
Rhomboaster cuspis																		x	x	x	x	x	x	x	x		x		
Rhomboaster spineus																		?											
Rhomboaster sp.																?		x	x							x			
Sphenolithus editus																							x					x	
Sphenolithus primus	x	x	x		x	x	x	x	x	x	x	x	x	x	x	x	x	x	x	x	x	x	x	x	x	x	x	x	x
Sphenolithus cf. S. radians																												x	x
Sullivania californica					x											x				x	x		x						
Sullivania consuetus	x				x	x	x	x	x	x					x	x	x		x	x	x		x	x	x		x	x	x
Sullivania "maxi" >15µ			x				x								x	x		x				x	x	x		x	x		
Sullivania sp. MINI						x		x		x		x	x		x	x				x	x	x	x				x		
Thoracosphaera sp.	x		x					x		x			x			x	x	x	x	x	x	x	x	x	x	x	x	x	x
Toweius creticulus						x	x	x													x		x					x	
Toweius eminens	x		x		x	x	x	x	x	x			x	x	x	x	x	x	x		x	x	x						
Toweius sp. ROUND					x			x	x	x									x		x		x	x					x
Tribrachiatus contortus																											x		
Zygodiscus adamas																		x					x						
NP, Martini, 1971	7/8					9a									9b								10a				10 b		11
CP, Okada & Bukry, 1980	6/7					8a									8b								9						9b

REWORKED CRETACEOUS	115	122	134	145	148	151	155	158	160	161	162	163	164	165	166	167	168	169	170	171	174	177	180	183	186	188	192	195	199
Arkhangelskiella cymbiformis																							x	x		x	x		
Biscutum sp.																												x	
Cribrosphaera ehrenbergii																								x			x		
Eiffellithus turriseiffelii																													
Lucianorhabdus cayeuxii																		x				x						x	
Micula decussata					x	x	x	x	x		x					x	x		x	x	x	x	x	x	x		x		x
Micula swastica					x			x														x							
Quadrum sp.																						?							
Prediscosphaera cretaceae								x	x												x			x					
Watznaueria barnesae																			x					x	x				

Abundance
A = abundant (>20%)
C = common (5-20%)
F = few (1-5%)
R = rare (<1%)
X = present
X = marker species

Preservation
G = good
M = moderate
P = poor

Table 2. *Stable isotopes ($\delta^{13}C$ and $\delta^{18}O$), calcite, phyllosilicates and quartz contents at Zomet Telalim, Israel*

Sample	Position (m)	Benthic (*Nuttallides truempyi*) $\delta^{13}C$	Benthic $\delta^{18}O$	Planktic (*Morozovella subbotinae*) $\delta^{13}C$	Planktic $\delta^{18}O$	Calcite (%)	Phyllo. (%)	Quartz (%)
ZT115	0.00	−0.25	−4.35			83.61	14.85	1.08
ZT117	0.30	0.82	−0.87			65.57	31.85	1.91
ZT119	0.60	0.88	−1.12			38.93	57.27	2.79
ZT120	0.75	0.40	−1.81			60.25	36.24	2.17
ZT125	1.40	0.10	−2.72			38.84	58.62	1.40
ZT126	1.50	0.02	−3.10	1.13	−3.96	64.70	31.92	2.15
ZT128	1.70	−0.57	−3.49	1.69	−4.22	51.60	43.84	2.66
ZT130	2.00	0.42	−2.74	1.72	−3.20	64.82	30.90	1.89
ZT133	2.35	0.31	−2.61	1.83	−3.69	54.80	38.41	2.22
ZT135	2.60	−0.79	−2.86	1.12	−3.80	61.71	32.66	1.98
ZT137	2.70			0.93	−3.89	66.57	29.57	1.41
ZT141	3.30	−0.61	−2.80			49.92	44.89	1.60
ZT143	3.50	−0.23	−2.27	1.15	−3.85	40.63	56.28	2.47
ZT144	3.60	−0.05	−2.29	1.12	−3.57	55.48	42.17	1.92
ZT146	3.75	−0.06	−2.24	1.49	−3.71	39.29	57.97	2.10
ZT148	4.00	0.27	−1.41	1.24	−3.25	51.95	44.37	3.19
ZT149	4.10	0.16	−1.14			42.14	53.66	3.73
ZT150	4.15	0.40	−1.50			32.83	62.77	3.68
ZT151	4.25	0.05	−1.71	0.93	−3.34	22.79	63.05	1.54
ZT153	4.45	−0.07	−1.93	1.24	−3.19	31.61	65.92	1.80
ZT155	4.65	0.22	−2.05			47.24	50.76	1.50
ZT156	4.75	0.07	−2.06	1.37	−3.41	43.51	53.83	1.70
ZT157	4.80	−0.43	−2.42	1.25	−3.64	48.12	48.26	3.18
ZT158	4.90	0.00	−2.28	1.70	−2.98	50.27	47.41	1.87
ZT159	5.00	−0.02	−2.15	1.37	−3.30	44.30	53.37	2.00
ZT160	5.10	−0.28	−2.01	1.22	−3.37	38.02	58.89	1.93
ZT161	5.20	−0.25	−2.27	1.42	−3.31	50.43	47.26	1.70
ZT162	5.25	−0.18	−1.90	1.41	−3.21	44.94	51.51	2.85
ZT163	5.35	−0.10	−2.19	1.36	−3.30	56.99	40.76	1.54
ZT164	5.45	0.02	−2.10	1.32	−3.25	60.77	37.38	1.51
ZT165	5.60	0.08	−2.07	1.33	−3.36	56.87	41.06	1.63
ZT167	5.80	−0.14	−2.47	1.04	−3.63	59.25	38.77	1.55
ZT168	5.85	−1.40	−2.75	0.16	−4.57	57.93	39.99	1.51
ZT170	6.00	−1.13	−2.47	0.02	−4.83	65.50	33.32	0.80
ZT172	6.20	−0.69	−2.65	0.21	−5.29	63.82	34.65	1.25
ZT174	6.30	−0.38	−2.51	1.10	−3.67	47.60	50.74	1.39
ZT176	6.50	0.02	−2.40	1.28	−3.48	60.73	37.49	1.42
ZT178	6.80	0.20	−2.21	1.62	−3.35	64.27	33.96	1.34
ZT180	6.90	−0.11	−2.18	1.41	−3.36	62.42	35.81	1.43
ZT183	7.20	0.15	−2.17	1.50	−3.55	73.69	24.51	1.43
ZT186	7.50	−0.06	−2.04	1.53	−3.20	74.88	23.33	1.61
ZT189	7.80	−0.03	−2.09	1.48	−3.20	68.84	29.59	1.39
ZT192	8.10	−0.24	−2.22	1.09	−3.25	42.83	55.33	1.71
ZT195	8.30	−0.31	−2.26	0.68	−3.35	88.09	11.13	0.71

walls lack infillings, most embryonic chambers are infilled with diagenetic calcite (Fig. 7). This problem of infilled or recrystallized foraminiferal test chambers is not only restricted to the Negev area, but has also been reported from lower Palaeogene sections in Egypt, Spain, Italy and Tunisia (Charisi & Schmitz 1995; Schmitz *et al.* 1996).

Magaritz *et al.* (1992) evaluated the effects of diagenetic alteration of skeletal carbonates on the $\delta^{18}O$ and $\delta^{13}C$ signals across the Cretaceous–Tertiary boundary and in early Palaeocene sections from the Negev. By comparing the isotopic values from bulk rock and two fine-grained size fractions, they concluded that although the $\delta^{13}C$ signals were not significantly altered, $\delta^{18}O$ signals were strongly affected by meteoric water during early diagenesis. Dissolution–recrystallization processes often do not significantly influence the magnitude of the $\delta^{13}C$ shift, even though the primary oxygen isotope values are overprinted by diagenesis (Veizer 1983). This difference may be explained by much larger temperature dependent fractionation during burial diagenetic cementation for oxygen than for carbon isotopes (Friedman & O'Neil 1977). These observations suggest a degradation of the primary $\delta^{18}O$ signal, though the $\delta^{13}C$ signal remains relatively unaltered at Zomet Telalim. Nevertheless, if foraminiferal tests are significantly infilled with diagenetic calcite of questionable origin (nannofossils, benthic and/or planktic foraminifera, aragonite) then the foraminiferal $\delta^{13}C$ values are probably in part related to the diagenetic calcite phases.

Carbon isotopes

At Zomet Telalim, changes in $\delta^{13}C$ values can be divided into three parts (Fig. 3, Table 2). Below 5.7 m, planktic

(*Morozovella subbotinae*) and benthic (*Nuttallides truempyi*) $\delta^{13}C$ values covary between 0.93‰ and 1.8‰ and 1‰ to −0.9‰, respectively. Maximum variability occurs in the lower 3 m of the section (zones P4, NP7/8). The interval from 3 m to 5.7 m (Zone P4 top and Subzone P5a) has relatively stable benthic and planktic $\delta^{13}C$ values. Between 5.7 m and 6.2 m planktic and benthic foraminifera $\delta^{13}C$ values decrease rapidly by 1.4‰ and 1.2‰, respectively. Above 6.2 m, planktic and benthic $\delta^{13}C$ values gradually increase to pre-excursion values. Throughout the Zomet Telalim section, benthic foraminifera exhibit lower $\delta^{13}C$ values than planktic foraminifera, resulting from the surface to deep-water vertical $\delta^{13}C$ gradient, which is related to biological carbon fractionation (Kroopnick *et al.* 1977).

The onset of the planktic and benthic carbon isotope excursion lies just above the benthic extinction event which, marks the beginning of the late Palaeocene thermal maximum (Kennett & Stott 1991; Bralower *et al.* 1995; Thomas & Shackleton 1996). However, the presence of a hiatus between Subzone P5a and P5b could have removed the lower part of the $\delta^{13}C$ excursion. The lower magnitude of this excursion at Zomet Telalim (1.2–1.4‰), as compared with 2.5–3‰ in other sections in the Negev and Egypt (Schmitz *et al.* 1996; Charisi & Schmitz 1998), may be due to non-deposition or erosion of the lower part of the $\delta^{13}C$ excursion at this hiatus.

Oxygen isotopes

Planktic $\delta^{18}O$ values vary between −3 and −4‰ throughout the section, except between 5.7 m and 6.2 m where a negative excursion of 1.9‰ occurs in the late Palaeocene (Fig. 3). From P4b to P4c (0 to 4.25 m), benthic $\delta^{18}O$ values fluctuate between −4.3‰ and −0.87‰ and between 4.25 m and 5.7 m, *Nuttallides truempyi* $\delta^{18}O$ values are stable and close to −2.1‰. The subsequent late Palaeocene thermal maximum interval (0.5 m thick) is marked by a minor negative excursion of 0.6‰ in benthic $\delta^{18}O$ values. Above this interval, values remain lower than below the interval (−2.3‰).

At Zomet Telalim planktic and benthic foraminiferal $\delta^{18}O$ values are lower than those recorded from most coeval marine sections worldwide. The recrystallization processes affecting foraminiferal tests (Fig. 6) have led to lower $\delta^{18}O$ values. Thus, palaeotemperature calculations using these oxygen isotope ratios are not reliable.

Despite the important role played by the diagenesis on the original $\delta^{18}O$ signal, some observations in the benthic and planktic $\delta^{18}O$ trends could suggest a partial preservation of the original signal in the Zomet Telalim basin. Except for the late Palaeocene thermal maximum interval, benthic and planktic $\delta^{18}O$ values are relatively stable and appear to follow the same trend throughout the section suggesting similar recrystallization rates for benthic and planktic foraminiferal tests (Fig. 3). Therefore, it appears difficult to explain the sudden decrease in planktic $\delta^{18}O$ values and the rapid post-$\delta^{18}O$ shift recovery (Fig. 3) as the result of changes in the recrystallization rate and the preferential effect on planktic foraminifera tests. Moreover a constant gradient of approximately 1.3‰ can be observed between the benthic and planktic $\delta^{18}O$ values (Fig. 3). Although the proportion of diagenetic infillings may play a significant role at Zomet Telalim, the retention of interspecific differences between the $\delta^{18}O$ values suggests the retention of the relict original oxygen isotopic ratio secreted in the foraminiferal test (Killingley 1983; Charisi & Schmitz 1995). In addition, the general trends of the benthic and planktic isotopic oxygen record shows strong similarities with those recorded from well-preserved foraminifera at Ben Gurion. During the late Palaeocene thermal maximum, the planktic $\delta^{18}O$ record exhibits a pronounced negative excursion (Lu *et al.* 1995), whereas $\delta^{18}O$ values measured on benthic foraminifera which lack infilling show only a 0.5‰ shift (Charisi & Schmitz 1998). Similar observations were made at Zomet Telalim.

Discussion

Reduced carbonate sedimentation

Various processes may result in a low calcite content, including decreased productivity of calcareous microplankton, relatively high quartz/phyllosilicate input during lower sea levels and carbonate dissolution. Low calcite values have been observed in the Ben Gurion section where Lu *et al.* (1995) suggested that carbonate dissolution may be the major cause of the pre-$\delta^{13}C$ excursion calcite minimum. At Zomet Telalim, dissolution is observed in foraminiferal tests in the calcite minima in Zone P4 (Fig. 3), but not further upsection. However, low sea levels corresponding to the upper parts of zones P4c and P5a (Haq *et al.* 1988) may account for the observed decrease in carbonate sediment supply as a result of increased terrigenous input and hence dilution of carbonates in the Zomet Telalim basin.

At Zomet Telalim, the coincidence of a high proportion of calcite at the time of the $\delta^{13}C$ excursion during the late Palaeocene thermal maximum is unusual since this event is generally associated with reduced carbonate contents in nearly all published records (e.g. Kennett & Stott 1990; O'Connell 1990; Adatte & Lu 1995; Bralower *et al.* 1995; Lu & Keller 1995; Lu *et al.* 1995; Kelly *et al.* 1996; Bolle *et al.* 1998). However, this high calcite content, coincident with the $\delta^{13}C$ shift, has not only been observed at Zomet Telalim, but also in other middle eastern Tethyan sections (Israel and Egypt) (Lu *et al.* 1995; Schmitz *et al.* 1996, 1997). Schmitz *et al.* (1997) interpreted these calcareous deposits as episodes of increased regional productivity. In the Ben Gurion section, a 2.5‰ $\delta^{13}C$ shift coincides with a strong increase in carbonate abundance to 90% (Schmitz *et al.* 1997), whereas at Zomet Telalim, the relatively slight increase in calcite to 78% coincident with a 1.3 negative $\delta^{13}C$ excursion, may be due to the presence of a discontinuity at the late Palaeocene thermal maximum interval. It is likely that the interval of the maximum of the $\delta^{13}C$ excursion and calcite values are missing at Zomet Telalim as suggested by the hiatus identified between subzones P5a/P5b.

Climate on the southeastern Tethys margin

During the early Palaeocene (zones P1 to P2), the adjacent coastal or continental areas of the southern Tethys margin were influenced by a warm and humid climate with high precipitation rates as indicated by the abundance of kaolinite observed in oceanic sediments in the Negev area (Arkin *et al.* 1972). Similar climatic conditions have been described in Tunisia where the high kaolinite content also suggests warmth and humidity in the early Palaeocene (Bolle *et al.* 1999). This climatic trend is in agreement with the humid and warm climate that marked the end of the Cretaceous both in this region (Arkin *et al.* 1972; Keller *et al.* 1998; Li *et al.* 2000) and worldwide (Barron & Washington 1982).

Palygorskite and sepiolite have frequently been observed in Atlantic sediments from the southern Angola basin to the deep basin of Morocco (Mélières 1977; Robert 1982; Maillot & Robert 1984). In the coastal basins and peri-marine environments of West Africa, palygorskite deposition starts to increase in the late Palaeocene where it is associated with smectite. Palygorskite almost exclusively dominates the clay fraction in the lower Eocene. This West African palygorskite episode indicates that low latitudes, especially coastal areas, experienced intensive aridity and evaporation, whereas humid conditions may have prevailed in the continental hinterland, as indicated by laterization processes observed on the African craton (Millot 1970; Robert & Chamley 1991). In the Middle Eastern Tethyan region, clay mineral data show similar trends to North and West Africa though with slight differences. In southeastern Egypt, the presence of kaolinite within marine sedimentary rocks and palaeobotanical and palynological data indicate high humidity on the continental hinterland from the upper Palaeocene to the early Eocene (Abou-Ela 1989; Hendricks *et al.* 1990; Strouhal 1993). High precipitation associated with warmer temperatures probably favoured intensive leaching of the parent rocks and formation of kaolinitic soils. Magnesium and silicon, the chemical elements essential for the crystallization of magnesium-rich palygorskite and sepiolite were dissolved, transported by running water into the sea and precipitated under warm and arid climates which favoured enhanced evaporation (Robert & Chamley 1991; Hendricks *et al.* 1990).

The gradual disappearance of kaolinite, coincident with the gradual increase in palygorskite, sepiolite and smectite, as well as mica and chlorite, suggests the progressive development of aridity in the Negev area. Increased aridity led to enhanced evaporation and chemical precipitation of palygorskite and sepiolite in the coastal basins and to poor drainage conditions which facilitated the formation of smectite on the adjacent land masses. At Ben Gurion I, kaolinite disappeared in the middle of Zone P3 whereas palygorskite and sepiolite increased markedly. In southern Tunisia, the Foum Selja section located in the El Kef Basin, where sedimentation was mainly influenced by the Saharan Platform to the south, shows similar trends (Bolle *et al.* 1999). The simultaneous disappearance of kaolinite in sections located at approximately the same palaeolatitude (*c.* 20°N), but separated by more than 2700 km (Tunisia to Israel) suggests a latitudinal change from humid and warm to arid conditions which affected the peri-marine environments of the southern Tethys margin during the Palaeocene. In the coastal basins of the Negev area, these arid climatic conditions were already initiated in the Danian (base of Zone P2) and fully developed largely in the Selandian (middle of Zone P3). Aridity persisted through the late Palaeocene and reached a maximum in the Ypresian, coincident with arid maxima observed in North Africa. The absence of palynomorphs in the sediments of Zomet Telalim reflects these arid climatic conditions and reduced vegetation on the adjacent land areas (H. Brinkhuis pers. comm.). During this time interval, gypsum deposits accumulated over vast areas of the southeastern Arabian Peninsula (Oberhänsli 1992) as a result of enhanced evaporation, whereas the persistance of kaolinite in southeastern Egypt suggests that humid conditions prevailed on the African craton (Hendricks *et al.* 1990).

Sea surface warming in the Negev area during the late Palaeocene thermal maximum?

The Negev area differs from other Tethyan sites by its location on the southeastern margin of the Tethys, a region affected by intermittent upwelling episodes (Benjamini & Eisenshtein 1995; Lu *et al.* 1995; Schmitz *et al.* 1997; Charisi & Schmitz 1998). Based on faunal and isotopic criteria observed in the Ben Gurion section (e.g. disappearance of radiolaria, maximum planktic/benthic foraminiferal ratio and elimination of the planktic $\delta^{13}C$ difference between the southern margin and deep basins), Lu *et al.* (1995) suggested a reduction in the upwelling intensity during the late Palaeocene thermal maximum. On the contrary, Schmitz *et al.* (1997) interpreted barium enrichment associated with increased P_2O_5, opaline-silica and $CaCO_3$ at Ben Gurion and Gebel Aweina in Egypt, as an episode of high productivity during the late Palaeocene thermal maximum in the Middle Eastern region. Moreover, at Ben Gurion Charisi & Schmitz (1998) speculated that benthic $\delta^{18}O$ values do not record temperature changes related to upwelling variations because bottom waters in this section were probably deeper than the active upwelling center.

Our study does not confirm increased upwelling activity in the Negev area during the late Palaeocene thermal maximum. The oxygen isotopic trends suggest sea-surface warming similar to Ben Gurion, whereas bottom waters remained unaffected. Moreover during the latest Palaeocene the thermal stratification of the water column of the Zomet Telalim basin increased as suggested by the benthic and planktic $\delta^{18}O$ gradient, which becomes higher during this time period (Fig. 3). Our apparently contradictory interpretation of the upwelling activity in the Negev area as compared with Schmitz *et al.* (1997) suggests the following possible scenarios for the observed surface warming at Zomet Telalim. First, the sea surface warming is regional and due to temporarily reduced upwelling as suggested by Lu *et al.* (1995). Alternatively, the Zomet Telalim basin may be less influenced by upwelling activity, in which case sea surface warming is simply a response to warmer climates associated with the aridity which dominates at the end of the Palaeocene in the adjacent coastal areas of the southern Tethys margin.

Palaeoproductivity changes

Benthic and planktic $\delta^{13}C$ records are persistently lower in the Middle Eastern Tethyan region than in coeval Tethys and Pacific sections (Lu *et al.* 1995; Charisi & Schmitz 1995, 1998; Schmitz *et al.* 1996) and reflect regional effects and the restricted character of the Middle Eastern region relative to the open ocean (Charisi & Schmitz 1998). These unusually light $\delta^{13}C$ values have been variously explained by enhanced input of organic matter of terrestrial origin, continental margin upwelling bringing $\delta^{13}C$-light waters to the surface, and palaeogeographic restriction of the Middle Eastern Tethys margin (Lu *et al.* 1995; Charisi & Schmitz 1995, 1998; Schmitz *et al.* 1996). The unusually low $\delta^{13}C$ values observed in this region are also consistent with increased aridity and associated warmer temperatures that affected the Negev area during the late Palaeocene to the early Eocene. Under warm and arid climatic conditions, palygorskite and sepiolite formed in restricted coastal basins with reduced surface water biological productivity. The light $\delta^{13}C$ composition associated with these low productivity restricted basins may have significantly influenced the negative $\delta^{13}C$ signal observed in the Negev area.

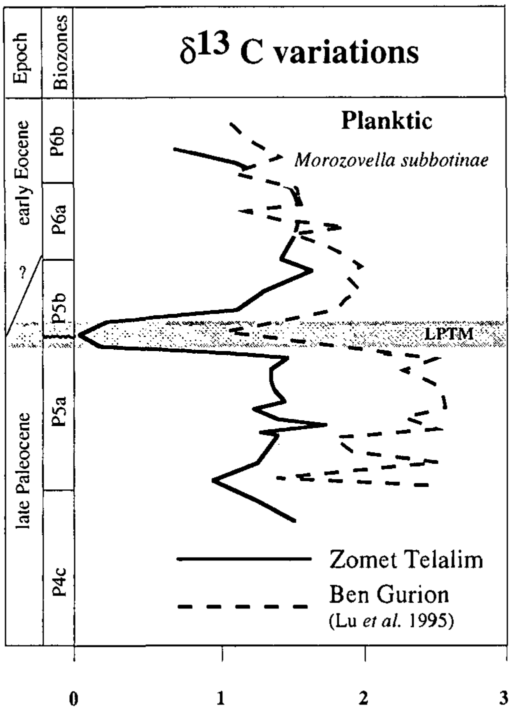

Fig. 8. Comparison of the planktic carbon isotope records of Zomet Telalim and Ben Gurion I sections across the late Palaeocene thermal maximum interval. For the Ben Gurion section, planktic stable isotopes data are from Lu *et al.* (1995).

Throughout the Zomet Telalim section, foraminiferal $\delta^{13}C$ values are constantly lighter than at Ben Gurion; planktic $\delta^{13}C$ values are 1.2‰ lower below and during the late Palaeocene thermal maximum, whereas the planktic records converge with a $\delta^{13}C$ difference of 0.6‰ above it (Fig. 8). Though Zomet Telalim represents a more open marine environment than Ben Gurion (Fig. 2), it is difficult to determine whether the palaeogeographic location of the two basins is the major cause for the difference in the $\delta^{13}C$ signal at the two sections. At Zomet Telalim, a combination of regional environmental factors and early diagenetic processes may have amplified the primary carbon isotopic signal and resulted in the unusually light $\delta^{13}C$ values, as compared to Ben Gurion.

Conclusions

Based on different criteria, the clay mineralogy observed in marine sedimentary rocks of Ben Gurion and Zomet Telalim indicate qualitative regional climatic changes. During the early Palaeocene, the southeastern Tethys margin experienced warm and humid climatic conditions with high rainfall. Arid climatic conditions progressively expanded on the coastal basins of the southeastern Tethys margin as indicated by the gradual disappearance of kaolinite and the increased abundance of palygorskite and sepiolite. Arid climatic conditions began in the Danian and persisted during the Selandian and Thanetian (late Palaeocene), reaching a maximum in the Ypresian (early Eocene).

During the late Palaeocene thermal maximum, warm climatic conditions associated with increased aridity may have led to sea surface warming as suggested by the planktic $\delta^{18}O$ excursion observed in the marginal Zomet Telalim basin, whereas bottom waters appear not to have been affected, assuming that the original oxygen isotopic signal is partly preserved.

Increase aridity in the Negev area could have induced a strong reduction in the surface-water biological productivity in the coastal basins, leading partly to the unusually light $\delta^{13}C$ values observed throughout the Zomet Telalim section. During the late Palaeocene thermal maximum, the low $\delta^{13}C$ values are amplified by the global short-term negative carbon isotope excursion which is observed in coeval sections worldwide, but whose cause remains an enigma.

The authors thank C. Benjamini from the University of Ben Gurion, Israel and G. Keller from Princeton University, USA, for the sampling of the studied sections. We are also grateful to G. Keller for providing important comments and helpful suggestions on this paper. We thank J. Richard for conducting X-ray preparations at the laboratory of mineralogy and petrology, University of Neuchâtel, Switzerland. We are sincerely grateful to R. Speijer (Bremen) and to an anonymous reviewer for impartial and constructive criticism of an early version. This study was supported by the Swiss National Foundation, No. 2100-043450.95/1.

References

ABOU-ELA, N.M. 1989. Lower Tertiary microflora from the Esna shale of the Red Sea coast, Egypt. *Revista Espanola de Micropaleontologia*, **21**, 189–206.

ADATTE, T. & LU, G. 1995. Clay mineral correlation across the Paleocene-Eocene boundary: evidence for global turnover from western to eastern Tethys (Abstract). *In: Geological Society af America 1995 annual meeting*. New Orleans, November 6–9, A305

——, RENTZEL, P. & KÜBLER, B. 1991. Etude minéralogique et sédimentologique du remplissage karstique de la grotte de Cotencher (Jura neuchételois, Suisse). *Eclogae geologicae Helvetiae*, **84**, 671–688.

——, STINNESBECK, W. & KELLER, G. 1996. Lithostratigraphic and mineralogic correlations near K/T boundary clastic sediments in northeastern Mexico: Implications for origin and nature of deposition. *In:* RYDER, G., FASTOVSKY, D. & GARTNER, S. (eds) *Cretaceous–Tertiary Event and Other Catastrophes in Earth History*. Geological Society of America Special Papers, **307**, 211–226.

ANGORI, E. & MONECHI, S. 1996. High resolution calcareous nannofossil biostratigraphy across the Paleocene-Eocene boundary at Caravaca (southern Spain). *Israel Journal of Earth Sciences*, **44**, 197–206.

ARENILLAS, I. 1996. *Los faraminiferos planctonicos del Paleoceno-Eoceno inferior: sistematica, bioestratigrafica, cronoestratigrafia y paleaceanografia*. PhD Thesis. Universidad de Zaragoza, Spain,

—— & MOLINA, E. 1996. Biocstratigrafia y evolucion de las asociaciones de foraminiferos planctonicos del transito Paleoceno-Eoceno en Alamedilla (Cordilleras Béticas). *Revista Espanola de Micropaleontologia*, **18**, 75–96.

ARKIN, Y., NATHAN, Y. & STARINSKY, A. 1972. Paleocene-Eocene environments of deposition in the northern Negev (southern Israel). *Geological Survey of Israel, Bulletin*, **56**, 1–18.

AUBRY, M.P. 1996. Towards an Upper Paleocene-Lower Eocene high resolution stratigraphy based on calcareous nannofossil stratigraphy. *Israel Journal of Earth Sciences*, **44**, 239–253.

AXELROD, D.I. 1984. An interpretation of Cretaceous and Tertiary biota in polar regions. *Palaeogeography, Palaeoclimatology, Palaeoecology*, **45**, 105–147.

BARRON, E.J. & WASHINGTON, W.M. 1982. Cretaceous Climate; A comparison of atmospheric simulations with the geologic records. *Palaeogeography, Palaeoclimatology, Palaeoecology*, **40**, 103–133.

BENJAMINI, C. 1992. The Paleocene-Eocene boundary in Israel – a candidate for the boundary stratotype. Neues Jahrbuch für Geologie und Paläontologie. *Abhandlungen*, **186**, 49–61.

—— & EISENSHTEIN, A. 1995. Record on the P/E catastrophe in two upper bathyal sections; northern Negev, Israel (Abstract). *In: Geological Society of America 1995, annual meeting*. New Orleans, November 6–9, A304

BENTOR, Y.K., VROMAN, A. & ZAK, I. 1965. *The Geological Map of Israel 1:250000 (Southern Sheet)*. Ministry of Labour, Survey Department, Tel Aviv.

BERGGREN, W.A. & MILLER, K.G. 1988. Paleogene tropical planktic foraminiferal biostratigraphy and magnetobiochronology. *Micropaleantology*, **34**, 362–380.

——, KENT, D.V., SWISHER III, C.C. & AUBRY, M.P. 1995. A revised Cenozoic Geochronology and Chronostratigraphy. *In:* BERGGREN, W.A., KENT, D., AUBRY, M.P. & HARDENBOL, J. (eds) *Geochronology, Time Scales, and Stratigraphic Correlation.* Society for Sedimentary Geology Special Publications, **54**, 129–212.

BLOW, W.H. 1979. *The Cenozoic Globigerinidae. A study of the morphology, taxonomy, evolutionary relationships and the stratigraphical distribution of some Globigerinidae (mainly Globigerinacea).* E. J. Brill, Leiden, Netherlands.

BOLLE, M.P., ADATTE, T., KELLER, G., VON SALIS, K. & BURNS, S. 1999. The Paleocene-Eocene transition in the Southern Tethys (Tunisia): Climatic and environmental fluctuations. *Bulletin de la Société géologique de France*, **170**, 661–680.

——, ——, ——, —— & HUNZIKER, J. 1998. Biostratigraphy, mineralogy and geochemistry of the Trabakua Pass and Ermua sections in Spain: Paleocene-Eocene transition. *Eclagae Geologicae Helvetiae*, **91**, 1–25.

BRALOWER, T.J., ZACHOS, J.C., THOMAS, E., PARROW, M., PAUL, C.K., KELLY, D.C., PREMOLI SILVA, I., SLITER, W.V. & LOHMANN, K.C. 1995. Late Paleocene to Eocene paleoceanography of the equatorial Pacific Ocean: Stable isotopes recorded at Ocean Drilling Program Site 865, Allison Guyot. *Paleoceanography*, **10**, 841–86.

BYBELL, L.M. & SELF-TRAIL, J.M. 1995. *Evolutionary, Biostratigraphic, and Taxonomic Study of Calcareous Nannofossils from a Continous Paleocene–Eocene Boundary Section in New Jersey.* United States Geological Survey, Professional Papers, **1554**.

CHAMLEY, H. 1989. *Clay Sedimentology.* Springer, Berlin, Heidelberg.

—— 1998. Clay Mineral Sedimentation in the Ocean. *In:* PAQUET, N. & CLAUER, N. (eds) *Soils and Sediments (Mineralogy and Geochemistry).* Springer Berlin, 269–302.

CHARISI, S.D. & SCHMITZ, B. 1995. Stable ($\delta^{13}C$ and $\delta^{18}O$) and strontium ($^{87}Sr/^{86}Sr$) isotopes through the Paleocene at Gebel Aweina, eastern Tethyan region. *Palaeogeography, Palaeoclimatology, Palaeoecology*, **116**, 103–129.

—— & —— 1998. Paleocene to early Eocene paleoceanography of the Middle East: The $\delta^{13}C$ and $\delta^{18}O$ isotopes from foraminiferal calcite. *Paleoceanography*, **13**, 106–118.

CORFIELD, R.M. & CARTLIDGE, J.E. 1992. Oceanographic and climatic implications of the Paleocene carbon isotope maximum. *Terra Nova*, **4**, 443–455.

DEBRABANT, P., FAGEL, N., CHAMLEY, H., DECONINCK, J.F., RECOURT, P. & TROUILLET, A. 1992. Clay Sedimentology, mineralogy and chemistry of Mesozoic sediments drilled in the northern Paris Basin. *Scientific Drilling*, **3**, 138–152.

DECONINCK, J.F. 1992. *Sédimentologie des argiles dans le Jurassique-Crétacé d'Europe occidentale et du Maroc.* Mémoire d'Habilitation Université de Lille 1, France.

DICKENS, G., O'NEIL, J., REA, D. & OWEN, R.M. 1995. Dissociation of oceanic methane hydrate as a cause of the carbon isotope excursion at the end of the Paleocene. *Paleoceanography*, **10**, 965–971.

——, CASTILLO, M. & WALKER, J.C. 1997. A blast of gas in the latest Paleocene: Simulating first-order effects of massive dissociations of oceanic methane hydrate. *Geology*, **25**, 259–262.

ESTES, R. & HUTCHISON, J.H. 1980. Eocene lower vertebrates from Ellesmere Island, Canadian Arctic Archipelago. *Palaeogeography, Palaeoclimatology, Palaeoecology*, **30**, 325–347.

FRIEDMAN, I. & O'NEIL, J.R. 1977. Compilation of stable isotope fractionation factors of geochemical interest. *In:* FLEISCHER, M. (ed.) *Data of Geochemistry.* United States Geological Survey Professional Papers **440-KK**, 12.

FERRERO, J. 1966. *Nouvelle méthode empirique pour le dosage des minéraux par diffroction R.X.* Rapport C.F.P (Bordeaux) **26**.

GAWENDA, P., WINKLER, W., SCHMITZ, B. & ADATTE, T. 1999. Climate and bioproductivity control on carbonate turbidite sedimentation (Paleocene to earliest Eocene Gulf of Biscay, Zumaia). *Journal of Sedimentary Research*, 69, 1253–1261.

GIBSON, T.G., BYBELL, L.M. & OWENS, J.P. 1993. Latest Paleocene lithologic and biotic events in neritic deposits of southwestern New Jersey. *Paleoceanography*, **8**, 495–514.

GINGERICH, P.D. 1980. Evolutionary patterns in early Cenozoic mammals. *Annual Review of Earth and Planetary Sciences*, **8**, 407–424.

HAQ, B.U., HARDENBOL, J. & VAIL, P.R. 1988. Mesozoic and Cenozoic chronostratigraphy and cycles of relative sea level change. *In:* WILGUS, C.K., HASTINGS, B.S., ROSS, C.A., POSAMENTIER, H.W., VAN WAGONER, J. & KENDALL, C.G. (eds) *Sea-level Changes: An Integrated Approach.* Society for Sedimentary Geology Special Publications **42**, 71–108.

HENDRICKS, F., LUGER, P. & STROUHAL, A. 1990. Early Tertiary Marine Palygorskite and Sepiolite Neoformation in SE Egypt. *Zeitschrift de Deutschen Geologischen Gesellschaft*, **141**, 87–97.

KARPOFF, A.M., LAGABRIELLE, Y., BOILLOTT, G. & GIRARDEAU, J. 1989. L'authigenèse océanique de palygorskite, par halmyrolyse de péridotites serpentinisées (marge de Galice): ses implications géodynamiques. *Comptes Rendus de l'Académie des Sciences de Paris*, **308**, 647–654.

KELLER, G. & BENJAMINI, C. 1991. Paleoenvironment of the Eastern Tethys in the early Paleocene. *Palaios*, **6**, 439–464.

——, ADATTE, T., STINNESBECK, W., STUBEN, D., KRAMAR, U., BERNER, Z. & VON SALIS, K. 1998. The Cretaceous-Tertiary transition on the shallow Saharan Platform of southern Tunisia. *Geobios*, **30**, 951–975.

KELLY, D.C., BRALOWER, T.J., ZACHOS, J.C., PREMOLI SILVA, I. & THOMAS, E. 1996. Rapid diversification of planktonic foraminifera in the tropical Pacific (ODP Site 865) during the Late Paleocene thermal maximum. *Geology*, **24**, 423–426.

KENNETT, J.P. & STOTT, L. 1990. Proteus and Proto-Oceanus: Paleogene oceans as revealed from Antarctica stable isotopic results. *Proceeding of the Ocean Drilling Program, Scientific Results*, **113**, 865–879.

—— & —— 1991. Abrupt deep-sea warming, palaeoceanographic changes and benthic extinctions at the end of the Paleocene. *Nature*, **353**, 225–229.

KILLINGLEY, J.S. 1983. Effects of diagenetic recrystallization on $^{18}O/^{16}O$ values of deep-sea sediments. *Nature*, **301**, 594–597.

KNOX, R.W. 1996. Correlation of the early Paleogene in northwest Europe: an overview. *In:* KNOX, R.W., CORFIELD, R.M. & DUNAY, R.E. (eds) *Correlation of the Early Paleogene in Northwest Europe.* Geological Society, London, Special Publications, **101**, 1–11.

KOCH, P.L., ZACHOS, J.C. & GINGERICH, P.D. 1992. Correlation between isotope records in marine and continental carbon reservoir near the Paleocene/Eocene boundary. *Nature*, **358**, 319–322.

KROOPNICK, P.M., MARGOLIS, S.V. & WONG, C.S. 1977. $\delta^{13}C$ variations in marine carbonate sediments as indicators of CO_2 balance between the atmosphere and the oceans. *In:* ANDERSON, N.R. & MALAHOFF, A. (eds) *The Fate of Fossil Fuel CO_2 in the Oceans.* Plenum New York, 295–321.

KÜBLER, B. 1983. *Dosage quantitatif des minéraux majeurs des roches sédimentaires par diffraction X.* Cahiers de l'Institut de Géologie de Neuchâtel Série AX 1.1 & 1.2.

—— 1987. *Cristallinité de l'illite, méthodes normalisées de préparations, méthodes normalisées de mesures.* Cahiers de l'Institut de Géologie de Neuchâtel Série ADX, 1–8.

LI, L., KELLER, G., ADATTE, T. & STINNESBECK, W. 2000. Late Cretaceous sea-level changes in Tunisia: a multidisciplinary approach. *Journal of the Geological Society, London*, **157**, 447–458.

LU, G. & KELLER, G. 1993. The Paleocene-Eocene transition in the Antarctic Indian Ocean : inference from planktic foraminifera. *Marine Micropaleontology*, **21**, 101–142.

—— & —— 1995. Planktic foraminiferal faunal turnovers in the subtropical Pacific during the Late Paleocene to Early Eocene. *Journal of Foraminiferal Research*, **25**, 97–116.

——, ADATTE, T., KELLER, G. & ORTIZ, N. 1998*a*. Abrupt climatic, oceanographic and ecologic changes near the Paleocene-Eocene transition in the deep Tethys basin: The Alamedilla section, Southern Spain. *Eclagae Geologicae Helvetiae*, **91**, 293–306.

——, KELLER, G., ADATTE, T. & BENJAMINI, C. 1995. Abrupt change in the upwelling system along the southern margin of the Tethys during the Paleocene-Eocene transition event. *Israel Journal of Earth Sciences*, **44**, 185–195.

——, —— & PARDO, A. 1998*b*. Stability and Change in Tethyan planktic foraminifera across the Paleocene-Eocene transition. *Marine Micropaleontology*, **35**, 203–233.

LUGER, P. & SCHRANK, E. 1987. Mesozoic to Paleogene transgressions in middle and southern Egypt: Summary of paleontological evidence. *In:* MATHEIS, G. & SCHANDELMEIER, H. (eds) *Current Research in African Earth Sciences.* Balkema Rotterdam, 199–202.

MAILLOT, H. & ROBERT, C. 1984. Significance of clay mineralogical and geochemical data, Walvis Ridge, Southeast Atlantic (DSDP Leg 75). *Initial Reports of the Deep Sea Drilling Project*, **25**, 843–862.

MAGARITZ, M., BENJAMINI, C., KELLER, G. & MOSHKOVITZ, S. 1992. Early diagenetic isotopic signal at the Cretaceous/Tertiary boundary, Israel. *Paleogeography, Paleoclimatology, Paleoecology*, **91**, 279–292.

MARTINI, E. 1971. Standard Tertiary and Quaternary calcareous nannoplankton zonation. *In:* FARINACCI, A. (ed.) *Proceedings 2nd Planktonic Conference, Roma 1970.* Technoscienza, **4**, 739–785.

MÉLIÈRES, F. 1977. X-ray mineralogy studies, Leg 41 DSDP, Eastern North Atlantic Ocean. *Initial Reports of the Deep Sea Drilling Project*, **41**, 1065–1086.

MILLOT, G. 1970. *Geology of Clays.* Springer, New York.

OBERHÄNSLI, H. 1992. The influence of the Tethys on the bottom waters of the early Tertiary ocean. *In:* KENNETT, J.P. (ed.) *The Antarctic Paleoenvironment: A Perspective on Global Change.* Antarctic Research Service, England, 167–184.

O'CONNELL, S.B.O. 1990. Variations in upper Cretaceous and Cenozoic calcium carbonate percentages, Maud Rise, Weddell Sea. *Proceeding of the Ocean Drilling Program, Scientific Results*, **113**, 971–984.

OKADA, H. & BUKRY, D. 1980. Supplementary modification and introduction of code numbers to the low-latitude coccolith biostratigraphic zonation (Bukry, 1973; 1975). *Marine Micropaleontology*, **5**, 321–325.

PAK, D.K. & MILLER, K.G. 1992. Paleocene to Eocene benthic foraminiferal isotopes and assemblages: implications for deepwater circulation. *Paleoceanography*, **7**, 741–761.

PARDO, A., KELLER, G. & OBERHÄNSLI, H. 1999. Paleoecologic and paleoceanographic evolution of the Tethyan realm during the Paleocene-Eocene transition. *Journal of Foraminiferal Research*, **29**, 37–57.

PERCH-NIELSEN, K. 1985. Cenozoic calcareous nannofossils. *In:* BOLLI, H.M. (ed.) *Plankton Stratigraphy*. Cambridge University Press Cambridge, 427–554.

PREMOLI-SILVA, I. & BOERMSA, A. 1984. Atlantic Eocene planktonic foraminiferal historical biogeographic and paleohydrologic indices. *Palaeogeography, Palaeoclimatology, Palaeoecology*, **67**, 315–356.

ROBERT, C. 1982. *Modalité de la sédimentation argileuse en relation avec l'histoire géologique de l'Atlantique Sud.* PhD Thesis, Université Aix-Marseille II, France.

—— & CHAMLEY, H. 1991. Development of early Eocene warm climates, as inferred from clay mineral variations in oceanic sediments. *Palaeogeography, Palaeoclimatology, Palaeoecology*, **89**, 315–332.

—— & KENNETT, J.P. 1992. Paleocene and Eocene kaolinite distribution in the South Atlantic and Southern Ocean: Antarctic climatic and paleoceanographic implications. *Marine Geology*, **103**, 9–110.

—— & —— 1994. Antarctic subtropical humid episode at the Paleocene-Eocene boundary: Clay-mineral evidence. *Geology*, **22**, 211–214.

SCHMITZ, B., CHARISI, S.D., THOMPSON, E. & SPEIJER, R.P. 1997. Barium, SiO2 (excess), and P_2O_5 as proxies of biological productivity in the Middle East during the Palaeocene and the latest Palaeocene benthic extinction event. *Terra Nova*, **9**, 95–99.

——, SPEIJER, R.P. & AUBRY, M.P. 1996. Latest Paleocene benthic extinction event on the southern Tethyan shelf (Egypt): Foraminiferal stable isotopic ($\delta^{13}C$, $\delta^{18}O$) records. *Geology*, **24**, 347–350.

SHACKLETON, N.J., CORFIELD, R.M. & HALL, M.A. 1985. Stable isotope data and ontogeny of Paleocene planktic foraminifera. *Journal of Foraminiferal Research*, **15**, 321–226.

SMITH, A.G., SMITH, D.G. & FUNNELL, B.M. 1994. *Atlas of Mesozoic and Cenozoic coastlines.* Cambridge University Press, Cambridge.

SPEIJER, R.P. 1994. *Extinction and recovery patterns in benthic foraminiferal paleocommunities across the Cretaceous/Paleogene and Paleocene/Eocene boundaries.* PhD Thesis, Universiteit Utrecht, Netherlands, Geologica Ultraiectina, **3**, 1–191.

STROUHAL, A. 1993. Tongeologische Entwicklungstrends in kretazischen und tertiären Sedimenten Nordostafrikas: regionale Fallbeispiele. *Berliner Geowissenschaftliche Abhandlungen*, **155**, 1–68.

THIRY, M. 1989. Geochemical Evolution and Paleoenvironments of the Eocene continental Deposits in the Paris Basin. *Palaeogeography, Palaeoclimatology, Palaeoecology*, **70**, 153–165.

THOMAS, E. 1990. Late Cretaceous through Neogene deep-sea benthic foraminifers (Maud Rise, Weddell Sea, Antarctica). *Proceedings of the Ocean Drilling Program, Scientific Results*, **113**, 571–594.

—— & SHACKLETON, N.J. 1996. The latest Palaeocene benthic foraminiferal extinction and stable isotope anomalies. *In:* KNOX, R.W., CORFIELD, R.M. & DUNAY, R.E. (eds) *Correlation of the Early Paleogene in Northwest Europe*. Geological Society, London, Special Publications, **101**, 401–441.

VAN MORKHOVEN, F.P., BERGGREN, W. & EDWARDS, A.S. 1986. Cenozoic cosmopolitan deep-water benthic Foraminifera. *Bulletin des Centres de Recherches Exploration-Production Elf-Aquitaine. Memoire*, **11**, 1–421.

VEIZER, J. 1983. Trace elements and isotopes in sedimentary carbonates. *In:* REEDER, R.J. (ed.) *Carbonates: mineralogy and chemistry.* Mineralogical Society of America Reviews in Mineralogy, **11**, 265–299.

WOLFE, J.A. 1980. Tertiary climates and floristic relationships at high latitudes in the northern hemisphere. *Palaeogeography, Palaeoclimatology, Palaeoecology*, **30**, 313–323.

ZACHOS, J., LOHMANN, K., WALKER, J.C.G. & WISE, S.W. 1993. Abrupt climate change and transient climates during the Paleogene: A marine perspective. *Journal of Geology*, **101**, 191–123.

Received 19 August 1999; revised typescript accepted 20 April 2000.
Scientific editing by Duncan Pirrie.